INVESTIGATING THE ENZYMATIC HYDROLYSIS OF CRYSTALLINE CELLULOSE USING FLUORESCENCE BASED ASSAYS – IMPLICATIONS OF SYNERGISM, BINDING AND PRODUCT INHIBITION

A Dissertation

Presented to the Faculty of the Graduate School

of Cornell University

In Partial Fulfillment of the Requirements for the Degree of

Doctor of Philosophy

by

Navaneetha Santhanam

August 2009

INVESTIGATING THE ENZYMATIC HYDROLYSIS OF CRYSTALLINE CELLULOSE USING FLUORESCENCE BASED ASSAYS – IMPLICATIONS OF SYNERGISM, BINDING AND PRODUCT INHIBITION

Navaneetha Santhanam, Ph. D.

Cornell University 2009

The hydrolysis kinetics of bacterial microcrystalline cellulose (BMCC) by the cellulases of *Thermobifida fusca* was studied using fluorescence based assays in three ways. First, the binding of fluorescence-labeled Cel5A, Cel6B and Cel9A in ternary synergistic mixtures was assessed. A rapid high-throughput binding assay using microwell plates was developed to measure the bound fractions of the three cellulases at varying mole ratios of Cel6B and Cel9A, with Cel5A fixed at 10% of the total cellulase loading. This study revealed that the bound fractions of cellulases in ternary mixtures were additive, unlike the hydrolytic activity which was synergistic. Second, an experimental system was developed for the application of high resolution fluorescence microscopy to examine the binding of individual Cel5A, Cel6B and Cel9A to immobilized cellulose with varying morphologies. The immobilization technique allowed deposition of cellulose morphologies ranging from nanoscale cellulose fibers, to microscale cellulose fibril mats to sub-millimeter scale cellulose particles. Fluorescently labeled Cel5A, Cel6B and Cel9A were successfully integrated with fluorescently labeled cellulose to obtain a miniaturized reaction system which retained the intrinsic binding and hydrolytic capabilities of cellulases. Direct visualization of the binding behavior of individual cellulases on cellulose with different morphologies was achieved using this system which showed that the binding behavior depended strongly on the morphology and complexity of cellulose

aggregates. Third, the significance of product inhibition by cellobiose as a rate-retarding factor in the hydrolysis of BMCC by Cel9A and Cel9A-68, its construct lacking the family 2 cellulose binding module, was investigated. Fluorescently labeled BMCC was used as the substrate for an analysis of initial rates in the presence of exogenous cellobiose. Increasing cellobiose concentrations ranging from 1- 5mM were found to decrease the initial rate by 10 - 30% but increasing cellobiose concentrations from 5 to 60 mM did not cause a further decline in initial rates, clearly ruling out classical competitive inhibition as a possible mechanism. No definitive correlation was observed between binding and cellobiose concentrations for both enzymes indicating that the presence of cellobiose does not lead to significant enhancement or inhibition of binding.

BIOGRAPHICAL SKETCH

Navaneetha Santhanam was born in Arakkonam, Tamil Nadu in 1981 and was raised in Jamshedpur, Jharkhand where, after 12 years of education she graduated from Hill Top School. She then moved to Chennai, Tamil Nadu in 1999 to get a Bachelor's degree in Chemical Engineering at Anna University. Somewhere along the way during her undergraduate years she decided she wanted to pursue higher education in the United States. In the fall of 2003 she came to Cornell University, Ithaca to take up the challenges of a Ph.D. in Biological and Environmental Engineering. Following the completion of her Ph.D. in June 2009, Navaneetha will begin research as a postdoctoral fellow at the Colorado Center for Biorefining and Biofuels at Fort Collins.

Dedicated to Appa and Amma

ACKNOWLEDGMENTS

This doctorate is a result of not just my research...it is the cumulative outcome of all the thoughtful things done by all the people who have helped me along the way. Firstly, I would like to express my gratitude for the mentorship and continuous support provided by my major advisor, Dr. Larry Walker. Not only does Larry ensure that every member of his team has full financial assistance throughout the time it takes to achieve their degree, but he also provides emotional and moral support, which is essential to students during the ups and downs of graduate life. Secondly, I would like to thank my committee members, Dr. David Wilson and Dr. Harold Craighead for providing the necessary guidance – either in the form of insights and interpretations of data or as recommendations for researchers to collaborate with. It was Diana Irwin who patiently taught me all the laboratory skills necessary to produce and work with cellulases. And Sue Fredenberg has almost been a foster mom to me at Cornell taking care of anything and everything I might need during my years as a graduate student in the Walker lab. I would like to thank the postdoctoral associates of the Walker lab – Stephane Corgie and Jose Moran-Mirabal – for the myriad brainstorming sessions which allowed me to bounce interesting research ideas off of them. I would like to thank all the graduate students who have provided the right milieu for work and relaxation at the Walker grad student office – Scott Pryor, Aaron Saathoff, Sarah Munro, Erin Brown, Linelle Fontenelle, Marie Donnelly, Ben Heavner, Jeremy Luterbacher and Hnin Aung. Former Walker lab graduates, Tina Jeoh , Caroline Corner and undergraduate Caroline Milne, who have immensely helped me whenever I reached out to them for advice or support, also deserve mention here. Finally, I owe all my success to my family – my parents who have continuously ensured the best education and unequivocally encouraged me in all my endeavors, despite the miles

that separate us and more recently, my husband for his boundless optimism, support and patience. And of course, I must stress that, errors if any, in this dissertation fall squarely on my own shoulders.

TABLE OF CONTENTS

LIST OF FIGURES

LIST OF TABLES

CHAPTER 1

INTRODUCTION

1.1 Background

Growing concerns regarding the impact of fossil fuel consumption on global climate change and energy security have led to the demand for the accelerated development of biofuels across the globe. Cellulosic ethanol has the potential to significantly reduce greenhouse gas emissions and replace petroleum based gasoline (Tilman, et al. 2006). In the United States, the Renewable Fuel Standard, as part of the Energy Independence and Security Act of 2007, mandates that 36 billion gallons of ethanol be produced annually by the year 2022, of which 16 billion gallons are expected to be produced from cellulosic feedstocks (U.S.DOE and USDA 2009). The biomass to ethanol production process involves three steps basic steps: (1) the pretreatment of feedstocks; (2) saccharification of pretreated feedstocks using enzyme cocktails; and (3) fermentation of the mixed sugars (Himmel, et al. 2007; Stephanopoulos 2007). The second step – enzymatic hydrolysis of pretreated feedstock – is the rate-limiting step which needs a 5-10 fold cost reduction in order to make cellulosic ethanol commercially viable (Himmel, et al. 2007; Stephanopoulos 2007).

More than two decades of empirical experimentation with cellulose hydrolysis have led to the identification of efficient cellulase preparations and effective feedstock pretreatment processes. However, the technology is still not mature enough to allow cellulosic ethanol to compete with the petroleum industry. Much progress has been made with regard to understanding the biochemistry of cellulases such as protein structure - function relationships and the different mechanisms of catalytic cleavage (Lynd, et al. 2002; Wilson and Irwin 1999). Despite much research, the kinetics of cellulose hydrolysis in terms of the intrinsic binding mechanisms, rate retardation and

diffusion limitations on the surface as well as within the porous cellulose substrate, are still not understood well enough to make this process commercially viable.

The driving force behind this research is the investigation of the fundamental mechanisms involved in the enzymatic hydrolysis of crystalline cellulose, so as to advance the current understanding of cellulose depolymerization kinetics. It addresses the kinetics of the cellulase-cellulose reaction system in three different ways. The first study investigates the binding of cellulases in ternary synergistic mixtures using a high-throughput binding assay conducted in microplate reactors. The second study involves the development of an experimental system for the application of high resolution microscopy to visualize the diffusion to, and binding of cellulases on cellulose fibrils at the nanoscale. The third probes the role of cellobiose inhibition on the activity and binding of an individual cellulase. All three studies take advantage of the precision and sensitivity of fluorescence based methods to characterize the cellulase-cellulose reaction system.

1.2 Research objectives

1.2.1 Objective One

Assess the binding behavior of cellulases in ternary synergistic mixtures on bacterial microcrystalline cellulose.

The efficient hydrolysis of crystalline cellulose requires a mixture of cellulases which can degrade cellulose using different catalytic modes. Based on their catalytic modes of action, cellulases have been classified as i) exocellulases, those that attack cellulose from the reducing and non-reducing ends and continue processively along the same chain, ii) endocellulases, those that cleave randomly along the cellulose chains and dissociate after cleavage, and iii) processive endocellulases, those that cleave randomly and continue processively along a chain (Wilson and Irwin 1999).

Such a mixture is found to have a cumulative activity that is several times higher than the sum of individual activities of its components, resulting in the phenomenon termed synergism (Woodward 1991). Different cellulases have also been observed to possess different binding affinities to crystalline cellulose (Bothwell, et al. 1997a; Kim et al. 1995; Medve, et al. 1994; Jung and Walker 2003). Hence, the question arises whether the binding behavior of cellulases in synergistic mixtures is different from their individual binding and whether their bound fractions in mixtures can provide useful clues about the mechanism of their synergistic activity. However, the measurement of bound fractions of cellulases in mixtures with more than two components has been limited by the lack of an accurate method for quantification of components in complex mixtures.

Jeoh et al. (2002) introduced the use of fluorescence to study binding in binary mixtures. Their method allowed direct measurement of bound cellulase concentrations and their experiments indicated a cooperative enhancement of cellulase binding in binary mixtures of *Thermobifida fusca* Cel5A, Cel6B and Cel9A at 50ºC . The major objective of this work was to extend the use of fluorescently labeled cellulases to study binding in ternary synergistic mixtures. In doing so, the key question to be answered was whether the binding of *T. fusca* cellulases exhibited cooperative or competitive behavior in ternary mixtures.

1.2.2 Objective Two

Elucidate the intrinsic mechanisms of cellulase-cellulose interactions at the scale of individual cellulose microfibrils through the use of high resolution microscopy.

In a heterogeneous reaction such as cellulose hydrolysis, where the enzyme is soluble and the substrate is insoluble, the effect of mass transfer from the solution

phase to the solid phase can play a key role in determining the overall reaction rate. This is because contact between the cellulase and cellulose can be established only by diffusion of cellulases to the cellulose surface (Lee and Fan 1980). Resistance to mass transfer is provided by the bulk solution phase and the stagnant film surrounding the cellulose particles. Following initial adsorption to the surface, penetration of the cellulase molecules into the pore structure of the cellulose substrate after certain time lapse, brings into effect the internal mass transfer resistance as well (Gan, et al. 2003; Lee and Fan 1980). Hence there is a need to elucidate the binding and diffusive properties of cellulases on the surface of cellulose fibrils and in the pore structure of its complex morphology.

The advancement of optical techniques based on fluorescence has reached a point where high spatial and temporal resolution is possible. Wide-field fluorescence microscopy in combination with high numerical aperture objectives and highly sensitive cameras has allowed the high resolution imaging of protein-surface interactions and protein receptor binding (Houseman, et al. 2002; Zhuang, et al. 2000). Fluorescence imaging techniques can be applied to study the inherent complexities of enzymatic cellulose depolymerization and to address the issues of mass transfer limitations. Previous studies (Jervis, et al. 1997) sought to measure the surface diffusion rates of bacterial cellulases from *Cellulomonas fimi* on thick cellulose films using fluorescence recovery after photobleaching. Despite their early success, there have been only limited applications of high-resolution optical techniques in the study of cellulases. Recently, wide-field fluorescence intensity measurements were performed on cellulose films in order to determine binding characteristics of cellulose binding domains (Pinto, et al. 2007). While these studies have made use of fluorescence to evaluate the average overall binding to the complex cellulose

morphology, they have not studied the cellulase-cellulose interactions at the most fundamental scale of the cellulose fibrils in the nanoscale range.

The goal of this study was to develop and validate an experimental system for the application of fluorescence microscopy to the cellulase-cellulose reaction system in order to elucidate binding of cellulases to the surface of cellulose microfibrils. The first objective was to obtain highly purified, active, fluorescent cellulases labeled with organic dye. The second objective was to fluorescently label and immobilize bacterial microcrystalline cellulose in a manner that would enable identification of single cellulose fibrils with widths in the order of 5-10 nm. The third and major objective of this study was to monitor the individual binding behavior of *T. fusca* Cel5A, Cel6B and Cel9A to immobilized BMCC morphologies using epifluorescence microscopy.

1.2.3 Objective Three

Investigate whether product inhibition by cellobiose leads to the rate retardation observed in cellulose hydrolysis by a processive endocellulase

A characteristic feature of the enzymatic hydrolysis of cellulose is the rapid decline in the rate of hydrolysis at any given enzyme to substrate ratio (Gusakov and Sinitsyn 1992; Ladisch, et al. 1983; Valjamae, et al. 1998; Zhang, et al. 1999; Zhang and Lynd 2004). Several factors have been considered responsible for the observed fall in the reaction rate such as product inhibition (Kruus, et al. 1995; Teleman, et al. 1995), substrate heterogeneity (Eriksson, et al. 2002; Valjamae, et al. 1998; Zhang, et al. 1999) and enzyme inactivation by fluid shear stress (Converse, et al. 1988; Eriksson, et al. 2002; Gan, et al. 2003). The aim of this study was to investigate whether product inhibition by cellobiose may be responsible for the nonlinear hydrolysis kinetics exhibited by purified cellulases. *T. fusca* secretes six cellulases of which Cel9A is the most active degrader of crystalline cellulose (Wilson 2004) and the

crystal structure of its construct Cel9A-68, which lacks the family 2 binding module, has been solved (Sakon, et al. 1997). Cellobiose has been reported to cause an enhancement in the binding of the catalytic domains of *Trichoderma reesei* (Palonen, et al. 1999; Stahlberg, et al. 1991). Hence probing the impact of cellobiose on the hydrolytic activity of intact Cel9A and Cel9A-68 on BMCC could provide useful insights on the intrinsic mechanism of crystalline cellulose hydrolysis. This study sought to test hypothesis that binding of cellobiose to the active site would prevent accessibility of the cellulose chains on the insoluble substrate to the active site of Cel9A-90 and Cel9A-68, leading to a decline in the reaction rate. It also addressed the question of whether the presence of cellobiose lead to increased or inhibited binding of Cel9A-68.

REFERENCES

Bothwell MK, Daughhetee SD, Chaua GY, Wilson DB, Walker LP. 1997a. Binding Capacities for *Thermomonospora fusca* E_3, E_4 and E_5, the E_3 Binding Domain, and *Trichoderma reesei* CBH I on Avicel and Bacterial Microcrystalline Cellulose. Bioresource Technology 60:169-178.

Converse AO, Matsuno R, Tanaka M. 1988. A Model of Enzyme Adsorption and Hydrolysis of Microcrystalline Cellulose with Slow Deactivation of the Adsorbed Enzyme. Biotechnol Bioeng 32:38-45.

Eriksson T, Karlsson J, Tjerneld F. 2002. A model explaining declining rate in hydrolysis of lignocellulose substrates with cellobiohydrolase I (Cel7A) and endoglucanase I (Cel7B) of *Trichoderma reesei*. Appl Biochem Biotechnol 101:41-60.

Gan Q, Allen SJ, Taylor G. 2003. Kinetic dynamics in heterogeneous enzymatic hydrolysis of cellulose: an overview, an experimental study and mathematical modelling. Process Biochemistry 38:1003-1018.

Gusakov AV, Sinitsyn AP. 1992. A Theoretical-Analysis of Cellulase Product Inhibition - Effect of Cellulase Binding Constant, Enzyme Substrate Ratio, and Beta-Glucosidase Activity on the Inhibition Pattern. Biotechnol Bioeng 40:663-671.

Himmel ME, Ding S, Johnson DK, Adney WS, Nimlos MR, Brady JW, Foust TD. 2007. Biomass Recalcitrance: Engineering Plants and Enzymes for Biofuels Production. Science 315:804-807.

Houseman BT, Huh JH, Kron SJ, Mrksich M. 2002. Peptide chips for the quantitative evaluation of protein kinase activity. Nat Biotechnol 20:270-274.

Jeoh T, Wilson DB, Walker LP. 2002. Cooperative and Competitive Binding in Synergistic Mixtures of *Thermobifida fusca* Cel5A, Cel6B and Cel9A. Biotechnology Progress 18:760-769.

Jervis EJ, Haynes CA, Kilburn DG. 1997. Surface diffusion of cellulases and their isolated binding domains on cellulose. J Biol Chem 272:24016-24023.

Jung H, Walker LP. 2003. Binding and Reversibility of *Thermobifida fusca* Cel5A, Cel6B and Cel48A and Their Respective Catalytic Domains to Bacterial Microcrystalline Cellulose. Biotechnol Bioeng 84:151-159.

Kim, D. W., Yoon, Y. H., Jeong, Y. K., Lee, J. K. and Jang,Y.H. 1995. Effect of adsorption of Endoglucanase on the degradation of microcrystalline cellulose. Bull. Korean Chem. soc 16:720-725.

Kruus K, Andreacchi A, Wang WK, Wu JHD. 1995. Product inhibition of the recombinant CelS, an exoglucanase component of the *Clostridium thermocellum* cellulosome. Appl Microbiol Biotechnol 44:399-404.

Ladisch MR, Lin KW, Voloch M, Tsao GT. 1983. Process Considerations in the Enzymatic-Hydrolysis of Biomass. Enzyme Microb Technol 5:82-102.

Lee YH, Fan LT. 1980. Kinetics of Hydrolysis of Insoluble Cellulose by Cellulase. Advances in Biochemical Engineering 17:131-168.

Lynd LR, Weimer PJ, van Zyl WH, Pretorius IS. 2002. Microbial Cellulose Utilization: Fundamentals and Biotechnology. Microbiol Mol Biol Rev 66:506-577.

Medve J, Stahlberg J, Tjerneld F. 1994. Adsorption and Synergism of Cellobiohydrolase I and II of *Trichoderma reesei* During Hydrolysis of Microcrystalline Cellulose. Biotechnol Bioeng 44:1064-1073.

Palonen H, Tenkanen M, Linder M. 1999. Dynamic interaction of *Trichoderma reesei* cellobiohydrolases Ce16A and Ce17A and cellulose at equilibrium and during hydrolysis. Applied and Environmental Microbiology 65:5229-5233.

Pinto R, Amaral AL, Carvalho J, Ferreira EC, Mota M, Gama M. 2007. Development of a method using image analysis for the measurement of cellulose-binding domains adsorbed onto cellulose fibers. Biotechnol Prog 23:1492-1497.

Sakon J, Irwin D, Wilson DB, Karplus PA. 1997. Structure and mechanism of endo/exocellulase E4 from *Thermomonospora fusca*. Nat Struct Mol Biol 4:810-818.

Stahlberg J, Johansson G, Petterson G. 1991. A New Model for Enzymatic Hydrolysis of Cellulose Based on the Two-Domain Structure of Cellobiohydrolase I. Bio/Technology 9:286-290.

Stephanopoulos G. 2007. Challenges in Engineering Microbes for Biofuels Production. Science; Science 315:801-804.

Teleman A, Koivula A, Reinikainen T, Valkeajarvi A, Teeri TT, Drakenberg T, Teleman O. 1995. Progress-Curve Analysis shows that Glucose Inhibits the Cellotriose Hydrolysis Catalyzed by Cellobiohydrolase II from *Trichoderma-Reesei*. Eur J Biochem 231:250-258.

Tilman D, Hill J, Lehman C. 2006. Carbon-Negative Biofuels from Low-Input High-Diversity Grassland Biomass. Science; Science 314:1598-1600.

U.S.DOE and USDA 2009. Sustainability of biofuels: Future Research Opportunities; Report from the October 2008 Workshop, DOE/SC-0114, U.S. Department of Energy Office of Science and U.S. Department of Agriculture

Valjamae P, V S, Pettersson G, Johansson G. 1998. The Initial Kinetics of Hydrolysis by Cellobiohydrolases I and II is Consistent with a Cellulose Surface - Erosion Model. European Journal of Biochemistry 253:469-475.

Wilson DB. 2004. Studies of *Thermobifida fusca* plant cell wall degrading enzymes. The Chemical Record 4:72-82.

Wilson DB, Irwin DC. 1999. Genetics and Properties of Cellulases. Advances in Biochemical Engineering Biotechnology: Recent Progress in Bioconversion 65:1-21S.

Woodward J. 1991. Synergism in Cellulase Systems. Bioresourse Technology 36:67-75.

Zhang S, Wolfgang DE, Wilson DB. 1999. Substrate heterogeneity causes the nonlinear kinetics of insoluble cellulose hydrolysis. Biotechnol Bioeng 66:35-41.

Zhang YHP, Lynd LR. 2004. Toward an aggregated understanding of enzymatic hydrolysis of cellulose: Noncomplexed cellulase systems. Biotechnol Bioeng 88:797-824.

Zhuang XW, Bartley LE, Babcock HP, Russell R, Ha TJ, Herschlag D, Chu S. 2000. A single-molecule study of RNA catalysis and folding. Science 288:2048-2051.

CHAPTER 2

LITERATURE REVIEW

2.1 Cellulose

2.1.1 Chemistry of cellulosic biomass

Plant cell walls comprise the most abundant renewable resource in the biosphere. The net carbon dioxide fixated annually by land plants has been estimated to be approximately 56×10^9 tonnes (Field, et al. 1998). Only about 2% of plant cell walls has been utilized by humans up till now in the form of wood for heating, as timber for construction and for textiles and paper (Pauly and Keegstra 2008). The idea of using sugars derived from biomass, which was first proposed in the 1970s, has now gained international momentum as a definite alternative to fossil fuels (Himmel, et al. 2007; Schubert 2006; Stephanopoulos 2007). Understanding the chemistry of cellulosic biomass is fundamental to effective utilization of this resource for production of biofuels. Plant cell walls are of two types – primary and secondary. The major component of primary cell walls is cellulose which comprises 40-60% of total plant biomass. In higher plants, cellulose occurs in the form of bundles of individual glucan chains called elementary fibrils or microfibrils, which are its fundamental structural unit (Haigler, et al. 1980). These microfibrils are enveloped in hemicellulose which consists of branched polymeric chains of aldopentoses (5-carbon sugars) such as xylose and arabinose and aldohexoses (6-carbon sugars) such as glucose, mannose and galactose. Cross-linked polysaccharides such as pectins form hydrated gels that hold the cell wall components together. In addition to the networks of pectins and hemicellulose, primary cell walls contain 2-10% structural glycoproteins and some enzymes and have 1-5% ionically and covalently bound minerals (O'Neill and York 2003).

Secondary cell walls develop inside primary cell walls after termination of cell growth and contain lignin. Lignin is a three-dimensional phenyl propane polymer which provides strength and rigidity to the plant. It is the residual portion of biomass that remains solid after hydrolysis (O'Neill and York 2003). Table 2.1 shows the typical values of cellulose, hemicellulose and lignin found in some selected cellulosic materials (Gong, et al. 1999). The composition of feedstocks for biofuel production is found to vary significantly among species. Lignin and hemicellulose are closely interlinked with cellulose as shown in Figure 2.1 and form a physical barrier to any type of biological or chemical hydrolysis of cellulose. Thus the first step in biomass conversion consists of disrupting the non-cellulosic matrix in order to expose the crystalline cellulose core and is termed the pretreatment step. Pretreatments convert the hemicellulose into soluble mono- and oligosaccharides which can be separated for further hydrolysis or fermentation. Several pretreatment methods such as steam explosion, ammonia explosion, dilute acid, liquid hot water and alkaline pretreatments have been investigated (Wyman, et al. 2005).

2.1.2 Structure of cellulose

Cellulose molecules consist of linear condensation polymers made up of D-anhydroglucopyranose units linked by β-1,4-glucosidic linkages. Condensation polymers are a class of polymers formed through a condensation reaction releasing a small molecule by-product, which in the case of cellulose, is water. One end of the cellulose chain is termed the reducing end because the hemiacetal ring is open, exposing the reducing aldehyde. The other end of the chain is called the non-reducing end because the C1 carbon in the hemiacetal is involved in the β-1,4-bond, preventing ring opening. This property provides directionality to cellulose chains. The repeating unit for cellulose is anhydrocellobiose since each anhydroglucose unit is rotated 180°

Table 2.1 Typical values of biomass composition in terms of cellulose, hemicellulose and lignin of certain cellulosic materials (Gong, et al. 1999)

Biomass Classification	Type	Cellulose (% dry weight)	Hemicellulose (% dry weight)	Lignin (% dry weight)
Herbaceous crops	Alfalfa hay	38	9	14
	Coastal Bermuda grass	25	35.7	6.4
	Switchgrass	45	31	12
Agricultural residues	Corn cobs	45	35	15
	Corn stover	41	21	17
	Wheat straw	36	28	29
Hardwood	Aspen	46	26	18
	Hybrid poplar	43	21	26
Softwood	Spruce	43	26	29
	Pine	44	26	29
Cellulose wastes	Newsprint	61	16	21
	Recycled paper sludge	50	10	n/a

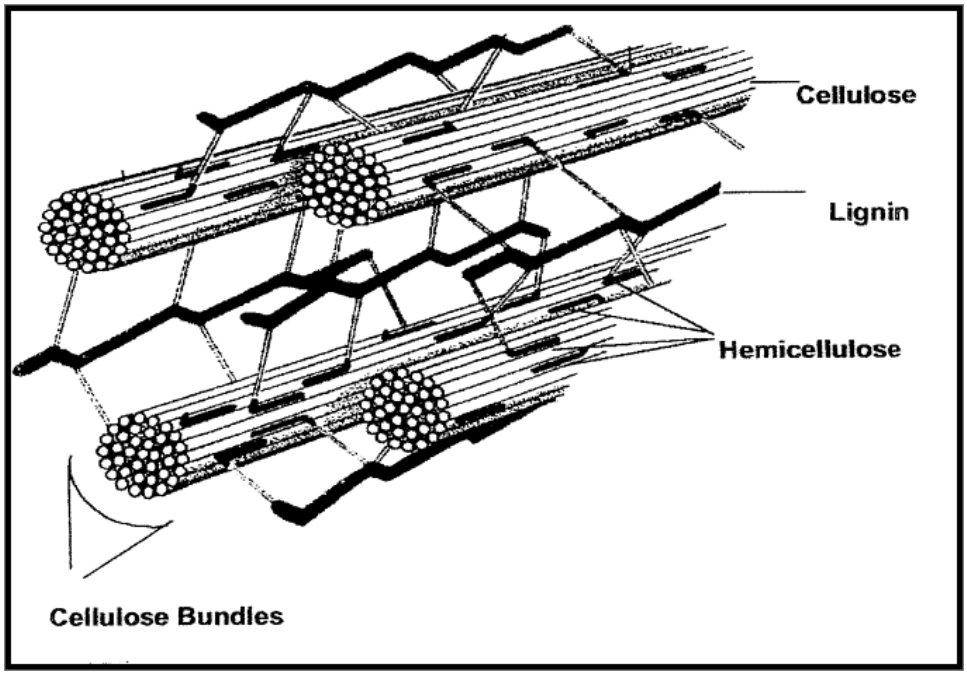

Figure 2.1 Diagrammatic representation of the association of cellulose with hemicellulose and lignin in the plant cell wall (Scott, et al. 2002).

with respect to its nearest neighbor producing a very symmetrical structure, as shown in Figure 2.2.

X-ray diffraction data of pure crystalline cellulose from various sources have indicated that cellulose crystals are made of chains arranged in layered sheets (Gardner and Blackwell, 1974). Within each sheet, the chains align parallel to each other and are linked by hydrogen bonds while the sheets are stacked by Van der Waals interactions (Gardner and Blackwell, 1974). The hydrophobicity of cellulose sheets makes cellulose resistant to chemical hydrolysis due to the formation of a dense aqueous layer near the hydrated cellulose surface (Matthews, et al. 2006) while the strong intra- and interchain hydrogen bonding networks make crystalline cellulose resistant to enzymatic hydrolysis (Nishiyama, et al. 2002).

While plant-based cellulose is an important resource for industrial purposes, cellulose is also synthesized by bacteria, amoebae, certain fungi, cellular molds, green algae and one group of animals, the tunicates (Brown 2004). Crystalline cellulose occurs in different forms, the most common ones being cellulose I and II. Studies have shown that cellulose I has two different suballomorphs, cellulose I_α which is dominant in bacterial and algal celluloses and I_β which is found in higher plants (Viëtor, et al. 2000). Cellulose I_α exists as a single-chain triclinic unit cell as shown in Figure 2.3b (Viëtor, et al. 2000). Of it's four crystal faces, the (100) and (010) faces present large hydrophilic surfaces rich in hydroxyl groups while the (110) and (1-10) faces present sharp edges which expose only one glucan chain to the surface [10]. The repeating unit of the (110) face is the cellobiose lattice which measures 1.07 nm along the axis of the glucan chain and 0.54 nm in the perpendicular direction.

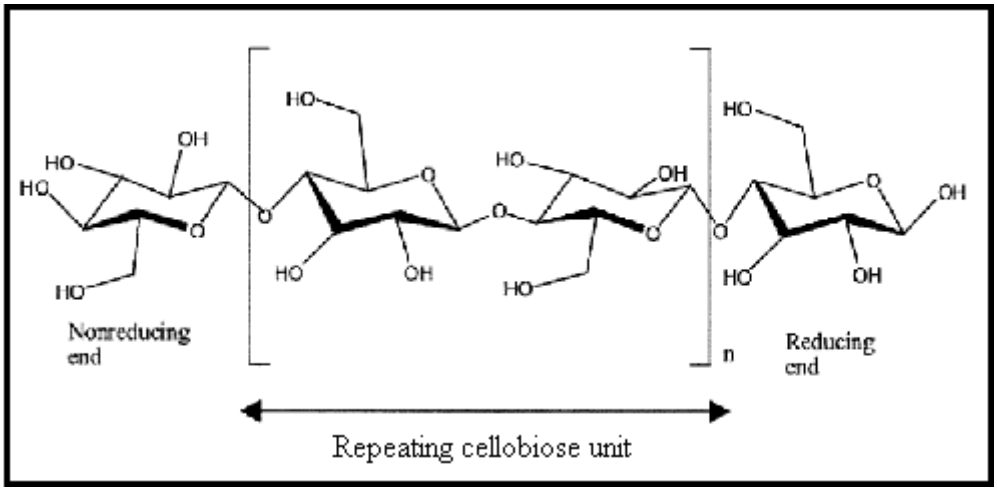

Figure 2.2 Structure of cellulose depicting β-1,4-linked anhydroglucose units.

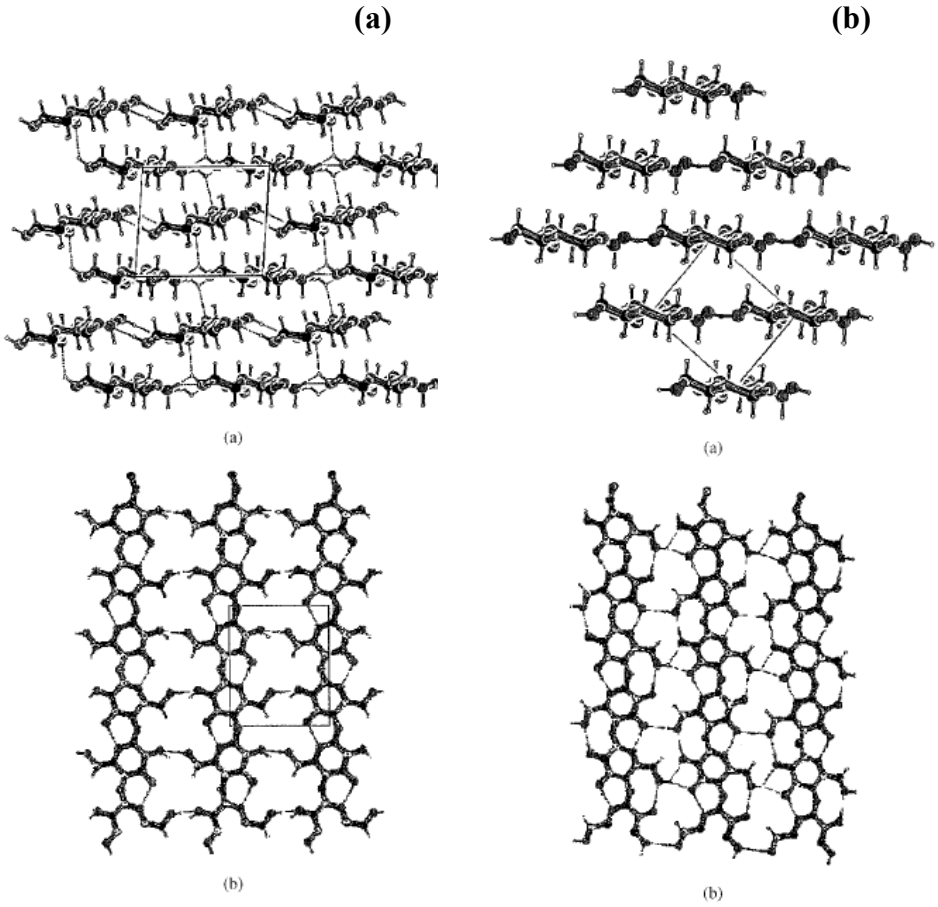

Figure 2.3 (a) The monoclinic model of cellulose I viewed along the chain axis (top) and perpendicular to the chain axis (below) and (b) The triclinic model of cellulose I viewed (top) along the chain axis and perpendicular to the chain axis (below).

Cellulose I_β is a lower energy, more stable allomorph with two non-equivalent chains per monoclinic unit cell, and its crystal structure is modeled to be as shown in Figure 2.3a (Viëtor, et al. 2000).

2.1.3 Model cellulosic substrates

In order to understand the mechanism of enzymatic hydrolysis of cellulose most biochemical studies use model substrates which are relatively free of non-cellulosic plant cell-wall-associated components, in order to simplify analyses (Tomme, et al. 1995a). Bacterial cellulose (BC) is model substrate prepared from the pellicle produced by *Acetobacter xylinum* and is available in never-dried form. Bacterial microcrystalline cellulose (BMCC) is prepared from BC by partial acid hydrolysis which removes some amorphous cellulose content (Valjamae, et al. 1999). Wood pulp is obtained after size reduction of wood by shredding, delignification, bleaching and washing (Klemm, et al. 1998) and Solka Floc is prepared from SO_2-bleached spruce pulp by ball-milling. Avicel, also known as microcrystalline cellulose or hydrocellulose, is prepared by partial acid hydrolysis of wood pulp followed by spray-drying of the washed pulp slurry and consists of 30-50% amorphous cellulose (Krassig 1993). Cotton cellulose is prepared from natural cotton by removal of wax, pectin and other colored components while Whatman No.1 filter paper is made from cotton pulp (Dong, et al. 1998). Phosphoric acid swollen cellulose (PASC) is prepared by swelling cellulose powder such as Avicel using concentrated phosphoric acid (Wood 1988).

The structural features of cellulosic materials are critical factors affecting the rate and extent of enzymatic hydrolysis. The accessibility of enzymes to cellulose is determined by properties such as the specific surface area, the crystallinity index, the degree of polymerization and particle size (Fan, et al. 1980; Grethlein 1985; Mandels

1985; Stone, et al. 1969; Wood and McCrae 1979). Investigation of the influence of these physical characteristics of these physical characteristics on enzymatic hydrolysis of model substrates and pretreated materials has been a subject of much research (Chang and Holtzapple 2000; Hong, et al. 2007; Ishizawa, et al. 2007; Jeoh, et al. 2007; Zhu, et al. 2008).

2.1.4 Accessible surface area

Cellulose is an insoluble, heterogeneous porous substrate and hence presents both internal and external surfaces (Cowling and Brown 1969; Stone, et al. 1969). The shape and size of the cellulose particles determine the external surface area while the capillary structure of the cellulose fibers and the size of the penetrating reactant determine the internal surface area (Walker and Wilson 1991). External surface area has been quantified using particle counters (Lee and Fan 1982). The internal surface has been quantified by the Brunauer-Emmett-Teller (BET) method which measures the surface of a dry sample available for adsorption to nitrogen molecules (Gharpuray, et al. 1983). However an important drawback of this technique is that it involves drying of the substrate, hence the results are not indicative of the properties of cellulose in its swollen state. Another problem of this technique is that since nitrogen is a much smaller molecule than cellulases, it has access to pores and cavities on the fiber surface that the cellulases cannot penetrate (Neuman and Walker 1992).

The solute exclusion technique overcomes both these disadvantages of the BET method by measuring the area available in the form of cavities and pores to dextran or polyethylene glycol molecules of various sizes in cellulose samples submerged in an aqueous medium, thus preventing the effects of shrinkage on pore structure caused by drying (Grethlein 1985). A linear correlation between initial hydrolysis rates and the pore size accessible to molecules of nominal diameter was

reported by Grethlein (1985). However, the correlation of pore volume to accessible surface area requires an assumption of the pore geometry (Mansfield, et al. 1999; Neuman and Walker 1992). The specific surface area obtained by the BET method and the solute exclusion method of some common substrates, is listed in Table 2.2.

Ishizawa et al. (2007) used solute exclusion and ^{1}H nuclear magnetic resonance thermoporometry to measure the porosity of wet dilute acid pretreated corn stover. Thermoporometric methods estimate pore volumes by using changes in physical properties of a substance, such as melting point depression, when it is confined to small spaces (Ishizawa, et al. 2007). NMR thermoporometry measures the fraction of unfrozen liquid as a function of temperature. At any specific temperature, the amount of unfrozen liquid is directly proportional to the pore volume of defined size (Ishizawa, et al. 2007). They found that pretreated corn stover appeared to have a more accessible pore volume that raw corn stover. However, Ishizawa et al. (2007) concluded that while the techniques used allowed the differentiation of porosity of pretreated and untreated materials, no correlation was found between pore size and the enzymatic digestibility of pretreated samples.

2.1.5 Crystallinity index

Another important structural feature that is believed to affect the rate of enzymatic hydrolysis of cellulose fibers is its degree of crystallinity (Wood 1975). A cellulose fiber contains crystalline and amorphous rEG Ions, with crystalline rEG Ions being more difficult to degrade. The crystallinity index is the percentage of total cellulose that is crystalline. Crystallinity of dried cellulose samples has been quantified using wide-angle X-Ray diffraction and the crystallinity indexes (CrI) of Cellulose I for various model substrates are shown in Table 2.3.

Table 2.2 Specific surface area of some model substrates measured by different techniques

Substrate	Measurement Technique	Specific Surface Area (m^2/g)	Reference
Avicel PH102	N_2 adsorption	1.8-5.4	(Lee and Fan 1982; Ryu, et al. 1982)
Solka Floc BW 40	N_2 adsorption	1.89-2.13	(Fan, et al. 1981; Ryu, et al. 1982)
Sigmacell 50	N_2 adsorption	1.84	(Fan, et al. 1981)
Acid Swollen cotton	Solute exclusion	10-100	(Stone, et al. 1969)
Mixed Hardwood	Solute exclusion	10.5	(Grethlein 1985)
	Solute exclusion	140	(Grethlein 1985)

Table 2.3 Crystallinity Index values for some model substrates

Substrate	Crystallinity Index (%)	Reference
Avicel PH 102	80.8-81	(Lee and Fan 1982; Ryu, et al. 1982)
Solka Floc BW 200	67.3	(Ryu, et al. 1982)
Solka Floc SW 40	74.3-76.7	(L. T. Fan 1981; Lee and Fan 1982)
Sigmacell 50	84.5	(L. T. Fan 1981)

Grethlein (1985) observed that dilute acid pretreatment of mixed hardwood and steam pretreated pine increased the specific surface area of the substrate but this change was found to be accompanied by an increase in its crystallinity. The crystallinity of lime pretreated hybrid poplar has been documented to have an impact on its digestibility, with reduction in crystallinity leading to increase in initial hydrolysis rates (Chang and Holtzapple 2000). Pretreatments selected to reduce crystallinity from 60% to 25 % were found to lead to tenfold improvement in digestibility (Zhu, et al. 2008).

The fact that any change in specific surface area is usually coupled with changes in substrate crystallinity leads to an uncertainty in drawing any definitive conclusions regarding the influence of either structural property on the rate and extent of hydrolysis (Walker and Wilson 1991). Another complicating factor is that hydrolysis is accompanied by a change in these properties (Walker and Wilson 1991). During enzymatic hydrolysis, cellulosic substrates also undergo a fragmentation process (Kyriacou, et al. 1987; Walker, et al. 1990). Studies using crude cellulases from *Thermobifida fusca* have shown that the rate of fragmentation varies linearly with the amount of bound cellulase (Walker, et al. 1990).

2.2 Cellulases

Cellulases are enzymes which catalyze the hydrolysis of the β-1-4-glycosidic linkage in cellulose. Conventionally, they have been divided into two fundamental types, endo-cellulases (EC 3.2.1.4) and exo-cellulases (EC 3.2.1.91) based on their mode of action. Though all cellulases share the same chemical specificity for the β-1,4-glucoside bonds of cellulose, they have evolved different specificities towards the more macroscopic properties of cellulose such as crystallinity and degree of polymerization. Assays have been developed to characterize and differentiate cellulases based on their activity on different model substrates (Teeri 1997). Cellulose

polymers solubilized by carboxymethyl or hydroxyethyl substitution are readily degraded by endocellulases resulting in a rapid decrease in the degree of polymerization (DP) and viscosity of the substrate (Shen, et al. 1995; Wood and Bhat 1988). Exocellulases seem to be limited by the availability of unsubstituted chain ends on the substrate and hence do not decrease their DP or viscosity (Shen, et al. 1995; Wood and Bhat 1988).

An important characteristic of some cellulases which can efficiently degrade crystalline cellulose is their "processivity" (Li, et al. 2007; Teeri 1997; Varrot, et al. 1999). Processivity is the ability of a cellulase molecule to adsorb to a cellulose chain, perform hydrolytic cleavage, translate along the same chain and continue to cleave bonds without dissociating until an obstruction or the end of the chain is reached (Wilson and Irwin 1999). On the basis of structural and mutational studies (Sakon, et al. 1997; Varrot, et al. 1999) it is hypothesized that single cellulose chains are fed into the active site of the processive cellulase and the enzyme slides along the cellulose chain aided by the cellulose binding module, while the product of hydrolysis diffuses away. It is believed that the main advantage of the processive mechanism of hydrolysis is that it prevents the re-association of the cellulose chain with the surrounding insoluble matrix once it has been detached from the crystal (Wilson 2004). Recent studies based on the enzymatic conversion of chitin have proposed that the processivity of chitinases, which is usually considered advantageous for improving substrate accessibility and beneficial for efficient hydrolysis, might be the factor responsible for hydrolysis being a slow reaction (Eijsink, et al. 2008).

Solid experimental evidence has yet to be obtained for directly relating the rate of processivity of cellulases with the rate of bond cleavage. Until now, processivity has been measured by determining the ratio of soluble reducing sugars to the insoluble reducing ends left on the substrate (Irwin, et al. 1993; Li, et al. 2007). This measure of

procession can be used to measure relative "processivity" since a standard curve of the absolute concentrations of reducing ends on the insoluble substrate cannot be prepared (Li, et al. 2007). Other techniques developed for measuring processivity involve analysis of hydrolysis products obtained from radioactive end-labeled cellulose (Nutt, et al. 1998) and the use of active site titration "burst" kinetics of fluorescent derivatized cellulose (Kipper, et al. 2005). The tritium label used to end-label cellulose has been found to be unstable under the alkaline conditions used to terminate the reactions (Nutt, et al. 1998). The active site titration studies are based on the assumption of steady state kinetics for the formation of a reaction intermediate, the validity of which is questionable for the heterogeneous cellulase-cellulose system.

Aerobic microorganisms such as fungi and bacteria produce mixtures of extracellular enzymes which are capable of completely degrading crystalline cellulose. These cellulases are made up of a minimum of two structural domains, the catalytic domain (CD) and the cellulose binding module (CBM). These two domains are usually joined together by a short linker peptide. The catalytic domain has an active site where the hydrolysis of a single glucan chain takes place. Using amino acid sequence alignment of the CDs, the cellulases have been classified into families such that all members of a family share the same basic three-dimensional structure and have the same stereochemistry for cleavage of the β-1,4-glucosidic linkage (Henrissat, et al. 1998).

Two stereochemically different mechanisms are possible for cellulose hydrolysis (Beguin and Aubert 1994). By the retaining mechanism enzymes carry out transglycosylation, producing cellobiose as the β anomer while in the inverting mechanism the first formed cellobiose is an α anomer. In both mechanisms, the role of two carboxyl side chains is critical. In inverting cellulases, one carboxyl side chain gets protonated to form a catalytic acid. It donates its proton to the glycosidic oxygen

of the leaving group. The other carboxyl side chain forms a catalytic base by removing a H-atom from the water molecule that attacks the C_1 carbon resulting in an inversion of the linkage from the β to the α configuration. In retaining cellulases, the C_1 carbon is attacked by the catalytic base resulting in the formation of a covalent intermediate with an inverted glycosidic bond, while a proton is donated to the glycosidic oxygen of the leaving group by the catalytic acid. A second step takes place in which the C_1 carbon is attacked by a water molecule causing another inversion of the linkage, resulting in overall retention of configuration. Figure 2.4 shows the two stereochemically different mechanisms of hydrolysis by cellulases (Wilson and Irwin 1999).

CBMs have also been classified into families based on sequence comparison, with family I CBMs being only of fungal origin and family 2 CBMs being only bacterial (Tomme, et al. 1995b). Fungal CBMs are small, usually made up of 33-36 amino residues while bacterial CBMs are larger consisting of about 100 amino acids (Wilson and Irwin 1999). Although structurally different, the CBMs of the these two families are all made up of β-sheets and have a flat face containing several aromatic and potential hydrogen-binding residues that are spaced in such a way as to stack against the glucose residues on the cellulose (Din, et al. 1994; Tormo, et al. 1996). These hydrophobic interactions increase binding stability. Three Trp residues are strictly conserved in all family 2 CBDs (Din, et al. 1994). Flexible polypeptide linkers connect the two domains, allowing them to function independently as well as in concert. Linkers are short amino acid sequences that are rich in Proline and Threonine. They are usually found to be O-glycosylated and it is believed that this protects them from proteolytic cleavage (Wilson and Irwin 1999). Linkers facilitate the ability of an enzyme to “desorb" or “slide" along a cellulose microfibril after hydrolytic activity (Wilson and Irwin 1999).

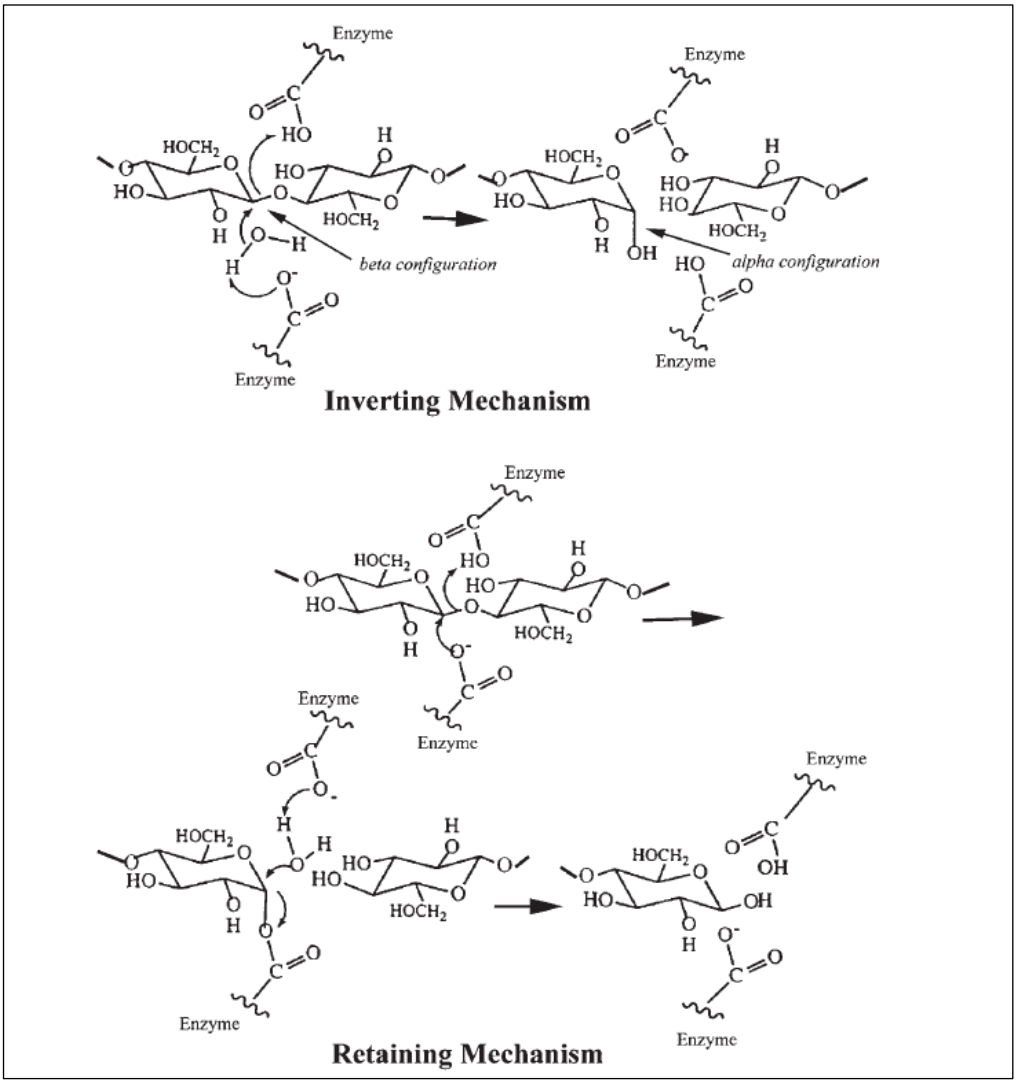

Figure 2.4 The two stereochemically different mechanisms of hydrolysis for cellulases

2.2.1 Cellulosomes

While aerobic fungi and bacteria produce mixtures of enzyme components which act in concert, anaerobic microorganisms such as the *Clostridia* adopt a different way to attack insoluble polysaccharides. They combine the essential glycosyl hydrolases, namely the cellulases, hemicellulases and carbohydrate esterases onto extracellular multi-enzyme complexes called cellulosomes (Lamed and Bayer 1988). The cellulosome is attached to the cell wall and is also tightly bound to the crystalline cellulose substrate (Lamed, et al. 1987; Mayer, et al. 1987), creating proximity between the cell and substrate which minimizes diffusional losses of hydrolysis products.

The cellulosome has a non-catalytic polypeptide called scaffoldin which has the multiple functions of binding the complex to cellulose, adhering it to the cell and also organizing its multiple enzyme subunits (Bayer, et al. 1985). Scaffoldin consists of a cellulose binding module and several duplicated non-catalytic domains called cohesins which interact with the cellulosomal enzymes. The modular enzymes each possess a catalytic domain and a dockerin domain which binds tightly to the cohesins of the scaffoldin (Shoham, et al. 1999). The most studied cellulosomal system is that of *Clostridium thermocellum* (Bayer, et al. 1998)which is a moderately thermophilic anaerobic bacterium (55-65°C) found in hot springs and wet, rotting biomass. The difficulty in producing large amounts of cellulosomes is a major drawback for their use in industrial applications. More detailed studies on the substrate-binding behavior, the interaction and arrangement of the catalytic modules and the dynamics of hydrolysis of crystalline cellulose need to be carried out in order to make cellulosomes suitable for commercial biomass conversion applications (Schwarz 2001).

2.2.2 Synergism

Long before the establishment of separation, purification and cloning methods to yield high purity cellulases, researchers recognized the fact that efficient hydrolysis of cellulose required a complex interacting collection of cellulases (Reese, et al. 1950; Wood 1968). The ability of two or more cellulases to work more effectively when added simultaneously rather than separately, in succession, is termed synergism (Irwin, et al. 1993; Walker, et al. 1993). A measure of synergism or the Degree of Synergistic Effect (DSE) is defined as the ratio of the activity of a cellulase mixture to the sum of activities of individual cellulases.

Mathematically, it is expressed as:

$$DSE = \frac{[RS]_{mix}}{\sum_{i}^{n}[RS]_i} \qquad (2.1)$$

where,

DSE = Degree of Synergistic Effect (dimensionless);

$[RS]_{mix}$ = Concentration of reducing sugars produced by hydrolysis by a mixture of enzymes (μM);

$[RS]_i$ = Concentration of reducing sugars produced by hydrolysis by individual enzymes (μM).

Some of the DSE values reported in literature have been listed in Table 2.4. While the DSEs of different cellulases measured under the same experimental conditions can be compared directly to gain insight on the synergizing ability of a given cellulase, comparison of DSE values obtained under different experimental conditions is

Table 2.4 Synergistic behavior observed in fungal and bacterial systems

Cellulases	Ratio	Substrate	DSE	References
T. reesei CBH I + EG I (exo-endo)	1:1	BMCC	2.8	(Henrissat, et al. 1985)
T. reesei CBH I + EG II (exo-endo)	1:1	BMCC	1.8	(Henrissat, et al. 1985)
T. reesei CBH I + EG II (exo-endo)	1:1	BMCC	1.5	(Henrissat, et al. 1985)
T. reesei CBH II + EG I (exo-endo)	1:4 1:1 4:1	BMCC	2.6 1.4 0.8	(Henrissat, et al. 1985)
T. fusca Cel5A + Cel9A (endo-endo)	1:3.3	Filter Paper	1.7	(Irwin, et al. 1993)
	1.11:1	BMCC	1.5	(Watson, et al. 2002)
T. fusca Cel6B + Cel9A	1:1	Filter Paper	1.9	(Irwin, et al. 1993)
(exo-endo)	1:4 1:1 4:1	BMCC	2.4 1.8 1.5	(Watson, et al. 2002)
T. fusca Cel6A + *T. reesei* CBH I (endo-exo cross synergism)	1:1 3:1	Avicel	1.6 1.9	(Bothwell, et al. 1993)
	1.6:1	Filter Paper	2.8	(Irwin, et al. 1993)
T. fusca Cel6B + *T. reesei* CBH I (exo-exo cross synergism)	0.25:1 1:1 3:1	Avicel	1.1 1.6 1.4	(Bothwell, et al. 1993)
	1:1	Filter Paper	2.5	(Irwin, et al. 1993)

questionable as it depends on several other factors which will be enumerated in the next section. The most popular and widely accepted model of synergy between endocellulases and exocellulases was developed by Eriksson et al. 1978 (Eriksson 1978; Wood and Mccrae 1978) to describe synergism observed with in fungal systems (Shoemaker, et al. 1983). They hypothesized that the endoglucanase preferentially attacks the cellulose crystal at its loosely packed 'amorphous' rEG Ions and creates chain ends for the exo acting cellobiohydrolases (CBHs). The CBH in turn releases cellobiose from the chains while β-glucosidase hydrolyzes the cellobiose to glucose.

It was also demonstrated that the same model was applicable to the synergistic behavior of bacterial cellulases and the existence of "cross-synergism" between bacterial and fungal systems has been documented (Bothwell, et al. 1993; Irwin, et al. 1993; Walker, et al. 1993). An underlying principle of this model for synergism is that substrate concentration is the limiting factor in hydrolysis for at least one enzyme. The presence of a complementary type of enzyme is considered to help overcome this limitation resulting in each enzyme stimulating the activity of the other (Tomme, et al. 1995a; Wilson 2004). Investigators have also observed synergism between exocellulases, namely between *T. reesei* CBH I and CBH II (Henrissat, et al. 1985; Nidetzky, et al. 1994). This type of synergy has been under question due to the disappearance of synergism observed between the CBH I and CBH II of *Penicillium pinophilum* after affinity purification of the mixture and its reappearance on the addition of small fraction of endocellulases (Wood, et al. 1989). However, *T. reesei* CBH I and CBH II purified using similar affinity purification have been known to display synergism on filter paper (Irwin, et al. 1993). These exoglucanases are considered to synergize due to their opposite stereospecificities, with one type attacking the cellulose chain from the reducing end and the other type attacking the chain from the non-reducing end.

2.2.3 Trichoderma reesei cellulases

Most commercial cellulase preparations are developed from the extracellular cellulases secreted by an isolate QM6a (Vinzant, et al. 2001) of the mesophilic filamentous fungus *Trichoderma reesei* owing to their high efficiency in degrading crystalline cellulose, coupled with cellulase production yields up to as much as 50-100g/l (Rabinovich 2006). The culture filtrate of *T. reesei* contains many cellulose degrading enzymes due to the existence of several isoenzymes and proteolytic fragments (Kubicek 1992). So far, seven *T. reesei* genes encoding cellulases have been cloned: Cel7A, an exocellulase or cellobiohydrolase, formerly CBH I, comprising roughly 60% of the supernatant; Cel6A, another exocellulase, formerly CBH II, comprising about 20% of the supernatant and five endocellulases Cel7B (EG I), Cel5A (EG II), Cel12A (EG III), Cel61A (EG IV), Cel45A (EG V) and two β-glucosidases which make up the rest of the culture fluid (Shoemaker, et al. 1983). Most *T. reesei* cellulases have a two domain structure with a catalytic domain and a cellulose binding module joined together by a highly glycosylated linker peptide (Kubicek 1992). CBH I and CBH II can achieve complete though slow hydrolysis of crystalline cellulose, even in the absence of endocellulases (Teeri 1997).

In order to identify and characterize the cellulolytic components of an organism, determination of the organization and regulation of the genes encoding them is essential (Tomme, et al. 1995a). Most of the cellulase genes cloned so far have been obtained from bacterial sources due to the relative ease of cloning of bacterial genes. Though bacteria produce cellulases at ten times lower yields compared to fungi, a major advantage of the former is their tenfold higher growth rates and their resistance to more severe growth conditions such as temperature and pH (Rabinovich 2006).

2.2.4 Cellulases of Thermobifida fusca

Thermobifida fusca YX (formerly *Thermomonospora fusca*) is a thermophilic soil bacterium belonging to the order *Actinomycetales*. It is a filamentous aerobe that degrades cellulose and hemicellulose. It is usually found in heated plant residues such as compost piles, decaying hay, manure heaps and paper mill waste with its optimum temperature for growth ranging from 48°C to 55°C (Wilson 2004). The culture supernatant of *T. fusca* YX contains a very active protease which hinders protein purification studies by creating multiple isozymes (Gusek, et al. 1988). This issue was overcome by isolation of a stable mutant of *T. fusca* named ER-1 which secreted the quantity of cellulases as the wild-type but lacked the protease (Wilson 1988). The extracellular crude cellulase mixture from ER-1 has been purified and characterized and is now known to contain six different cellulases, two small cellulose binding modules and a xylanase (Calza, et al. 1985; Irwin, et al. 1993). An intracellular β-glucosidase and an extracellular xyloglucanase have also been isolated and characterized (Irwin, et al. 2003; Spiridonov and Wilson 2001).

The biosynthesis of *T. fusca* cellulases has been shown to be induced by the presence of cellobiose and repressed by readily metabolized carbon sources such as glucose and cellobiose, in the growth medium (Lin and Wilson 1987). A study of the levels of individual enzymes produced by *T. fusca* on different carbon sources such as Solka Floc, ground grass, CMC, cellobiose, xylose and glucose showed that the lowest level of cellulase was synthesized on xylose as the carbon source while the highest level was synthesized in cultures grown on microcrystalline cellulose, Solka Floc (Spiridonov and Wilson 1998). The six cellulases secreted by *T. fusca* are Cel9B (formerly E1), Cel6A (E2), Cel6B (E3), Cel9A (E4), Cel5A (E5) and Cel48A (E6). In order to better understand the different modes of action of these six cellulases, it is interesting to study and compare a classical

exocellulase (Cel6B) and the unique processive endocellulase (Cel9A). Listed in Table 2.5 are the properties of these three *T.fusca* cellulases.

The catalytic domains of *T. fusca* cellulases belong to four different structural families namely 9, 6, 5 and 48. Cel6A, an endocellulase and Cel6B, an exocellulase belong to the same structural family. Similarly, Cel9A is a new type of 'processive' endocellulase while Cel9B is a classical endocellulases and they belong to the same structural family. Since all six of the *T. fusca* cellulases have very different characteristics, it is believed that they have been derived from different organisms rather than having formed as a result of gene duplication (Wilson 2004). A mesophilic bacterium, *Cellulomonas fimi*, has a remarkably similar set of six glycosyl hydrolases as *T. fusca*, belonging to the same catalytic and cellulose binding module families and exhibiting very similar activity. The major difference between them is that their family 2 CBMs are located at different ends for all but one of their six cellulases.

2.2.5 T. fusca Cel5A

Cel5A (EC 3.2.1.4) is a 46.3 kDa classical endocellulase as indicated by its high CMC activity (Table 2.5). It is made up of a family 5 CD joined to a family 2 CBM by a short peptide linker. The X-ray crystal structure of a mutant (Glu355Gln) of its catalytic domain in complex with cellotetraose has been determined at 1.77 Å recently (Berglund, et al. 2007) when the cellulase was expressed in Bacillus subtilis and is shown in Fig 2.5. Studies on fragments of Cel5A obtained by proteolysis have revealed that its 14 kDa family 2 CBM was located on its N-terminus (Mcginnis and Wilson 1993). Cel5A by itself has low activity on crystalline substrates such as BMCC (Watson, et al. 2002). However, very small quantities of it in combination with processive cellulases like Cel6B or Cel9A lead to very high synergistic action on BMCC (Watson, et al. 2002). Binding of Cel5A to BMCC has been found to be

Table 2.5 *T. fusca* Cel5A, Cel6B and Cel9A characteristics (Wilson 2004)

Specie	Mode of action/ Mechanism	MW (kDa)	Iso-electric Point (pI)	CD family / CBM family	Specific Activity (μmole cellobiose / min / μmole cellulase)			
					CMC	SC	FP	BMCC
Cel5A (E_5)	Endo/ Retaining	46.3	4.5	5 / II	2840	90.4	0.83	15
Cel6B (E_3)	Exo/ Inverting	59.6	3.1	6 / II	0.30	1.50	0.13	2
Cel9A (E_4)	Endo/ Inverting	90.4	3.6	9 / II, IIIc	475	202	1.03	19.1

irreversible (Bothwell, et al. 1997b).

2.2.6 T. fusca Cel6B

Cel6B (EC 3.2.1.91) is a 59.6 kDa classical exocellulase which has low activity on CMC (Table 2.5). Based on the high ratio of soluble to insoluble reducing sugars obtained by incubation of filter paper with Cel6B, it is known to be a processive exocellulase (Irwin, et al. 1993). It shows optimum catalytic activity at 50°C and pH 7 (Wilson 1988; Zhang, et al. 1995). Cel6B has been shown to attack cellulose chains from the non-reducing end (Barr, et al. 1996). The Cel6B gene has been successfully cloned into, sequenced and over-expressed in *Streptomyces lividans* and *Eschericia coli* (Zhang, et al. 1995). The C-terminal family 6 CD made up of 423 amino acids, accounts for 46 kDa of its molecular weight and is linked to an N-terminal family 2 CBM by a proline-serine rich linker peptide (Zhang, et al. 1995). The linker has been found to be lightly glycosylated, containing about 5% sugars (Wilson 1988), though the structural or functional purpose of the sugar content is still not very clear (Zhang, et al. 1995). By itself, Cel6B also has very low activity on most substrates, however, in conjunction with endocellulases or with a reducing-end directed exocellulase it shows a high degree of synergistic effect.

Though the crystal structure of *T. fusca* Cel6B is not available to date, the detailed three-dimensional structures have been obtained for *T. fusca* Cel6A (an endocellulase) (Spezio, et al. 1993), *Trichoderma reesei Cel6A* (formerly CBH II, an exocellulase) (Rouvinen, et al. 1990) and Cel6A from *Humicola insolens* (an exocellulases) (Varrot, et al. 1999). Besides sequence similarities, the three structures enclosed in a tunnel covered by two loops while the active site of the endocellulase was found to have very short loops leading to a more open active site structure

Figure 2.5: X-Ray crystal structure of the catalytic domain of *T. fusca* Cel5A (E5) E355Q in complex with cellotetraose (Berglund, et al. 2007)

share similar topologies and have certain conserved amino acid residues located close to their active sites. The active site of both exocellulases have been found to be (Rouvinen, et al. 1990; Spezio, et al. 1993; Varrot, et al. 1999)

The catalytic residues of *T. fusca* Cel6B were believed to be Asp274 as the catalytic acid and Asp226 as the catalytic base based on sequence and functional similarity with *T.reesei* Cel6A (Zhang, et al. 2000). By conducting site-directed mutation studies, Zhang et al. 2000 examined the roles of pertinent non-catalytic residues in and near the active site. Mutations in aromatic residues Trp 331, Trp332 and His326 were found to significantly decrease activity on crystalline substrates, specifically on BMCC. The flexibility of the loops forming the tunnel in the active site was found to have significance in the activity of the exocellulase on crystalline substrates. Certain mutations which were chosen with the aim of increasing its thermostability were found not to improve it beyond that of the wild type Cel6B (Zhang, et al. 2000). However recent site-directed mutagenesis and kinetics studies show that while Asp 274 is the catalytic acid, mutation of the highly conserved, putative catalytic base residues Asp226, Asp497 and Glu495, as well as Ser232 and Tyr220 revealed the absence of a single identifiable catalytic base residue (Vuong and Wilson 2009).

2.2.7 T. fusca Cel9A

Cel9A (EC 3.2.1.4) is a unique 90.4 kDa cellulase which exhibits the characteristics of an endocellulase as well as those of an exocellulase (Irwin, et al. 1993). Of all the *T. fusca* cellulases it has the highest individual activity on crystalline cellulose and it also has relatively high activity on soluble CMC. It produces a majority of soluble oligosaccharides (about 87%) from filter paper; typically only exocellulases release as much as 90% or more soluble reducing sugars while

endocellulases usually release into solution only 60-70 % of the reducing ends they produce, with about 30-40% remaining on the insoluble substrate (Irwin, et al. 1993). Another unusual characteristic of Cel9A is that it shows synergism with endocellulases as well as both types of exocellulases (Irwin, et al. 1993), while classical endocellulases do not synergize with other endocellulases. Cel9A retains greater than 70% of its activity between pH 4.7 and pH 10.1 (Irwin, et al. 1998). Structurally, Cel9A is made up of four domains; a 51.4 kDa N terminal family 9 catalytic domain, a family 3c cellulose binding module, a fibronectin-like Pr/Ser/Thr rich linker and a family 2 cellulose binding module at the C-terminus (Irwin, et al. 1998).

The Cel9A CD and the family 3c CBM are homologous to the CelD domain and the scaffoldin CBM from *Clostridium thermocellum*, respectively (Sakon, et al. 1997). Limited proteolysis of Cel9A produces a 68 kDa fragment containing the CD and the family 3c CBM (Irwin, et al. 1998). The crystal structure of this fragment has been determined by X-ray crystallography at 1.9 Å resolution (Sakon, et al. 1997) and has been shown in Figure 2.6. The CD is made of an $(\alpha/\alpha)_6$ barrel fold and is rigidly attached to the CBM 3c which consists of an antiparallel β-sandwich fold. These two domains interact in two loop rEG Ions. A shallow cleft runs through the CD and forms the substrate binding site. At one end, the cleft is blocked by a loop of residues while at the other end it merges and is aligned with the flat face of the family 3c CBM (Sakon, et al. 1997). In order to study the interactions between the substrate and key residues in the active site, the crystal structure of Cel9A-68 was also determined with soluble oligosaccharides liganded to the active site (Sakon, et al. 1997). Comparison of the structure of Cel9A soaked with oligosaccharides with that of free Cel9A allowed observation of the catalytic water molecule in the free structure and revealed the conformational changes that occurred on substrate binding. With the help of these

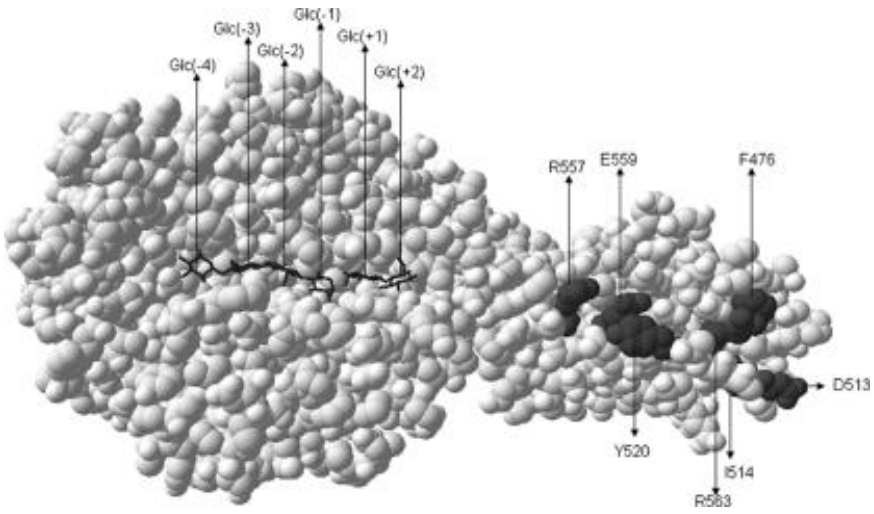

Figure 2.6 Space-filled structure of Cel9A-68 (4TF4) with six glucose molecules in the catalytic cleft. Enzyme product structure was obtained after soaking the crystals in cellopentaose (Li, et al. 2007).

enzyme-oligosaccharide complexes the active site was identified and the locations of six glycosyl binding sites numbered -4,-3,-2,-1,+1,+2 from the non-reducing end to the reducing end were established. Glu 424 was found to be the catalytic acid while the catalytic base was considered to be formed by the coordinated action of Asp55 and Asp58 (Zhou, et al. 2004).

Sakon et al. (1997) hypothesized that the flat face of the CBM, consisting of a strip of conserved polar residues bound to three adjacent cellulose chains, with the CD feeding the central chain into its active site cleft. After hydrolytic cleavage of the glucosidic bond, the weakly held product would diffuse into solution while the cellulase would still be held onto the crystalline cellulose by the CBM. The cellulase would then move processively on the cellulose strands, with the active site determining the position which would lead to cleavage of cellotetraose units. A Tyr206Ser mutant studied by Zhou et al. (2004) showed very poor activity with almost no processivity leading the investigators to hypothesize that a charged network formed between Tyr206, Asp55, Glc(-1)01, Asp58 and His125 was responsible for catalytic activity. Studies by Li et al. (2007) have proved this hypothesis to be true and have confirmed that Asp58 is the catalytic acid while Asp55 appears to be an integral supporting residue. The family 3c CBM has been considered important for Cel9A's processivity as well as binding behavior (Irwin, et al. 1998). However Li et al. (2007) found that mutations of key residues in the family 3c CBM did not interfere with the cellulase's processivity while mutations introduced in the CD caused significant decline in processivity, leading the authors to postulate that processivity is primarily controlled by equilibrium binding of the CD.

2.3 Cellulose Hydrolysis

Cellulose hydrolysis is a heterogeneous reaction system in which an insoluble porous substrate is degraded by an ensemble of soluble enzymes. Early investigators have attempted to describe the cellulase-cellulose reaction system using Michaelis Menten kinetics (Howell and Stuck 1975; Huang 1975; Okazaki and Mooyoung 1978) by assuming a state of dynamic equilibrium between the enzyme, the substrate, the enzyme-substrate complex and the products. However, the Michaelis-Menten model is valid, only for homogeneous reaction systems. The fundamental premise of this model is the pseudo-steady-state assumption which implies that the concentration of the enzyme-substrate complex is constant over time. While this holds for enzyme-substrate complexes in solution it fails for biphasic systems (Bothwell et al. 1997a, Lynd, et al. 2002). Results of such kinetic models cannot be expected to accurately describe insoluble cellulose hydrolysis since the latter has macroscopic properties which continuously change as the hydrolysis reaction proceeds thereby inherently affecting the rate of hydrolysis.

Factors affecting the reaction kinetics of the hydrolysis of cellulose can be grouped under the following subheadings:

1. the structural features of cellulose such as crystallinity and accessible surface area;
2. the binding behavior of the cellulases in the system -- formation of cellulase-cellulose reaction intermediate complex, productive and non-productive adsorption , and desorption;
3. the nature of the cellulase system used -- its composition in terms of endocellulases, exocellulases and β-glucosidases and the synergistic interactions of the component cellulases;

4. product inhibition of cellulases by soluble end products such as cellobiose and inactivation of adsorbed cellulases over time;
5. mass transfer considerations such as bulk diffusion of cellulases, two-dimensional diffusion or surface mobility of cellulases and internal resistance to cellulase diffusion in pores.

Some of these factors which are relevant to the present study are addressed in detail in this literature review.

2.3.1 Effects of physical properties of cellulose

One of the early investigations that focused attention on the effects of the structural features of cellulose on its enzymatic hydrolysis was conducted by Fan et al. (1980). They attempted to experimentally determine the specific surface area (SSA) and crystallinity indices of three types of pure cellulosic substrates and to observe how these parameters affected and were affected by the rate of hydrolysis. They used the nitrogen adsorption technique to measure the SSA and powder X-ray diffraction to measure the crystallinity of cellulose, performing ball milling to obtain substrates with different crystallinity indices. The authors reported that the SSA increased during the course of hydrolysis but they did not find any direct correlation between the extent of hydrolysis and the SSA. Hence the increase in SSA with time did address the issue of whether the cellulose became more accessible to cellulases leading to a favorable condition for extended hydrolysis times. However, in a similar study following the above work Lee and Fan (1982) analyzed the initial reaction rates of cellulose hydrolysis, and derived an empirical relationship for the formation of the enzyme substrate complex as a linear function of the SSA.

$$(ES)_o = a + b\,(SSA)_o \qquad (2.2)$$

where,

$(ES)_o$ = initial apparent extent of enzyme adsorption (g / L),

a and b = linear parameters to be determined by linear regression of data, a (g/L), b (g^2/L)

$(SSA)_o$ = initial specific surface area of the substrate (m^2/g).

The initial specific surface area was found to increase drastically from 3.9 m^2/g to 27 m^2/g corresponding to a change in initial hydrolysis rates from 9g/l-h to 13g/l-h. When examining the effect of crystallinity, Fan et al. (1980) observed that the glucose production at 8 hrs decreased linearly with an increase in CrI of the cellulosic substrate and based on experimental data derived the following empirical expression relating CrI to the extent of cellulase adsorption:

$$k_o = \alpha - \beta (CrI)_o \qquad (2.3)$$

where,

k_o = effectiveness of the initial extent of soluble protein adsorption (%),

α and β = linear parameters to be determined by linear regression of data (dimensionless),

$(CrI)_o$ = initial crystallinity index of the substrate (%).

Initial crystallinity index values were found to be 37.5 % at initial hydrolysis rates of 20g/l-h and increased to 77% at low initial rates of around 4.9 g/l-h. However they also found only a 6 % increase in cellulose crystallinity during the course of 96 h of hydrolysis which lead them to conclude that factors other than crystallinity were responsible for the decrease in hydrolysis rate with time. Hence, increasing SSA favored cellulase binding and initial hydrolysis rates while CrI seemed to inhibit hydrolysis leading to a gradual decrease in the overall extent of hydrolysis.

Based on the results of these experiments, Fan and Lee (1983) developed a mechanistic model describing the relationship between crystallinity, specific surface area and the hydrolysis rate. They also accounted for the fall in reaction rate over time by incorporating product inhibition by cellobiose and glucose. The final expression of their model was as follows:

$$R = \frac{d(P)}{dt} = \frac{d(S)}{0.9dt} = k_o \phi (ES)^e \tag{2.4}$$

$$= k_o \left[1 - \left[\frac{(S)_o - (S)}{(S)_o} \right]^n \right] \left[\frac{(ES)_o}{(S)_o}(S) \right] \left[1 - k_{P_1}(P_1) \right] \left[e^{-k_{P_2}(P_2)} \right] \tag{2.5}$$

where,

R = apparent hydrolysis rate (g/L/h^{-1}),

$\frac{d(P)}{dt}$ = rate of product formation (g/L/h),

k_o = effectiveness of adsorbed soluble protein to promote hydrolysis (h^{-1}),

ϕ = relative digestibility of residual cellulose determined experimentally,

$(ES)^e$ = effective portion of the apparent extent of soluble protein adsorption (g/L),

$(S)_o$ = =initial substrate concentration, (g/L),

(S) = cellulose concentration (g/L),

$(ES)_o$ = initial extent of soluble enzyme adsorption (g/L),

n = dimensionless parameter for the structural transformation of cellulose,

k_{P1}, k_{P2} = constants (L/g),

P_1 = glucose concentration (g/L),

P_2 = cellobiose concentration (g/L).

Fan and Lee (1983) appear to have adopted a realistic approach towards the cellulase-cellulose system by studying the structural changes in the solid phase as well as the concentration changes in liquid phase. However, their study had several significant drawbacks. They employed crude *Trichoderma reesei* culture filtrate which contains many different cellulases with varying modes of action on cellulose. The combined behavior of these components is much more complex than that of single enzyme acting on a heterogeneous substrate (Woodward 1991). The use of the nitrogen adsorption technique to measure SSA deserves scrutiny. The size of cellulase molecules is about 50-100 kDa while that of a nitrogen molecule is only 28 daltons. This implies that the nitrogen molecules would diffuse into pores which would be inaccessible to cellulase molecules. The nitrogen adsorption method also requires drying of cellulose which causes collapse of the pore structure leading to underestimation of the pore volume (Grethlein 1985).

Grethlein (1985) used a solute exclusion technique to estimate the influence of pore size distribution on the rate of enzymatic hydrolysis. The use of hydrated dextran solutes whose size is comparable to that of cellulase molecules, provides a much more convincing measure of the accessibility of cellulases to cellulose. Grethlein (1985) assumed a geometric model of the substrate, considering the 'pores' in the cell wall to be made up of parallel slits between multiple lamellae. Thus the model surface was made up of parallel plates separated by pores of different widths, which would exclude polymeric probes of different sizes. The following equation was applied to estimate surface area of this substrate model:

$$\Delta A = \frac{2\Delta V}{\omega} \qquad (2.6)$$

where:

ΔA = incremental surface area (m^2/g),

ΔV = incremental pore volume (m^3/g),

w = average pore width (m)

The SSA could then be calculated by plotting the total inaccessible pore volume as a function of the molecular probe diameters. Adopting this methodology Grethlein (1985) found a positive linear correlation between the SSA and the extent of hydrolysis, in stark contrast with the results of Fan and Lee (1983). Hence a proper technique to measure the substrate's SSA needs to be used before concluding whether SSA affects cellulose hydrolysis. One aspect to be noted regarding specific surface area measured in terms of the pore volume is that it is assumed that the external surface area of the substrate is negligible. However, adsorption in the initial stages for non saturating enzyme concentrations and at short reaction times, takes place on the external surface of cellulose. Hence to capture initial reaction kinetics, techniques to measure surface adsorption of cellulases are essential.

2.3.2 Binding behavior of cellulases

The adsorption of cellulases to cellulose is the step that establishes contact between the enzyme and the substrate and hence is considered the prerequisite to hydrolytic activity. The classical Langmuir theory for gas adsorption has been found applicable to adsorption from solution, provided the solution is sufficiently dilute (Adamson 1983). It is expressed as follows:

$$E_b = \frac{E_{b,m} K_a E_f}{1 + K_a E_f} \tag{2.7}$$

where:

E_b is the bound enzyme concentration (μmol/g)

$E_{b,m}$ is the adsorptive capacity of the substrate (μmol/g)

E_f is the free enzyme concentration (μmol/L)

E_t is the total enzyme concentration (μmol/L)

K_a is the association constant (L/μmol)

The basic assumptions of the classical Langmuir isotherm are:

1. adsorption takes place as a monolayer and that the energy of the adsorbed species is equal over the entire surface;
2. the surface is homogeneous, implying that only one type of binding site is present;
3. the adsorption of one molecule does not affect the adsorption energy of the other molecules (there are no lateral interactions or cooperativity);
4. only one type of adsorption species is present;
5. the solution is dilute; and
6. the adsorption is completely reversible and the rates of adsorption and desorption are at equilibrium.

Several investigators have found that this model provides very good fits to the experimental adsorption data of cellulase acting on cellulose (Beldman, et al. 1987; Converse and Girard 1992; Gilkes, et al. 1992; Hoshino, et al. 1992; Kim, et al. 1992; Stahlberg, et al. 1991; Woodward, et al. 1988a; Bothwell et al. 1997a, Jung et al. 2002). It is simple and widely used mainly because the interpretation of its parameters is straightforward.

2.3.2.1 Binding studies with crude cellulase preparations

Lee et al. (1982) and Ooshima et al. (1983) conducted studies investigating how the adsorption behavior of cellulases was affected by the physical properties of the substrate. Ooshima et al. (1983) employed a commercial enzyme preparation from *Trichoderma viride* and used Avicel as substrate. They prepared cellulose samples of varying crystallinity by partially pre-hydrolyzing Avicel with cellulase for various

reaction times. The adsorption behavior of the *T. viride* cellulase was compared with that of bovine serum albumin (BSA). BSA did not adsorb to cellulose so they concluded that the binding of cellulases was specific. They applied the Langmuir isotherm and found that the maximum binding capacity decreased while the adsorption equilibrium constant increased with increasing crystallinity. According to the Langmuir theory, $E_{b,m}$ must be independent of temperature but Ooshima et al.(1983) found the $E_{b,m}$ decreased linearly with increasing temperature. They measured CMC activity to determine the endocellulase content of their enzyme mixture but they did not have any direct measure for the exocellulase or the β-glucosidase present in the mixture. Using their limited capabilities for enzyme differentiation and quantification they concluded that CMCases (endocellulases) have a greater tendency to adsorb at lower temperatures while Avicelases (exocellulases) adsorb more at higher temperatures.

Building on the hypothesis that the adsorption behavior of cellulases would provide significant clues to the mechanism of synergistic hydrolysis Ryu et al. (1984) used the culture filtrate from *T. reesei* on Avicel and two varieties of Solka Floc to characterize adsorption kinetics. Ryu et al. (1984) also employed CMC activity and filter paper (FP) activity to differentiate between endocellulases and exocellulases respectively. In order to determine the effect of addition of a type of cellulase to a reaction mixture, they supplemented crude cellulase after 1 h with either cellobiohydrolase (CBH) or endoglucanase (EG). Addition of CBH as the supplement caused the CMC activity of the free solution to increase immediately and significantly. Similarly, addition of endoglucanase to the reaction mixture caused the FP activity in the bulk solution to increase. This phenomenon was observed on all three substrates tested and led the authors to conclude that the two types of cellulases were competing with each other to adsorb to common binding sites on the substrate, with the degree of

competitiveness depending on the adsorbent properties. On the basis of their experimental results, Ryu et al. (1984) proposed a mechanistic model with the following steps; that CBH competed with EG bound to its own active sites on cellulose, EGs randomly adsorbed, cleaved bonds and desorbed and the presence of CBHs and EGs simultaneously resulted in a coordinated competitive adsorption pattern that led to enhanced hydrolysis activity.

The validity of the results obtained by Ryu et al. (1984) results is questionable due to the fact that they partially purified their culture filtrate and selected two out of the four fractions obtained by ion-exchange chromatography based on each having either predominant FP activity and very little CMC activity or vice-versa without providing any numbers regarding what amount of activity distinguished the terms "predominant" and "little". This implies that even their purified components were basically mixtures of the endocellulases and CBHs at different ratios. It has been pointed out that the ratios of the individual components play a crucial role in synergism (Baker, et al. 1998; Henrissat, et al. 1985; Jeoh, et al. 2002; Nidetzky and Claessens 1994; Walker, et al. 1993; Watson, et al. 2002; Woodward, et al. 1988a; Woodward, et al. 1988b). Hence the reliability of Ryu et al. (1984)'s data is highly questionable.

2.3.2.2 Binding studies with purified cellulases

A substantial improvement in the purity of cellulase components used to investigate cellulase kinetics was obtained in the late 1970s and 1980s. Beldman et al. (1987) were one of the first who succeeded in purifying four endocellulases and two exocellulases from *T. viride* crude and to study cellulase adsorption (Beldman, et al. 1987) as well as synergism (Beldman, et al. 1988). The most significant results of their work were:

1. The DSE was a function of the ratio of enzymes since they found that the maximum DSE occurred at much lower endocellulase to exocellulase ratio for one combination of endo- and exocellulases as compared to another combination. The authors believed that the optimum DSE dependence on cellulase molar ratio was more due to the individual adsorption behavior rather than the specific activity of the individual cellulases.
2. The DSE was a function of the nature of the substrate based on the low degree of synergism observed on amorphous phosphoric acid swollen cellulose as compared to those observed on Avicel using the same combination of endo- and exocellulases on the two substrates.

Though this was the first study to examine the effect of mole ratios on DSE, a major drawback of the work is that they recombined the pure components by keeping the endocellulase concentration fixed without maintaining a fixed total cellulase molar concentration. Since it has been shown (Wood and Bhat 1988; Woodward, et al. 1988a) that the DSE is a function of the total cellulase molar loading, it is imperative that the total cellulase concentration be fixed in order to observe any effects due to the binding of individual cellulases.

The question of the reversibility and competition in cellulase adsorption was addressed by Kyriacou et al. (1988) who used radioactive labeling of different purified cellulase components, EG I, EG II, EG III and CBH I of *T. reesei* to overcome the uncertainties involved in quantification based on activity measurements. Adsorption experiments were conducted at 5°C and equilibrium exchange between bound and free cellulases was demonstrated. On simultaneous addition, 2.5 times more CBH I was found to adsorb compared to EG I. On sequential addition, when CBH I was added first and allowed to reach equilibrium followed by EG I, CBH I bound to its maximum binding capacity while EG I bound only to 26% of its maximum capacity. However,

when EG I was added first it bound to 87 % of its maximum capacity and CBH I when added sequentially bound to 92% of its capacity. CBH I and to a lesser extent EG I competed with EG II and EG III in similar experiments.

At 50°C very little competition was observed between the endoglucanases but the extent of CBH I adsorption was close to its saturation. The predominance in the adsorption of CBH I over the EGs at both temperatures led the authors to conclude that competitive adsorption of the individual components had a strong influence on the hydrolytic mechanism. Though the authors have measured the adsorption behavior of the individual cellulases in binary mixtures, they did not provded any correlation between the adsorption data and the hydrolysis data for conclusive proof that competitive adsorption leads to synergistic hydrolysis.

The Langmuir adsorption isotherm has been applied to describe the equilibrium binding of *T. fusca* Cel5A, Cel6B, Cel9A, Cel6B binding module and *T. reesei* CBH I to two different substrates, Avicel and BMCC by Bothwell et al. (1997a). The maximum adsorptive capacities and the association constants they obtained are shown in Table 2.6. They observed that the maximum adsorption capacities ($E_{b,m}$) for all the cellulases and for the binding domain were 9-30 fold higher on BMCC than on Avicel and concluded that this was due to the enzymes finding more accessible sites on BMCC than on Avicel. The association constants for all the cellulases and binding domain were different for the two substrates but did not reveal any obvious trend in affinity. A power relationship was found to exist between the molecular weights of the *T. fusca* cellulases and their maximum adsorptive capacities for both substrates. This led the authors to point out that the binding capacities were not only a function of the substrate accessibility but also of the size of the cellulase in question. However, the behavior of CBH I did not comply with the same power relationship with respect to molecular weight and had a lower $E_{b,m}$ on

Avicel as well as BMCC despite having the lowest molecular weight. This implied that the binding mechanisms for fungal and bacterial cellulases could be inherently different, probably due to the difference in their binding domains.

Bothwell et al. (1997) acknowledged that their binding data had some inherent error correlation associated with the cellulase quantification technique which led to an increase in the standard deviation of sample measurements with increasing total cellulase concentration. Dilution of samples to ensure that the absorbance at 280 nm was within the linear range for protein concentration measurements was found to be responsible for this error. Hence though adsorption saturation was validated by at least three data points, the magnitude of the error bars on bound cellulase concentration values raises the possibility of the $E_{b,m}$ not being accurately determined.

An important feature that must be considered when evaluating cellulase adsorption is its modular two domain structure. Each domain has its own binding behavior and when combined by the linker peptide, the two act in concert to lead to the observed intact cellulase adsorption. In order to better understand the contributions of the individual domains to the overall binding trends, Jung et al. (2002a, 2002b, 2003) determined how the binding of the CBD and the CD compared with the binding of the intact enzyme for *T. fusca* Cel5A, Cel6B and Cel48A (reducing end attacking exocellulase). Jung et al. (2002) hypothesized that the CBMs appeared to first bind to the easily accessible surface and once this was saturated they penetrated the surface in the interstices. A model was developed comprising of three submodels to describe the three regions in the binding behavior, as follows:

Langmuir binding:
$$f_1(x) = \frac{\beta_{01} x}{1 + \beta_{11} x} \tag{2.8}$$

Table 2.6 Langmuir constants obtained by Bothwell et al. (1997a)

Cellulase Species	Avicel PH102 (40g/l)		BMCC (1g/l)	
	$E_{b,max}$ (μmol/g)	K_m (l/μmol)	$E_{b,max}$ (μmol/g)	K_m (l/μmol)
Cel6B	0.40	0.20	11.4	0.10
Cel6B CBM	1.77	0.182	16.5	0.124
Cel9A	0.34	0.077	9.7	0.044
Cel5A	0.67	0.22	12.0	0.13
CBH I	0.48	0.09	4.6	0.28

Interstice Penetration: $$f_2(x) = \max\left(\frac{\beta_{01}}{1+\beta_{11}}, \beta_{02} + \beta_{12}x\right) \quad (2.9)$$

Interstice Saturation: $$f_3(x) = \min\left(\max\left(\frac{\beta_{01}}{1+\beta_{11}x}, \beta_{02} + \beta_{12}x\right), \beta_{03}\right) \quad (2.10)$$

where :

$f_i(x)$ = bound CBM concn in μmol/g substrate

x = free CBM concn. in μmol/L

Complete reversibility was found to occur for the CBMs only in the Langmuir rEG Ion while irreversibility in the Interstice penetration and Interstice Saturation rEG Ions of the isotherm were considered to be a result of entrapment in the pores. Jung et al. (2002) found that the binding affinity of the CBMs increased at lower temperature and that Cel5A CBM had lower affinity than the two exocellulase CBMs. At 5°C all three CDs were found to bind rapidly but they desorbed with the progress of the reaction due to loss of binding sites. At the same temperature, the endo CD was found to bind 1.5-4 times as much as the exo-CDs. A two-substrate model developed by Nidetzky & Steiner (1993) was applied to account for binding to an easily hydrolysable fraction as follows:

$$E_b = E_1 \exp(-k_d t) + E_2 \quad (2.11)$$

where:

E_b = total bound enzyme, μmol/g,

E_1 = is the initially bound enzyme to easily hydrolysable fraction of the substrate, μmol/g,

E_2 = the bound enzyme to recalcitrant fraction of the substrate μmol/g,

k_d = the first-order desorption constant, h^{-1},

t = reaction time, h.

The endo-CD was found to saturate the easily hydrolyazable fraction (EHF) first and then bind to the recalcitrant fraction (RF) as a function of remaining concentration. The exo-CDs were found to partition between the EHF and the RF at a constant ratio. Hydrolysis by the endo-CD at 5°C was found to level off with increase in concentration but was found to increase for the exo-CDs. Cellobiose was found to inhibit binding for all three CDs and most strongly for the Cel6B CD. At 50°C an interesting phenomenon was observed: CDs of Cel5A and Cel48A showed an increase in the binding corresponding to the percent conversion of BMCC while CD Cel6B showed a decrease in binding. The methods employed to measure the binding behavior failed to provide an insight into the reason for this unexpected behavior of the Cel6B CD.

Intact Cel5A, Cel6B, Cel48A bound irreversibly to the BMCC at 5°C and it was suggested that this could be due to the irreversible binding of the CDs at this temperature. At 50°C intact Cel5A and Cel48A showed lower binding than their CBM while Cel6B exhibited higher binding than either of its domains. One problem with the binding data of Jung et al. (2002a, 2002b, 2003) is that they present their bound cellulase per amount of initial substrate as opposed to per amount of residual substrate. While their quantification works well for the non-hydrolytic activity of CBMs at 5°C, it fails to capture the dynamic changes in the substrate quantity with the progress of the reaction in the case of CDs and intact cellulases, especially at 50°C where degradation rapidly changes the residual amount of substrate which significantly affects the amount of enzyme bound to it.

Though all the above studies, and several others, have used the Langmuir isotherm to describe the binding behavior of cellulases, the physical significance of parameters obtained from it is questionable since there has been growing evidence that the cellulase-cellulose system does not satisfy some of the key assumptions namely;

the existence of more than one type of binding site has been predicted (Jung, et al. 2002; Linder and Teeri 1997; Medve, et al. 1997; Medve, et al. 1998); the adsorption of cellulases of one type would affect the adsorption behavior of other cellulases (Jeoh, et al. 2002); the presence of more than one type of species in cellulase systems with varying affinities for cellulose (Ooshima, et al. 1983; Jeoh, et al. 2002) and the complete or partial irreversibility of cellulase adsorption (Beldman, et al. 1987; Jung and Walker 2003; Kyriacou, et al. 1989; Palonen, et al. 1999).

The binding study conducted by Bothwell et al. (1997a) showed that the binding capacities for *T. fusca* Cel5A, Cel6B and Cel9A were 18-30 times higher on BMCC than on Avicel. In order to explore the effect of substrate accessibility on the extent of conversion and on synergism, Watson et al. (2002) tested three binary cellulase mixtures of *T. fusca* Cel5A, Cel6B and Cel9A over a range of cellulase molar ratios and total molar cellulase concentrations on BMCC and Avicel. Watson et al. (2002) observed that the maximum DSE and the greatest sensitivity of DSE to the cellulase mole fractions occurred at the lowest total enzyme to substrate (E/S) ratio. Cel9A, which has the lowest binding capacity on BMCC was found to achieve the highest extent of conversion on BMCC while Cel5A which has the highest binding capacity on BMCC had the lowest extent of conversion. In order to obtain 80% conversion, about 500 nmol/g of the Cel9A+Cel6B mixture was required while the Cel6B+Cel5A and Cel9A+Cel5A mixtures required 1500 nmol/g and 1250 nmol/g respectively. While Watson et al. (2002) established the relationship between enzyme-substrate loading, varying mole ratios and the extent of conversion in binary mixtures, they did not look at the extent of binding of the cellulase components in the binary mixtures. Jeoh et al. (2002) sought to answer the question of whether the observed synergism in hydrolysis in binary mixtures was a result of differential binding in mixtures. Jeoh et al. (2002) established a fluorescence based quantification

technique to measure bound concentrations in individual and binary mixture reactions of *T. fusca* Cel5A, Cel6B and Cel9A on BMCC. They observed that at 5ºC, the binding extents of cellulases in mixture reactions were only 22-70% of their binding in individual reactions. At 5ºC the extents of conversion were less than 1.5% for all reactions studied and the DSE < 1 indicating anti-synergistic hydrolysis at this temperature. The Degree of Synergistic Binding (DSB) was defined by Jeoh et al. (2002) as:

$$DSB = \frac{\dfrac{E_{b,mix}}{S_{res,mix}}}{\displaystyle\sum_{i=1}^{3}\left[\frac{E_{b,individual}}{S_{res,individual}}\right]} \tag{2.12}$$

where:

DSB = degree of synergistic binding (dimensionless)

$E_{b,mix}$ = bound concentration of enzyme in the mixture (μM)

$S_{res,mix}$ = concentration of residual BMCC in the mixture (g/L)

$[E_{b,individual}]_i$ = bound concentration of enzyme *i* when acting individually (μM)

$[S_{res,individual}]_i$ = concentration of residual BMCC in the individual component reaction (g/L)

The anti-synergistic mixtures were found to have DSB < 1. The largest reduction in binding was observed for Cel5A, in the mixture of Cel5A+Cel9A and the mixture of Cel5A+Cel6B. The binding levels of Cel6B were unaffected by the presence of Cel9A in the mixture of Cel6B+Cel9A. At 50 ºC, the same three binary mixtures achieved extents of conversion of the order of 10-12% and DSE > 1. At this temperature, the cellulases in mixtures bound up to 40-126% higher extents compared to their binding in individual reactions. Jeoh et al. (2002) concluded that the lower

extents of binding at 5ºC resulted from a competition for binding sites between cellulases in binary mixtures while the enhanced extents of binding observed at 50ºC were due to cooperative binding between them at this temperature.

In a subsequent study, Jeoh et al. (2006) examined the effect of varying molar ratios in binary mixtures of *T.fusca* Cel5A, Cel6B and Cel9A and the recalcitrance of BMCC on the DSE and the DSB. BMCC was exhaustively hydrolyzed by the CD of *T.fusca* Cel5A to produce a recalcitrant form of BMCC referred to as pre-hydrolyzed BMCC (PHBMCC). DSE was found to be sensitive to molar ratio as found by Watson et al. (2002) however, DSE was found to decrease on the more recalcitrant PHBMCC. It was expected that the bound ratios of cellulases in mixtures would reflect their loaded ratios since all three cellulases had homologous family 2 CBMs. However the measured bound ratios in mixtures were found to be different from the loaded ratios both for BMCC and PHBMCC, suggesting that the CDs of these cellulases had a significant contribution to their overall binding affinities. For mixtures of Cel6B+Cel9A, Cel6B showed increased binding in mixtures substantiating the hypothesis that endocellulases increase the availability of free ends for exocellualses. However for mixtures of Cel5A+Cel6B, Cel5A showed enhanced binding indicating that the hypothesis did not hold for this mixture. For mixtures of Cel5A+Cel9A, Cel9A was observed to have enhanced binding levels indicating that the classical endocellulase (Cel5A) caused increased in binding of the processive endocellulase (Cel5A). Thus the work of Jeoh et al. (2006) revealed that synergism in binding was accompanied by synergism in binding.

A recent study by Ma et al. (2008) examined the relationship between irreversibly bound *T. reesei* CBH I and the initial rate of hydrolysis of Whatman CF11 cellulose. The authors measured the total bound, reversibly bound and irreversibly bound CBH I concentration in two ways; by UV absorbance and by Surface Plasmon

Resonance (SPR). SPR is an optical technique used to measure the mass of protein adsorbed (Hlady and Buijs 1996). They found the rate of cellulose hydrolysis to decline with increasing surface density of irreversibly bound CBH I over a reaction time of 30 minutes. A similar trend was observed between rate of hydrolysis and total bound enzyme. The declining initial rate coupled with increasing adsorption of enzyme was attributed to a greater extent of nonproductive binding compared to productive binding. The amount of reducing ends on the residual substrate was determined and found to be nearly constant. The specific activity of the irreversibly bound enzymes at different time points was measured using the soluble substrate pNPC (Deshpande, et al. 1984) and compared with activity of total unbound enzyme and total enzyme added. The relative specific activity of enzyme in free solution was found to decrease by 40% from the specific activity of the initial CBH I added. However the relative specific activity of irreversibly bound CBH I was found to decrease by 70 % after 10 min intervals, over 30 minutes. This decline in activity was complemented by measurement of circular dichroism spectra of the irreversibly bound CBH I, which showed changes in conformation of the bound enzyme over time. The authors inferred that the conformation change was linked to the decrease in pNPC activity. They concluded that the decline in hydrolysis rate was a function of the irreversibly adsorbed enzyme rather than the total adsorbed enzyme. The low activity observed over extended reaction times was attributed to the activity of reversibly bound enzyme.

This work uses two methodologies – SPR and UV absorbance – to measure the irreversible and reversible CBH I bound concentrations, thus eliminating any method related errors in enzyme concentration measurements. The decreasing pNPC activity of irreversibly adsorbed enzyme over time appears to indicate that irreversible binding leads to poor activity. A time course of the extent of irreversible binding allowed the

authors to determine a correlation between the binding behavior and the reaction rate at short reaction times.

2.4 Use of optical techniques for the study of cellulase-cellulose interactions

The advances in fluorescence imaging methods have revolutionized the study of biological phenomena at the micro and nanoscale. The application of optical techniques to the study of cellulase-cellulose interactions has been sporadic in the past decade and has only recently become an area of much interest and significance. The first study to apply Fluorescence Recovery After Photobleaching (FRAP) to demonstrate the lateral mobility of cellulases bound to immobilized cellulose was conducted by Jervis et al (1997). FRAP is a spectroscopic technique in which a small, well defined rEG Ion on a surface containing bound fluorescent species, is irreversibly photobleached with a high-powered light source (Axelrod, et al. 1976). The gradual recovery of fluorescence in the bleached rEG Ion due to subsequent migration of unbleached fluorescent species from the surrounding rEG Ions is monitored at low power to obtain information about the mobility of the fluorescent species. The concept of FRAP is described pictorially in Figure 2.7.

In their study using the bacterial cellulases from *Cellulomonas fimi*, Jervis et al. (1997) labeled an exo-beta-1-4-glycanase (Cex), an endo-beta-1-4-glucanase (CenA), and their respective isolated cellulose-binding domains (CBDs) with fluorescein isothiocyanate (FITC). An inactive endocellulase mutant was used to prevent any surface degradation while the wild type glycanase was used as it has very low activity on cellulose. Labeled cellulases were purified by passing them twice through Sephadex G50 size exclusion gel columns and pooling fractions containing significant quantities of protein. On an average, 1.5-2.2 moles of FITC were estimated to be bound per mole of protein. The microcrystalline cellulose substrate used for this

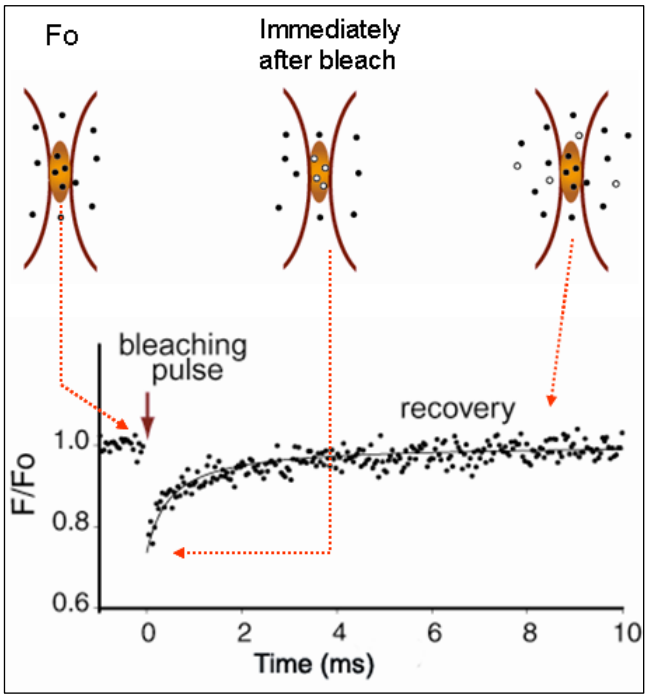

Figure 2.7: Fluorescence Recovery After Photobleaching. On a surface of the sample specimen a well defined rEG Ion is bleached and the recovery of fluorescence in the rEG Ion as a result of diffusion from neighboring rEG Ions is monitored (Lippincott-Schwartz, et al. 2001)

study was obtained from the cell wall of the marine algae *Valonia ventricosa.* Sheets of approximately 1μm thickness were peeled off from the cell wall and dried on glass coverslips. The conditions used for drying were, however, not specified. This immobilized substrate was first rehydrated by incubation with buffer followed by addition of labeled cellulase. Equilibrium conditions were established over 3 h and the supernatant was replaced by fresh buffer. FRAP experiments by Jervis et al. (1997) were conducted at room temperature, using a confocal microscope, which has the advantage of allowing the monitoring of fluorescence photobleaching recovery at a well defined image plane. Bleached spots were produced using a high-powered laser beam and the beam was attenuated to monitor the fluorescence recovery. The averaged radial profile of the fluorescence intensity within the bleached spot was fit by nonlinear least squares regression to a model function, assuming the bleached spot had a Gaussian profile.

The diffusion coefficients and the mobile fractions obtained for the *C. fimi* cellulases and their CBDs have been listed in Table 2.7. Estimating the free solution diffusion coefficient for the cellulases to be of the order of 10^{-6} cm^2/s from the Stokes-Einstein equation, the authors observed the two-dimensional diffusion coefficient to be approximately four orders of magnitude lower than that in free solution. Surface coverage density was defined as the ratio of bound cellulase to maximum bound cellulase. The diffusion rate of the CBD_{Cex} was found to increase with surface coverage up to 90% surface coverage and then decrease. Ideally, for a single sorbant species diffusing on a homogeneous surface containing a single type of adsorption sites, the surface diffusivity is predicted to have zero order dependence on surface concentration at low surface coverage with a definitive decrease in the diffusivity when the surface coverage approaches saturation (Scalettar, et al. 1988). The observed non-ideal behavior of the CBD_{Cex} diffusivity with respect to surface coverage

showed that the cellulase-cellulose system does not conform to the simplified model of a single self-diffusing species moving on a homogeneous crystalline lattice.

While FRAP provides measurements of surface diffusivity and the mobile fraction on the surface it has certain unavoidable drawbacks. First, FRAP measures the average self-diffusion rate. Hence it cannot distinguish different components diffusing at different rates. It has been speculated that the observed surface diffusion coefficient is the result of the mean of a fast diffusing fraction corresponding to a productively bound fraction and a slower fraction bound non-productively to the surface (Jervis, et al. 1997). Thus this technique lacks the sensitivity to separate multiple components (Lippincott-Schwartz, et al. 2001). Second, Jervis et al. (1997) admit that very little information is obtained regarding the nature of the immobile fraction. For Cex and CBD_{Cex} about 35% of the bound cellulases appear to be immobilized on the cellulose surface. While the authors hypothesize that the immobile species could be a result of the trapping of the CBDs onto the chain ends or discontinuities on the crystal, there is no experimental evidence to show that this is the case. The FRAP technique is also not quantitative enough to give absolute concentrations of bound cellulases.

Pinto et al (2007) developed a method based on image analysis of widefield fluorescence intensity measurements to quantify the surface concentrations of CBD-FITC conjugates bound to cellulose films. Cellulose films were produced on glass slides by evaporation of a solution of cellulose acetate in acetone. In this work image analysis algorithms were developed to convert fluorescence intensities of bound CBDs into corresponding concentrations. In a subsequent study (Pinto, et al. 2008) using the algorithms developed in the above work, they used image analysis and confocal microscopy to quantify CBD-FITC bound to three substrates, namely, Whatman CF11 fibers , amorphous cellulose and Sigmacell 20. Amorphous cellulose was prepared by

Table 2.7: Surface diffusion rates and mobile fractions for *C.fimi* Cex and its CBD and a catalytically inactive mutant of CenA and its CBD (Jervis, et al. 1997).

Molecule	Surface Diffusion coefficient (cm^2/s)	Mobile fraction
CenA	2.9 ± 0.5 (10-11)	0.85 ± 0.07
CenA CBD	1.9 ± 0.4 (10-11)	0.89 ± 0.07
Cex	4.1 ±0.5 (10-11)	0.65 ± 0.05
Cex CBD	3.1 ±0.4 (10-11)	0.65 ± 0.06

phosphoric acid swelling of Whatman CF11 fibers. Sigmacell 20 is a commercial cellulosic substrate obtained by separation of mechanically crushed cellulose fibers with an average particle size of 20 μm.

Adsorption assays were carried out using CBD concentration of 20 mg per g of cellulose fiber at 4˚C for 30 minutes. The CBDs used in their studies belonged to CBH I of *T.reesei.* These CBDs have a single amine in the N-terminal of the linker rEG Ion, which was used to specifically label the CBDs with FITC. Unconjugated FITC was separated from CBD-FITC conjugates using Bio-Gel columns packed with P4 resin and equilibrated with buffer. The surface concentration of CBDs on Whatman CF11 fibres was estimated to be 25.2×10^{-13} mol/mm^2, for a saturating CBD loading of 60 mg/L. Estimating the density of monolayer of CBDs to be around 3.08×10^{-13} mol/mm^2 based on a CBH I of dimensions 3.0×1.8 nm, the results indicated that the surface coverage of fiber with CBD-FITC was much higher than a monolayer. The authors used confocal imaging to analyze the fluorescence in the fibers at different depths to verify penetration of CBDs into the porous structure of the CF11 fiber.

The advantage of confocal microscopy is that it allows imaging of individual optical sections in sequence along the depth of the sample (Schatten and Pawley 1988). In conventional widefield epifluorescence microscopy, the resolution of the features in the focal plane is obscured by the fluorescence emitted from the sample throughout the excitation volume. The fine details are difficult to retrieve specially for specimens of thickness greater than 2 μm. Confocal microscopy uses spatial filtering techniques to exclude fluorescence emitted from areas around the focal plane, thus reducing much of the background information while allowing optical sectioning of the sample (Fellers and Davidson 2004). Figure 2.8 shows the images of the CF11 fiber taken at different optical sections. The interior of the fibres was found to have higher

fluorescence intensity than the exterior sections, providing visual proof of the penetration of CBDs into the pores of the substrate. While this result corroborates the pore entrapment model developed by Jung et al (2002), the extent of penetration as exhibited by the higher fluorescence in the pores needs closer examination. The authors have not quantified the purity of their labeled CBD-FITC samples in terms of removal of unconjugated fluorophore. The separation of labeled protein from unreacted fluorophore by gel filtration is now known to be inefficient (Moran-Mirabal, et al. 2008). Hence the possibility that the presence of unreacted dye in the CBD-FITC sample is responsible for the fluorescence of the interior of the fibres due to diffusion of free fluorophore into the pores, cannot be ruled out completely.

Pinto et al (2008) verified the pore entrapment of CBDs using Transmission Electron Microscopy (TEM) – immunolabeling analysis of CBD treated CF11 fibers. The surface coverage for amorphous cellulose was found to be 50 % greater than that for the crystalline Whatman CF11. This result follows from the fact that preparation of amorphous cellulose by phosphoric acid swelling of Whatman CF11 causes it to present a greater total surface area for adsorption of CBDs. Sigmacell 20 was found to adsorb CBDs to an extent similar to that observed with amorphous cellulose. The work of Pinto et al.(2007, 2008) is significant in that it provides a means of quantifying the concentration of bound enzyme achieved by calibrating the fluorescence intensity with enzyme loading rather than expressing it as relative intensity. Studies conducted at non-saturation enzyme loadings using the above methodology would provide interesting clues to enzyme binding behavior.

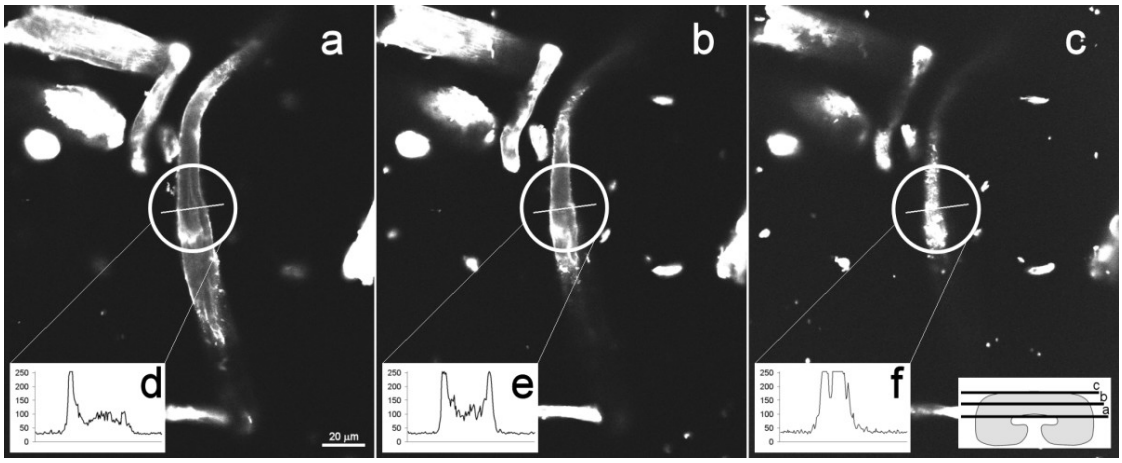

Figure 2.8 (a), (b), (c) Confocal microscopy images of optical sections of CBD-FITC adsorbed to CF 11 fibers. Insertions (d), (e) and (f) show the pixel intensities obtained at the rEG Ion indicated by the white circle (Pinto, et al. 2008).

2.5 Fluorescent cellulose derivatives

The use of fluorescence to detect cellulolytic activity was introduced by Helbert et al. (2003) who devised a miniaturized assay to rapidly screen crude enzyme extracts. A commercial dye, 5-(4,6-dichlorostriazinyl) aminofluorescein (DTAF), which has the ability to fluoresce as well as to react with the hydroxyl moiety of polysaccharides, was used to label bacterial cellulose. An ethylene diamine treatment was applied to the bacterial cellulose to open up its mesh-like structure so that it could be deposited as thin films onto the wells of microplates. This treatment was found to change the crystal structure of bacterial cellulose from cellulose I to cellulose III and the change was monitored using X-ray diffractrometry. Different amounts of DTAF were then added to the treated cellulose suspension in alkali, either as a single step labeling or as a multi-step labeling. In the single-step labeling the amount of DTAF added was varied. In the multistep labeling, the amount of DTAF was fixed and the labeling procedure was repeated on the same sample sequentially for a number of times. Unreacted DTAF was removed by repeated washes with water. The mean degree of substitution of BMCC labeled with DTAF was determined by elemental composition analysis and was expressed as:

$$D_S = \frac{M_{DTAF}}{M_{AGU}} \qquad 2.13$$

where :

M_{DTAF} = Moles of DTAF, (MW_{DTAF} = 492.28);

M_{AGU} = Moles of anhydroglucose units, (MW_{AGU} = 162);

D_S = Mean degree of substitution

Films of labeled cellulose were cast on the bottoms of microplates by drying at 37 °C. Enzymatic hydrolysis assays were set up by adding known amounts of *Humicola insolens* complex or purified *H. insolens* endocellulases Cel6B and Cel45A

followed by incubation at 37 °C for fixed time periods. Similar reactions were set up for the digestion of DTAF labeled suspensions of cellulose. Enzymatic activity was determined by measuring the reducing ends produced by the ferricyanide assay. The amount of fluorescence released by films and suspensions into the supernatant was also quantified. For single-step labeling reactions, the extent of fluorescence released by the *H. insolens* complex was found to vary linearly with the amount of DTAF added up to 40 mg of DTAF per 100 mg of cellulose, after which it reached a plateau. For the multi-step grafting reactions, the D_S was found to increase linearly with the number of successive labeling steps but the amount of fluorescence released by the *H. insolens* complex was found to increase up to the fourth step followed by a decrease up to the seventh step. This indicated an inhibition of enzymatic activity by excess DTAF labeling.

The amount of reducing sugars produced by *H. insolens* crude cellulase was found to decrease with increasing degree of substitution, in direct contrast to the trend observed with fluorescence released by the complex. However, the amount of reducing sugars produced by endocellulase Cel6B were unaffected by the degree of substitution. The authors reasoned that the amount of fluorescence released was dependent on the mode of action of cellulases. The *H. insolens* crude cellulase had a majority of cellobiohydrolases and was expected to have high processivity. Helbert et al (2003) explained that processive enzymes would attack ends of the cellulose chain, release reducing sugars and would continue to act processively on the same cellulose chain until they reached a DTAF labeled glucose moiety, which would prevent any further cleavage along the same cellulose chain. The endocellulases would, on the other hand, attack the cellulose chain randomly releasing reducing sugars and would be affected to a lesser degree by the presence of DTAF on the chain. Figure 2.9 shows the predicted pattern for release of fluorescence and reducing sugars from labeled

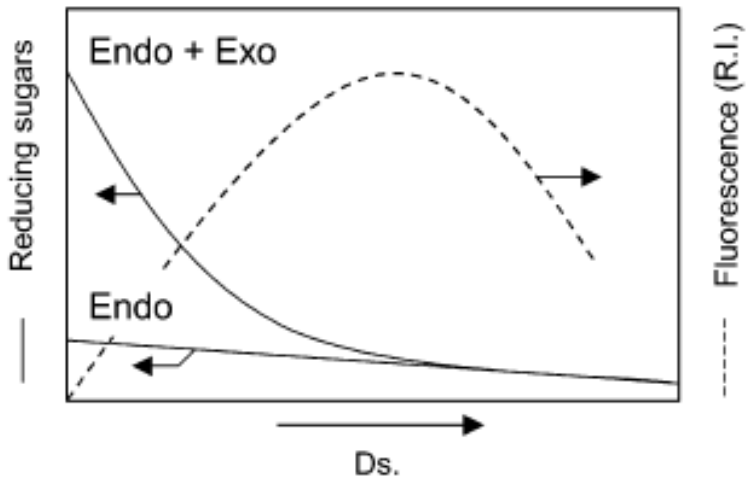

Figure 2.9 Prediction of pattern of release of fluorescence and reducing sugars by endocellulases and mixtures of endocellulases and exocellulases (Helbert, et al. 2003)

cellulose as a function of the degree of substitution. The authors anticipated using this pattern as a basis for accounting for the cellulolytic composition of any crude cellulase mixture.

The films of cellulose in microwell plates were found to be suitable substrates for detecting minute quantities of enzyme activity. However, this will be complicated by the synergistic activity of an enzyme mixture. The films were found to be immobilized strongly enough to the well bottoms to allow pipetting out of the supernatant for fluorescence detection. The fluorescence released by cellulose III films was found to be thrice as much as that released by cellulose I. The authors envisioned the use of this assay for cellulase activity screening and detection on robotic platforms due to the ease of automation of the steps. However, they failed to characterize the fluorescence releasing pattern of a pure exocellulase, which could be different for that of mixtures containing both endocellulases and exocellulases. The presence of processive endocellulases in the mixture would also affect the pattern of fluorescence released. Hence their prediction of the application of this assay is not completely tested in their experimental work.

2.6 Product inhibition studies of cellulose hydrolysis

A typical characteristic of the enzymatic hydrolysis of cellulose is a pronounced rate retardation, which becomes evident even at a low degree of conversion (20-30%) of the substrate (Beltrame, et al. 1984; Converse, et al. 1988; Holtzapple, et al. 1984d; Howell and Stuck 1975; Howell 1978; Ladisch, et al. 1983; Lee and Fan 1983; Ohmine, et al. 1983; Gusakov, et al. 1985b). This decline in the reaction rate becomes even more pronounced over extended reaction times and the reaction almost stops before all the substrate is consumed (Gusakov and Sinitsyn 1992; Valjamae, et al. 1998; Zhang, et al. 1999) . In order to improve the economic viability of the production of liquid renewable fuels by the enzymatic hydrolysis of cellulosic biomass, it is essential to be able to diagnose the cause for this decline in the rate and develop an understanding of the mechanisms involved in order to reliably predict the kinetics of cellulose hydrolysis for application to commercial scale reactors. Several factors have been considered responsible for the observed fall in the reaction rate, namely;

- Inhibition of enzyme by soluble end products such as cellobiose and, to a lesser extent, glucose (Gusakov, et al. 1985a; Holtzapple, et al. 1984d).
- Change in the nature of the substrate – its morphology, crystallinity and heterogeneity – with the progress of hydrolysis (Lee and Fan 1983; Zhang, et al. 1999)
- Deactivation of enzyme due to causes other than bulk product inhibition, such as exposure of adsorbed cellulases to fluid shear stress in the reaction zone or non-productive binding (Converse, et al. 1988; Gan, et al. 2003)

Though there has been general agreement in literature that most cellulases are inhibited by either cellobiose or glucose or both, the mechanism of product inhibition of cellulose hydrolysis has been a topic of much controversy.

2.6.1 Mechanisms of inhibition

Product inhibition is caused by reaction products that behave as reversible inhibitors. These are compounds that form dynamic complexes with enzymes causing a change in the catalytic properties of the enzyme, which results in reduced enzymatic activity (Cornish-Bowden 2004). Three major classifications of the mechanisms for reversible enzyme inhibition are competitive inhibition, non-competitive inhibition and uncompetitive inhibition.

2.6.1.1 Competitive inhibition

Competitive inhibitors are usually analogs of the substrate and compete with the substrate to bind to the active site of the enzyme. The mechanism for this type of inhibition is depicted schematically below.

$$E + S \xrightarrow{k_1} ES$$
$$ES \xrightarrow[k_{-1}]{} E + S$$
where $$ES \xrightarrow{k_2} E + P$$
$$E + I \xrightarrow{K_I} EI$$

E = Enzyme; S = Substrate; P = Product; I = Inhibitor;

k_1, k_{-1},k_2 = Rate constants;

$K_M^{'}$ = Dissociation constant for enzyme substrate complex formation

K_I = Dissociation constant for enzyme inhibitor comples

Assuming rapid equilibrium, the equilibrium constants for the enzyme-substrate and enzyme-in complex formation are:

$$K_M^{'} = \frac{[E][S]}{[ES]} \qquad (2.14)$$

)

$$K_I = \frac{[E][I]}{[EI]} \qquad (2.15)$$

A material balance of enzyme species gives:

$$[E_0] = [E] + [ES] + [EI] \tag{2.16}$$

While the rate of product formation is given by:

$$v = k_2[ES] \tag{2.17}$$

Substituting the expression for the enzyme substrate complex, the rate of enzymatic conversion can be developed to be:

$$v = \frac{V_m[S]}{K_M^{'}\left[1 + \frac{[I]}{K_I}\right] + [S]} \tag{2.18}$$

or

$$v = \frac{V_m[S]}{K_{m,app}^{'} + [S]} \tag{2.19}$$

where)

V_m= the maximum forward velocity of the reaction

$K^{'}_{m,app}$ = the apparent dissociation constant for the ES complex

whose value is give by

$$K_{m,app}^{'} = K_m^{'}\left(1 + \frac{[I]}{K_I}\right) \tag{2.20}$$

The net effect of competitive inhibition is an increase in the value of the apparent dissociation constant of the enzyme substrate complex accompanied by a reduced reaction rate. Competitive inhibition can be overcome by using high substrate concentrations.

2.6.1.2 Non-competitive inhibition

The inhibitors which are non-competitive are not substrate analogs and bind to sites other than the active site of the enzyme. However their binding to the enzyme

diminishes the enzyme affinity to the substrate. The mechanism for non-competitive inhibition can be described as below:

$$E + S \xrightarrow[K_M]{} ES \xrightarrow[k_2]{} E + P$$
$$E + I \xrightarrow[K_I]{} EI + S$$
$$EI + S \xrightarrow[K_M]{} ESI$$
$$ES + I \xrightarrow[K_I]{} ESI$$

Deriving the rate equation in a manner similar to that for competitive inhibition, the rate of the reaction is found to be

$$v = \frac{V_{m,app}}{\left(1 + \frac{K_m^{'}}{[S]}\right)} \tag{2.21}$$

Where

$$V_{m,app} = \frac{V_m}{\left(1 + \frac{[I]}{K_I}\right)} \tag{2.22}$$

The effect observed in the presence of a non-competitive inhibitor is a reduction in the maximum forward velocity of the reaction, which cannot be overcome by increasing the substrate concentrations. In some cases of non-competitive inhibition where the ESI complex can form a product, the maximum velocity is decreased while the dissociation constant is increased.

2.6.1.3 Uncompetitive inhibition

Uncompetitive inhibitors differ from non-competitive inhibitors in that they only bind to the ES complex and have no affinity to bind to the free enzyme. The scheme for this type of inhibition is given below:

$$E + S \xrightarrow{K_m^{'}} ES \xrightarrow{k_2} E + P$$
$$ES + I \xrightarrow{K_I} ESI$$

The equation for the rate of the reaction can be derived as:

$$v = \frac{V_{m,app}[S]}{K'_{m,app} + [S]} \tag{2.23}$$

where

$$V_{m,app} = \frac{V_m}{1 + \frac{[I]}{K_I}} \tag{2.24}$$

$$K_{m,app} = \frac{K'_m}{1 + \frac{I}{K_I}} \tag{2.25}$$

The presence of an uncompetitive inhibitor leads to a reduction in the maximum reaction velocity as well as the enzyme dissociation constant with the former effect being more pronounced than the latter. The overall effect is a reduction in the reaction rate.

A summary of the results of the work of different research groups on cellulase product inhibition has been shown in Table 2.8. The observed variation in the patterns of inhibition reported are attributed to several causes (Gusakov and Sinitsyn 1992; Holtzapple, et al. 1990). Cellulase preparations used in product inhibition studies have usually been treated as one single enzyme. It is however well known that the term 'cellulase', unless qualified as purified, actually implied a mixture of at least three major components namely; endoglucanases, exoglucanases and β-glucosidases (Wilson and Irwin 1999; Wood 1975; Wood and Mccrae 1978). Each of these components has a specific mode of action (Irwin, et al. 1993), activity, binding affinity (Bothwell, et al. 1997a) and domain structure (Henrissat, et al. 1998). Attributing a single inhibitory effect on a mixture of three different enzyme species can be an erroneous assumption.

Table 2.8 Summary of cellulase inhibition studies in literature (Holtzapple, et al. 1990)

Enzyme source	Substrate	Inhibitor	Reference
Competitive Inhibition			
T.reesei	Wheat straw	Glucose,cellobiose	(Gonzalez, et al. 1989)
T.reesei	Solka Floc	Cellobiose	(Ryu and Lee 1986)
T.viride	Solka Floc	Glucose,cellobiose	(Huang 1975)
T.viride	Cotton waste	Glucose	(Beltrame, et al. 1984)
T.viride	Microcrystalline cellulose	Lumped products	(Converse, et al. 1988)
Theroretical	---	Glucose, cellobiose	(Okazaki and Mooyoung 1978)
Noncompetitive Inhibition			
T.reesei	Solka FLoc	Lumped products	(Holtzapple, et al. 1984d)
T.viride	Solka Floc	Glucose, cellobiose	(Howell and Stuck 1975)
T.fusca	Cellulose azure	Glucose, cellobiose	(Holtzapple, et al. 1984a)
T.fusca	Aspen	Cellobiose	(Holtzapple, et al. 1984b)
Uncompetitive Inhibition			
T.viride	Cotton waste	Glucose	(Beltrame, et al. 1984)
Empirical Inhibition			
T.reesei	Solka Floc	Glucose, cellobiose	(Fan and Lee 1983)

The composition of the products formed by cellulose hydrolysis using a cellulase preparation also needs to be taken into account in order to understand product inhibition. Different products can have different inhibitory effects on different components of the cellulase preparation used. Glucose is known to inhibit β-glucosidases (Gong, et al. 1977) while cellobiose inhibits exoglucanases (Gusakov, et al. 1985b). Characteristics of the cellulosic substrate, such as its pore structure, crystallinity and specific surface area influence the kinetics of cellulose hydrolysis (Fan, et al. 1980; Fan, et al. 1981; Grethlein 1985) leading to nonlinearity in the reaction kinetics. Since the hydrolysis reaction itself takes place at the solid-liquid interface diffusional limitations can occur. The kinetic equations traditionally used to describe product inhibition were derived for homogenous enzymatic reactions and may not be directly applicable to a heterogeneous system.

2.6.2 Methods of modeling product inhibition of cellulose hydrolysis

Enzymatic hydrolysis is usually studied by measurement of the *amount* of product formed or the *amount* of substrate remaining at one or several time points. On the other hand, most kinetic models are developed in terms of *rates* of reaction. This introduces a fundamental mismatch between the data collected and the kinetic model formulated to describe the system (Duggleby 1995). This mismatch can be resolved using two methods. The first method is to integrate the model to give an equation describing the time course of the reaction. The second method is to differentiate the data to determine reaction rates (Duggleby 1995) .

2.6.3 Product inhibition models based on analysis of progress curves

Integration of a kinetic model has several inherent advantages (Duggleby 1995).

- The change in concentration of the substrate is automatically adjusted for, with the progress of the reaction. This provides information about the dependence of the enzyme on the substrate concentration.
- The products formed as a result of the progress of the reaction have the correct stereochemistry and are free of any impurities which may be introduced in a deliberately added external product. This provides information about the dependence of the enzyme on the product concentration.
- As a result of the above conditions, considerably more information can be extracted from each assay so that the complete description of the kinetic behavior of the reaction system can be obtained through fewer experiments.

However, the use of progress curves for reaction rate measurements has a limitation which prevents it from being the popular method of choice. The shape of the progress curve depends on several other factors such as slow deactivation of the enzyme or change of substrate reactivity. Such information may not easily be extractable from the integrated equation.

Progress kinetic curves using integrated Michaelis-Menten equations have been used by Bezerra et. al. (Bezerra and Dias 2004) to investigate the influence of cellobiose on the kinetics of hydrolysis of Avicel by the *T. reesei* exogluconase Cel7A. The reaction mechanism used by Bezerra et. al. is called the linear "Mixed inhibition model with substrate and parabolic inhibition" (MISPI) and is depicted schematically below:

$$ES' \xrightarrow{K_{IS}} E \xrightarrow{K_m} ES \xrightarrow{k_{cat}} P$$

$$E \xrightarrow{K_{ic}} EI$$

$$ES \xrightarrow{K_{iu}} EIS$$

$$EII \xrightarrow{K_{ip}} EI \xrightarrow{K_{is}} EIS$$

A key assumption inherent to the MISPI model is that the cellulases form productive (ES) and non-productive enzyme substrate complexes (ES'). Productive complexes (ES) lead to cellulose hydrolysis with the release of enzyme and cellobiose while the non-productive complexes (ES') remain catalytically inactive. The authors base their model on the hypothesis that the existence of productive and nonproductive complexes reflects the possible interactions between enzyme and substrate but does not reflect the transformation of the substrate structure itself. Parabolic inhibition was considered in order to account for the fact that the 3D structure of the Cel7A covers several binding sites, with the assumption that the parabolic inhibition would be probable as soon as a minimum of two cellobiose molecules were bound to the active site. The eight different linear inhibition models derived were as shown in Table 2.9. Using the reaction mechanism depicted and assuming Michaelis-Menten kinetics, the rate equation for the general model (MISPI) was derived to be:

$$v = \frac{VS_0}{K_m\left(\left(1+\frac{S_0}{K_{is}}\right)+\frac{P}{K_{ic}}\left(1+\frac{P}{K_{ip}}\right)\right)+S_0\left(1+\frac{P}{K_{iu}}\right)} \qquad (2.26)$$

Considering the cellulose chain to have thousands of cellobiose units, the above rate equation was integrated using the assumption that the release of reducing sugars was not accompanied by any significant decrease in the reaction sites, or in other words, the substrate concentration was assumed constant.

Table 2.9. Formulation of eight modified Michaelis-Menten kinetics models (units of K_{is}, K_{ip}, K_{iu} are g/L) (Bezerra, et al. 2004)

Model	Assumption
The mixed inhibition model with parabolic inhibition (MIPI)	$K_{is} = \infty$ $K_{ip} = \infty$
The mixed inhibition model with substrate (MISI)	K_{is} and $K_{ip} = \infty$
The mixed inhibition model	K_{iu}, K_{ip}, $K_{is} = \infty$
The competitive inhibition model (CI)	$K_{ic} = K_{iu}$, $K_{ip} = \infty$, $K_{is} = \infty$
The noncompetitive inhibition model (NCI)	$K_{ic} = \infty$, $K_{ip} = \infty$, $K_{is} = \infty$
The uncompetitive inhibition model (UCI)	

The integration was performed as follows:

$$V\int_0^t dt = \left(\frac{K_m}{S_0} + \frac{K_m}{K_{is}} + 1\right)\int_{P_0}^{P_t} dP + \left(\frac{K_m}{S_0 K_{ic}} + \frac{1}{K_{iu}}\right)\int_{P_0}^{P_t} PdP + \frac{K_m}{S_0 K_{ic} K_{ip}}\int_{P_0}^{P_t} P^2 dP \tag{2.27}$$

$$t = \frac{1}{V}\left\{\left(\frac{K_m}{S_0} + \frac{K_m}{K_{is}} + 1\right)\left(P_t - P_0\right) + \left(\frac{K_m}{S_0 K_{ic}} + \frac{1}{K_{iu}}\right)\frac{1}{2}\left(P_t^2 - P_0^2\right) + \left(\frac{K_m}{K_{ic} K_{ip} S_0}\right)\frac{1}{3}\left(P_t^3 - P_0^3\right)\right\} \tag{2.28}$$

where:

S = substrate;

P = reaction product, cellobiose;

P_t = product at time t min;

S_0 = substrate at time t = 0;

P_0 = product at time t = 0

Progress curve analysis can be used to study only those reaction systems where the shape of the process curve depends entirely upon the changes in reactant concentrations that are brought about only by the catalyzed reaction. It is imperative to show that the enzyme does not get progressively inactivated over time and that there are no uncatalyzed side reactions in the assay. Selwyn's test is used to indicate whether a given system is suitable for progress curve analysis studies (Duggleby 1995). It is based on the fact that the general form of the integrated equations can be expressed as:

$$\left[E_0 t\right] = f\left(P, k, [X]_0\right) \tag{2.29}$$

where:

X_0 = the initial substrate concentration;

E_0 = the total enzyme concentration;

P = the amount of product formed

k = the various rate constants;

Selwyn's test states that the plots of P vs [E_ot] obtained for a range of enzyme concentrations should be superimposable unless there is instability of enzyme, substrate or products. The authors show that the Cel7A Avicel system passes the Selwyn's test criterion indicating that there is no inactivation of enzyme over the time period examined. The parameters for the different models were estimated using the non-linear regression method DUD (does not use derivatives). Results of the progress curve analysis showed that the hydrolysis of cellulose by Cel7A was inhibited competitively with parameter values obtained as

$$K_m = 3.8\text{mM}$$

$$K_{in} = 0.041\text{mM}$$

$$K_{cat} = 2/\text{h}$$

The only drawback of the work by Bezerra et al. (2004) lies in their rate equation, equation 2.25. They have started out with the assumption that the substrate concentration at any time t remains unchanged and equal to initial substrate concentration. The assumption that when the enzyme concentration is low compared to the substrate concentration, the instantaneous substrate concentration is approximately equal to the initial substrate concentration ($S \approx S_0$) holds only for soluble substrates and not for insoluble cellulose. A material balance is necessary to account for the cellulose hydrolyzed to cellobiose and the formation of non-productive enzyme substrate complexes. The lack of any such material balance undermines the credibility of the model equations developed by Bezerra et al. (2004).

Progress curve analyses have also been used by Teleman et al. (1995) to show that glucose inhibits cellotriose hydrolysis by *T. reesei* Cel6A. The use of a soluble

substrate provides little information about the inhibitory effects of products when the substrate is insoluble.

2.6.4 Product inhibition models based on analysis of initial rates

Traditionally, most biochemical studies have used the method of determining the rates, specifically initial rates, by measuring the tangents to the reaction progress curves at zero time. The reasons for the popularity of the method of initial rates are:

- There is no probability for the enzyme to have undergone any partial inactivation at the very start of the reaction
- The concentration of the substrate is exactly equal to the concentration added to the reaction
- At the start of the reaction, the concentration of potentially inhibitory products formed as a result of the reaction is vanishingly small

An important feature of a product inhibition study based on initial rates is that a significant amount of product is usually deliberately added to the system at the start of the reaction to study inhibitory effects. This condition makes the accurate measurement of the initial rate formation of the same product in the presence of its high background concentration, extremely tricky. Such measurements can be fraught with experimental errors. Use of a labeled substrate has been devised as a means to overcome this limitation (Gruno, et al. 2004; Gusakov, et al. 1985a; Holtzapple, et al. 1984c). The rate of substrate hydrolysis can then be monitored easily by measuring the rate of dye release irrespective of the high sugar background concentration.

Gruno et al. (2004) used reducing end-specific tritium labeled bacterial cellulose and amorphous cellulose to perform an initial rate-based quantitative study of the effect of cellobiose on the action of the purified cellulases *Trichoderma reesei*

Cel7A , Cel5A and Cel12A. The schematic representation of the reaction mechanism proposed is as follows.

$$E \underset{k_{-1}}{\overset{k_1[S]}{\rightleftarrows}} ES' \underset{k_{-6}+k_{cat}}{\overset{k_6}{\rightleftarrows}} ES \xrightarrow{k_{cat}} P$$

$$E \underset{k_{-2}}{\overset{k_2[I]}{\rightleftarrows}} EI$$

$$ES' \underset{k_{-4}}{\overset{k_4[I]}{\rightleftarrows}} EIS$$

$$EI \underset{k_{-3}}{\overset{k_3[S]}{\rightleftarrows}} EIS$$

Accounting for the multiple glucosyl-unit binding tunnel structure of Cel7A, the authors assumed that the enzyme could complex with the substrate in different ways. In a productive complex, a glucosidic bond was in the right position for cleavage to occur. In a non-productive complex, the substrate had to be moved to be in the correct position. The rate expression for the steady state according to this reaction mechanism was obtained as below using the method of King and Altman (King and Altman 1956).

$$v = \frac{\dfrac{k_{cat} e_0 [S]}{1+K_{ES}\left(1+\frac{[I]}{K_{EIS}}\right)}}{[S] + \dfrac{K_s K_{ES}\left(1+\dfrac{[I]}{K_{EI}}\right)}{1+K_{ES}\left(1+\dfrac{[I]}{K_{EIS}}\right)}} \qquad (2.30)$$

where:

e_0 = Total enzyme concentration (μM);

[S] = free substrate concentration (g/L);

[I] = free inhibitor concentration (g/L);

[E] = free enzyme concentration (μM);

[EI] = enzyme-inhibitor complex (μM. g/L);

[EIS] = enzyme-inhibitor-substrate ternary complex (μM. g^2/L^2);

[ES] = productive enzyme-substrate complex (μM. g/L);

[ES']= non-productive enzyme-substrate complex (μM. g/L)

The equilibrium constants were defined as:

$$K_S = \frac{k_{-1}}{k_1}$$

$$K_{EI} = \frac{k_{-2}}{k_2}$$

$$K_{EIS} = \frac{k_{-4}}{k_4}$$

$$K_{ES} = \frac{k_{-6} + k_{cat}}{k_6}$$

The fundamental simplifying assumption made in the model was that the 2nd order rate constants for the binding of substrate were not affected by the inhibitor and the rate constants for the binding of the inhibitor were not affected by the substrate; i.e. $k_1 = k_3$ and $k_2 = k_4$.

The proposed mechanism suggests that when catalytic cleavage takes place, besides the formation of cellobiose, there is the formation of a nonproductive enzyme substrate complex rather than a free enzyme. This is taken into account such that the next rate constant for the conversion of ES to ES' is the sum of k_{-6} and k_{cat} rather than just k_{-6} alone. Thus the authors define K_{ES} as a dimensionless parameter which describes the ratio of nonproductive enzyme substrate complex (ES') to the productive enzyme substrate complex (ES) or

$$K_{ES} = \frac{[ES']}{[ES]} \qquad (2.31)$$

Two limiting conditions result depending on whether the ES complex or the ES' complex is dominant:

Condition 1: When the productive enzyme substrate complex is prevalent then $K_{ES} << 1$.

This implies that the term $1+K_{ES}\left(1+\frac{[I]}{K_i}\right)$ approaches 1. Then equation 2.29 reduces to:

$$v=\frac{k_{cat}\cdot e_0\cdot[S]}{[S]+K_S\cdot K_{ES}\left(1+\frac{[I]}{K_{EI}}\right)} \qquad (2.32)$$

This is the expression for competitive inhibition. The affinity of the enzyme for the substrate and the limiting rate are then given by:

$$K_M = K_S\cdot K_{ES}$$
$$V_{\lim} = k_{cat}\cdot e_0$$

Condition 2: When the nonproductive enzyme substrate complex prevails and $K_{ES}>>1$. Then the $1+K_{ES}\left(1+\frac{[I]}{K_i}\right)$ term can be approximated by $K_{ES}\left(1+\frac{[I]}{K_i}\right)$

Then equation 2.29 reduces to:

$$v=\frac{\frac{k_{cat}\cdot e_0\cdot[S]}{K_{ES}\left(1+\frac{[I]}{K_{EIS}}\right)}}{[S]+\frac{K_S\left(1+\frac{[I]}{K_{EI}}\right)}{\left(1+\frac{[I]}{K_{EIS}}\right)}} \qquad (2.33)$$

This results in a mixed type inhibition which has noncompetitive inhibition as a special case i.e. when $K_{EI} = K_{EIS}$

The affinity of the enzyme for the substrate and the limiting rate are then given by:

$$V_{\lim}=\frac{k_{cat}\cdot e_0}{1+K_{ES}}$$
$$K_M=\frac{K_{ES}\cdot K_S}{1+K_{ES}} \qquad (2.34)$$

The initial rates of reaction were based on the measured rates of release of soluble sugars after 5 or 10 s of reaction. These time points were considered to be acceptable as they were in the linear rEG Ion of the time course. Reducing end labeled bacterial

cellulose, [^{3}H]-BC, was used as the substrate for Cel7A while reducing end labeled amorphous cellulose, [^{3}H]-amorphous cellulose, was used as the substrate for endoglucanases Cel5A and Cel12A. Substrate concentrations which were required for the half limiting release rate of label were calculated using nonlinear regression methods.

A significant and necessary condition for the use of radioactively reduced substrates in a product inhibition study is that the label is released only as a result of the activity of the cellulase and not due to other reactions. At the initial stage of hydrolysis, the authors found that at a fixed [^{3}H]-BC concentration, a linear relationship existed between the released cellobiose and released label. The correlation was acceptable for Cel7A, Cel7B and Cel12 A however for Cel5A the release of reduced primary end groups was not an indicator of the general activity of the enzyme. The authors admit that a major drawback of their experiments was the use of tritium labeled celluloses, especially under alkaline conditions. Alkalification was used as the most reliable method for rapid (5-10 s time scale) termination of the cellulase reaction. However, the tritium label used was unstable under the alkaline conditions used for termination. Hence the authors accept that the relative instability of the tritium labeled celluloses under alkaline conditions set the limits for the sensitivity of their product inhibition assay and prevented them from making an experimentally accurate assessment of the exact type of inhibition.

The apparent inhibition constants obtained for the enzymes tested were as follows:-

Cel7A (cellobiohydrolase) : 1.6±0.5 mM

Cel5A (endoglucanase) : 34±6 mM

Cel7B (endoglucanase) : 11±3 mM

The mechanism for product inhibition proposed by Gruno et al. (2004) seems to be more realistic than earlier mechanisms in literature as it takes into account the two domain structure of cellulases while describing the formation of productive and nonproductive complexes. The idea that for a tunnel shaped structure of Cel7A a nonproductive complex could also occur when the cellulose chain was already captured in the active site adds to the value of the mechanism. However, the use of an unstable radioactively labeled substrate renders the methods unreliable and reduces the credibility of the experimental data and consequently the effectiveness of the model.

2.6.5 Inhibition of cellulase binding

Since adsorption of cellulases to the insoluble cellulose surface is a prerequisite for hydrolysis to take place, the rate of hydrolysis would essentially be a function of the bound enzyme concentration (Lee and Fan 1982; Walker and Wilson 1991). The effect of cellobiose on the adsorption of *T. reesei* Cel7A (CBH I) and its individual domains was investigated by Stahlberg et al. (1991). Cellobiose at 10 mM and 100 mM was added to the protein solution before incubation with Avicel at 20°C from 0 to 20 h. The binding of the intact CBH I and the cellulose binding module were found to be unaffected by the cellobiose, but the binding of the catalytic domain was found to increase over time in the presence of cellobiose, while its desorption rate was observed to be slower. Stalhberg et. al.(1991) concluded that since the amount of enzyme bound was enhanced due to the presence of cellobiose, desorption could not be due to simple product inhibition but would have been brought about by structural modifications of the substrate due to hydrolysis. They hypothesized that in spite of enhanced binding, the inhibition of cellulase activity due to the presence of cellobiose in the reaction could be a result of the retardation of the desorption of cellulases.

Another study investigating the effect of cellobiose on the binding behavior of *T. reesei* CBH I and CBH II was conducted by Palonen et al.(1999) who conducted binding experiments by incubating cellulases and their individual domains in buffer containing different amounts of cellobiose, ranging from 0.02 mM to 16 mM. The cellobiose concentrations expected to be present as a result of hydrolysis at the end of the experiments ranged from 2.5 mM to 3 mM. Palonen et al. (1999) found that binding of the catalytic domains (CDs) of both CBH I and CBH II were affected by cellobiose even at concentrations lower than 1 mM. The amount of bound CBH I CD doubled in the presence of 1.5 mM cellobiose and the amount of CBH II CD increased five times. On the contrary, in the presence of 1.6 mM cellobiose in the reaction the binding of the intact CBH II was found to decrease slightly while the binding of intact CBH I was found to be unchanged. Though the authors reported the effect of cellobiose on the binding behavior, they did not make any explicit comments on the correlation between the effect of cellobiose on the binding vis-à-vis its inhibitory effect on the hydrolytic activity of the cellulases and their catalytic domains.

The influence of cellobiose on the binding behavior of the CDs of *T. fusca* Cel5A, Cel6B and Cel48A was studied by Jung and Walker (2002) who employed cellobiose at 10 mM and 100 mM concentrations and monitored bound enzyme concentration over a 6 h reaction time at 5°C. The 100mM cellobiose concentration used was about 30 times the cellobiose concentration that would be produced by complete hydrolysis under those reaction conditions (Jung and Walker 2002). For all three cellulase CDs, the binding was found to be inhibited by the presence of cellobiose. The CDs of Cel6B and Cel48A appeared to be inhibited to a greater extent than the CD of Cel5A, with binding to the easily hydrolysable fraction being of the substrate being most affected. The effect of increasing cellobiose concentration tenfold was observed by the lower binding of Cel6B CD in the presence of 100mM

cellobiose compared to 10 mM. Binding of Cel6B CD was found to return to its initial level after 1 h of incubation in the presence of 10 mM cellobiose and no inhibition was observed between 1 and 6h. The CD of Cel48A appeared not be inhibited except for the initial 5s in the presence of 100 mM cellobiose. Jung et al. (2002) (Jung and Walker 2002) also concluded that the desorption of CDs was not a result of product inhibition and was more a function of the dynamically changing substrate morphology, as suggested by Stahlberg et al.(1991).

REFERENCES

Adamson AW. Physical Chemistry of Surfaces. New York; Wiley 1983

Axelrod D, Koppel DE, Schlessinger J, Elson E, Webb WW. 1976. Mobility Measurement by Analysis of Fluorescence Photobleaching Recovery Kinetics. Biophys J 16:1055-1069.

Baker JO, Ehrman CI, Adney WS, Thomas SR, Himmel ME. 1998. Hydrolysis of Cellulose Using Ternary Mixtures of Purified Cellulases. Applied Biochemistry and Biotechnology 70-72:395-403.

Barr BK, Hsieh YL, Ganem B, Wilson DB. 1996. Identification of Two Functionally Different Classes of Exocellulases. Biochemistry 35:586-592.

Bayer EA, Setter E, Lamed R. 1985. Organization and Distribution of the Cellulosome in *Clostridium-Thermocellum*. Journal of Bacteriology 163:552-559.

Bayer EA, Shimon LJW, Shoham Y, Lamed R. 1998. Cellulosomes - Structure and ultrastructure. Journal of Structural Biology 124:221-234.

Beguin P, Aubert JP. 1994. The Biological Degradation of Cellulose. Fems Microbiology Reviews 13:25-58.

Beldman G, Voragen AGJ, Rombouts FM, Pilnik W. 1988. Synergism in Cellulose Hydrolysis by Endoglucanases and Exoglucanases Purified from *Trichoderma viride*. Biotechnol Bioeng 31:173-178.

Beldman G, Voragen AGJ, Rombouts FM, Searle-van Leeuwen MF, Pilnik W. 1987. Adsorption and Kinetic Behavior of Purified Endoglucanases and Exoglucanases from *Trichoderma viride*. Biotechnol Bioeng 30:251-257.

Beltrame PL, Carniti P, Focher B, Marzetti A, Sarto V. 1984. Enzymatic-Hydrolysis of Cellulosic Materials - a Kinetic-Study. Biotechnol Bioeng 26:1233-1238.

Berglund GI, Gualfetti PJ, Requadt C, Gross LS, Bergfors T, Shaw A, Saldajeno M, Mitchinson C, Sandgren M. 2007. The Crystal Structure of the Catalytic Domain of *Thermobifida fusca* Endoglucanase Cel5A in Complex with Cellotetraose.

Bezerra RMF, Dias AA. 2004. Discrimination among eight modified Michaelis-Menten kinetics models of cellulose hydrolysis with a large range of substrate. Appl Biochem Biotechnol 112:173-184.

Bothwell MK, Daughhetee SD, Chaua GY, Wilson DB, Walker LP. 1997a. Binding Capacities for *Thermomonospora fusca* E_3, E_4 and E_5, the E_3 Binding Domain, and *Trichoderma reesei* CBH I on Avicel and Bacterial Microcrystalline Cellulose. Bioresource Technology 60:169-178.

Bothwell MK, Walker LP, Wilson DB, Irwin DC, Price M. 1993. Synergism Between Pure *Thermomonospora fusca* and *Trichoderma reesei* Cellulases. Biomass and Bioenergy 4:293-299.

Bothwell MK, Wilson DB, Irwin DC, Walker LP. 1997b. Binding Reversibility and Surface Exchange of *Thermomonospora fusca* E3 and E5 and *Trichoderma reesei* CBH I. Enzyme and Microbial Technology 20:411-417.

Brown RM. 2004. Cellulose structure and biosynthesis: What is in store for the 21st century? Journal of Polymer Science Part a-Polymer Chemistry 42:487-495.

Calza RE, Irwin DC, Wilson DB. 1985. Purification and Characterization of 2 Beta-1,4-Endoglucanases from *Thermomonospora-Fusca*. Biochemistry 24:7797-7804.

Chang VS, Holtzapple MT. 2000. Fundamental factors affecting biomass enzymatic reactivity. Appl Biochem Biotechnol 84-6:5-37.

Converse AO, Girard DJ. 1992. Effect of Substrate Concentration on Multicomponent Adsorption. Biotechnology Progress 8:587-588.

Converse AO, Matsuno R, Tanaka M. 1988. A Model of Enzyme Adsorption and Hydrolysis of Microcrystalline Cellulose with Slow Deactivation of the Adsorbed Enzyme. Biotechnol Bioeng 32:38-45.

Cornish-Bowden A. 2004. Fundamentals of Enzyme Kinetics. London:Portland Press. 422 p.

Cowling EB, Brown W. 1969. Structural Features of Cellulosic Materials in Relation to Enzymatic Hydrolysis. Advances in Chemistry Series 152-&.

Deshpande MV, Eriksson KE, Pettersson LG. 1984. An Assay for Selective Determination of Exo-1,4,-Beta-Glucanases in a Mixture of Cellulolytic Enzymes. Anal Biochem 138:481-487.

Din N, Forsythe IJ, Burtnick LD, Gilkes NR, Miller RC, Warren RAJ, Kilburn DG. 1994. The Cellulose-Binding Domain of Endoglucanase-a (Cena) from *Cellulomonas-Fimi* - Evidence for the Involvement of Tryptophan Residues in Binding. Molecular Microbiology 11:747-755.

Dong XM, Revol JF, Gray DG. 1998. Effect of microcrystallite preparation conditions on the formation of colloid crystals of cellulose. Cellulose 5:19-32.

Duggleby RG. 1995. Analysis of Enzyme Progress Curves by Nonlinear-Regression. Methods Enzymol 249:61-90.

Eijsink VGH, Vaaje-Kolstad G, Varum KM, Horn SJ. 2008. Towards new enzymes for biofuels: lessons from chitinase research. Trends Biotechnol 26:228-235.

Eriksson KE. 1978. Enzyme Mechanisms Involved in Cellulose Hydrolysis by Rot Fungus *Sporotrichum-Pulverulentum*. Biotechnol Bioeng 20:317-332.

Fan LT, Lee YH. 1983. Kinetic-Studies of Enzymatic-Hydrolysis of Insoluble Cellulose - Derivation of a Mechanistic Kinetic-Model. Biotechnol Bioeng 25:2707-2733.

Fan LT, Lee YH, Beardmore DR. 1981. The Influence of Major Structural Features of Cellulose on Rate of Enzymatic-Hydrolysis. Biotechnol Bioeng 23:419-424.

Fan LT, Lee Y-, Beardmore DR. 1980. Mechanism of the Enzymatic Hydrolysis of Cellulose: Effects of Major Structural Features of Cellulose on Enzymatic Hydrolysis. Biotechnol Bioeng 22:177-199.

Fellers TJ, Davidson MW. 2004. Theory of Confocal Microscopy. Olympus FluoView Resource Center 2009:

Field CB, Behrenfeld MJ, Randerson JT, Falkowski P. 1998. Primary production of the biosphere: Integrating terrestrial and oceanic components. Science 281:237-240.

Gan Q, Allen SJ, Taylor G. 2003. Kinetic dynamics in heterogeneous enzymatic hydrolysis of cellulose: an overview, an experimental study and mathematical modelling. Process Biochemistry 38:1003-1018.

Gardner KH, Blackwell J. 1974. Structure of Native Cellulose. Biopolymers 13:1975-2001.

Gharpuray MM, Lee YH, Fan LT. 1983. Structural Modification of Lignocellulosics by Pretreatments to Enhance Enzymatic-Hydrolysis. Biotechnol Bioeng 25:157-172.

Gilkes NR, Jervis E, Henrissat B, Tekant B, Jr. M, Warren RAJ, Kilburn DG. 1992. The Adsorption of Bacterial Cellulase and its Two Isolated Domains to Crystalline Cellulose. The Journal of Biological Chemistry 267:6743-6749.

Gong CS, Cao NJ, Du J, Tsao GT. 1999. Ethanol Production from Renewable Resources. Recent Progress in Bioconversion of Lignocellulosics 207-241.

Gong CS, Ladisch MR, Tsao GT. 1977. Cellobiase from *Trichoderma-Viride* - Purification, Properties, Kinetics, and Mechanism. Biotechnol Bioeng 19:959-981.

Gonzalez G, Caminal G, Demas C, Lopezsantin J. 1989. A Kinetic-Model for Pretreated Wheat Straw Saccharification by Cellulase. J Chem Technol Biotechnol 44:275-288.

Grethlein HE. 1985. The Effect of Pore-Size Distribution on the Rate of Enzymatic-Hydrolysis of Cellulosic Substrates. Bio-Technology 3:155-160.

Gruno M, Väljamäe P, Pettersson G, Johansson G. 2004. Inhibition of the *Trichoderma reesei* cellulases by cellobiose is strongly dependent on the nature of the substrate. Biotechnol Bioeng 86:503-511.

Gusakov AV, Sinitsyn AP. 1992. A Theoretical-Analysis of Cellulase Product Inhibition - Effect of Cellulase Binding Constant, Enzyme Substrate Ratio, and Beta-Glucosidase Activity on the Inhibition Pattern. Biotechnol Bioeng 40:663-671.

Gusakov AV, Sinitsyn AP, Gerasimas VB, Savitskene RY, Steponavichus YY. 1985a. A Product Inhibition Study of Cellulases from *Trichoderma-Longibrachiatum* using Dyed Cellulose. J Biotechnol 3:167-174.

Gusakov AV, Sinitsyn AP, Klyosov AA. 1985b. Kinetics of the Enzymatic-Hydrolysis of Cellulose .1. a Mathematical-Model for a Batch Reactor Process. Enzyme Microb Technol 7:346-352.

Gusek TW, Wilson DB, Kinsella JE. 1988. Influence of Carbon Source on Production of a Heat-Stable Protease from *Thermomonospora-Fusca* YX. Applied Microbiology and Biotechnology 28:80-84.

Haigler CH, Malcolmbrown R, Benziman M. 1980. Calcofluor White St Alters the Invivo Assembly of Cellulose Microfibrils. Science 210:903-906.

Helbert W, Chanzy H, Husum TL, Schulein M, Ernst S. 2003. Fluorescent cellulose microfibrils as substrate for the detection of cellulase activity. Biomacromolecules 4:481-487.

Henrissat B, Driguez H, Viet C, Schulein M. 1985. Synergism of Cellulases from *Trichoderma reesei* in the Degradation of Cellulose. Bio/Technology 3:722-726.

Henrissat B, Teeri TT, Warren RAJ. 1998. A scheme for designating enzymes that hydrolyse the polysaccharides in the cell walls of plants. Febs Letters 425:352-354.

Himmel ME, Ding S, Johnson DK, Adney WS, Nimlos MR, Brady JW, Foust TD. 2007. Biomass Recalcitrance: Engineering Plants and Enzymes for Biofuels Production. Science 315:804-807.

Hiroshi Ooshima,Masaru Sakata Yoshio Harano. 1983. Adsorption of cellulase from *Trichoderma viride* on cellulose. Biotechnol Bioeng 25:3103-3114.

Hlady V, Buijs J. 1996. Protein adsorption on solid surfaces. Curr Opin Biotechnol 7:72-77.

Holtzapple M, Cognata M, Shu Y, Hendrickson C. 1990. Inhibition of *Trichoderma-Reesei* Cellulase by Sugars and Solvents. Biotechnol Bioeng 36:275-287.

Holtzapple MT, Caram HS, Humphrey AE. 1984a. Determining the Inhibition Constants in the HCH-1 Model of Cellulose Hydrolysis. Biotechnol Bioeng 26:753-757.

Holtzapple MT, Caram HS, Humphrey AE. 1984b. A comparison of two empirical models for the enzymatic hydrolysis of pretreated poplar wood. Biotechnol Bioeng 26:936-941.

Holtzapple MT, Caram HS, Humphrey AE. 1984c. Determining the inhibition constants in the HCH-1 model of cellulose hydrolysis. Biotechnol Bioeng 26:753-757.

Holtzapple MT, Caram HS, Humphrey AE. 1984d. The HCH-1 model of enzymatic cellulose hydrolysis. Biotechnol Bioeng 26:775-780.

Hong J, Ye X, Zhang Y-P. 2007. Quantitative determination of cellulose accessibility to cellulase based on adsorption of a nonhydrolytic fusion protein containing CBM and GFP with its applications. Langmuir 23:12535-12540.

Hoshino E, Kanda T, Sasaki Y, Nisizawa K. 1992. Adsorption Mode of Exo-Cellulases and Endo-Cellulases from Irpex-Lacteus (Polyporus, Tulipiferae) on Cellulose with Different Crystallinities. Journal of Biochemistry 111:600-605.

Howell JA. 1978. Enzyme Deactivation during Cellulose Hydrolysis. Biotechnol Bioeng 20:847-863.

Howell JA, Stuck JD. 1975. Kinetics of Solka Floc Cellulose Hydrolysis by *Trichoderma-Viride* Cellulase. Biotechnol Bioeng 17:873-893.

Huang AA. 1975. Kinetic Studies on Insoluble Cellulose-Cellulase System. Biotechnol Bioeng 17:1421-1433.

Irwin D, Shin D-, Zhang S, Barr BK, Sakon J, Karplus PA, Wilson DB. 1998. Roles of the Catalytic Domain and Two Cellulose Binding Domains of *Thermomonospora fusca* E4 in Cellulose Hydrolysis. Journal of Bacteriology 180:1709-1714.

Irwin DC, Cheng M, Xiang BS, Rose JKC, Wilson DB. 2003. Cloning, expression and characterization of a family-74 xyloglucanase from *Thermobifida fusca.* European Journal of Biochemistry 270:3083-3091.

Irwin DC, Spezio M, Walker LP, Wilson DB. 1993. Activity Studies of 8 Purified Cellulases - Specificity, Synergism, and Binding Domain Effects. Biotechnol Bioeng 42:1002-1013.

Ishizawa CI, Davis MF, Schell DF, Johnson DK. 2007. Porosity and its effect on the digestibility of dilute sulfuric acid pretreated corn stover. J Agric Food Chem 55:2575-2581.

Jeoh T, Wilson DB, Walker LP. 2002. Cooperative and Competitive Binding in Synergistic Mixtures of *Thermobifida fusca* Cel5A, Cel6B and Cel9A. Biotechnol. Progress 18:760-769.

Jeoh, T., Wilson DB and Walker LP. 2006. Effect of Cellulase Mole Fraction and Cellulose Recalcitrance on Synergism in Cellulose Hydrolysis and Binding. Biotechnol. Progress 22: 270-277.

Jeoh T, Ishizawa CI, Davis MF, Himmel ME, Adney WS, Johnson DK. 2007. Cellulase digestibility of pretreated biomass is limited by cellulose accessibility. Biotechnol Bioeng 98:112-122.

Jervis EJ, Haynes CA, Kilburn DG. 1997. Surface diffusion of cellulases and their isolated binding domains on cellulose. J Biol Chem 272:24016-24023.

Jung H, Walker LP. 2003. Binding and Reversibility of *Thermobifida fusca* Cel5A, Cel6B and Cel48A and Their Respective Catalytic Domains to Bacterial Microcrystalline Cellulose. Biotechnol Bioeng 84:151-159.

Jung H, Walker LP. 2002. Binding of *Thermobifida fusca* CD_{Cel5A}, CD_{Cel6B} and CD_{Cel48A} to Easily Hydrolyzable and Recalcitrant Cellulose Fractions on BMCC. Enzyme and Microbial Technology 31:941-948.

Jung H, Wilson DB, Walker LP. 2002. Binding Mechanisms for *Thermobifida fusca* Cel5A, Cel6B and Cel48A Cellulose-Binding Modules on Bacterial Microcrystalline Cellulose. Biotechnol Bioeng 80:380-392.

Kim DW, Kim TS, Jeong YK, Lee JK. 1992. Adsorption-Kinetics and Behaviors of Cellulase Components on Microcrystalline Cellulose. Journal of Fermentation and Bioengineering 73:461-466.

King EL, Altman C. 1956. A Schematic Method of Deriving the Rate Laws for Enzyme-Catalyzed Reactions. J Phys Chem 60:1375-1378.

Kipper K, Väljamäe P, Johansson G. 2005. Processive action of cellobiohydrolase Cel7A from *Trichoderma reesei* is revealed as 'burst' kinetics on fluorescent polymeric model substrates. Biochem J 527.

Klemm D, Philipp B, Heinze T, Heinze U,Wagenknecht W. 1998. Comprehensive cellulose chemistry. I. Fundamentals and analytical methods. Weinheim: Wiley-VCH.

Krassig HA. 1993. Cellulose: structure,accessibility and reactivity. Yverland,Switzerland : Gordon & Breach

Kubicek CP. 1992. The Cellulase Proteins of *Trichoderma reesei*: Structure, Multiplicity, Mode of Action and Regulation of Formation. In: Fiechter A, editor. Enzymes and Products from Bacteria, Fungi and Plant Cells. Berlin, Heidelberg:Springer-Verlag. p 1.

Kyriacou A, MacKenzie CR, Neufeld RJ. 1987. Detection and Characterization of the Specific and Nonspecific Endoglucanases of *Trichoderma reesei*: Evidence Demonstrating Endoglucanase Activity by Cellobiohydrolase II. Enzyme and Microbial Tecnhnology 9:25-32.

Kyriacou A, Neufeld RJ, MacKenzie CR. 1989. Reversibility and Competition in the Adsorption of *Trichoderma reesei* Cellulase Components. Biotechnol Bioeng 33:631-637.

L. T. Fan YHLDRB. 1981. The influence of major structural features of cellulose on rate of enzymatic hydrolysis. Biotechnol Bioeng 23:419-424.

Ladisch MR, Lin KW, Voloch M, Tsao GT. 1983. Process Considerations in the Enzymatic-Hydrolysis of Biomass. Enzyme Microb Technol 5:82-102.

Lamed R, Bayer EA. 1988. The Cellulosome of *Clostridium-Thermocellum*. Advances in Applied Microbiology 33:1-46.

Lamed R, Naimark J, Morgenstern E, Bayer EA. 1987. Specialized Cell-Surface Structures in Cellulolytic Bacteria. Journal of Bacteriology 169:3792-3800.

Lee, S. B., Shin, H. S. and Ryu,D.D.Y. 1982. Adsorption of cellulase on cellulose : Effect of Physicochemical properties of cellulose on adsorption and rate of hydrolysis. Biotechnol. Bioeng. 24:2137-2153.

Lee YH, Fan LT. 1983. Kinetic-Studies of Enzymatic-Hydrolysis of Insoluble Cellulose .2. Analysis of Extended Hydrolysis Times. Biotechnol Bioeng 25:939-966.

Lee YH, Fan LT. 1982. Kinetic-Studies of Enzymatic-Hydrolysis of Insoluble Cellulose - Analysis of the Initial Rates. Biotechnol Bioeng 24:2383-2406.

Li Y, Irwin DC, Wilson DB. 2007. Processivity, Substrate Binding, and Mechanism of Cellulose Hydrolysis by *Thermobifida fusca* Cel9A. Appl. Environ. Microbiol. 73:3165-3172.

Lin E, Wilson DB. 1987. Regulation of Beta-1,4-Endoglucanase Synthesis in *Thermomonospora-Fusca*. Applied and Environmental Microbiology 53:1352-1357.

Linder M, Teeri TT. 1997. The Roles and Function of Cellulose-Binding Domains. Journal of Bacteriology 57:15-28.

Lippincott-Schwartz J, Snapp E, Kenworthy A. 2001. Studying protein dynamics in living cells. Nat Rev Mol Cell Biol 2:444-456.

Lynd LR, Weimer PJ, van Zyl WH, Pretorius IS. 2002. Microbial Cellulose Utilization: Fundamentals and Biotechnology. Microbiol Mol Biol Rev 66:506-577.

Ma A, Hu Q, Qu Y, Bai Z, Liu W, Zhuang G. 2008. The enzymatic hydrolysis rate of cellulose decreases with irreversible adsorption of cellobiohydrolase I. Enzyme Microb Technol 42:543-547.

Mandels M. 1985. Applications of Cellulases. Biochemical Society Transactions 13:414-416.

Mansfield SD, Mooney C, Saddler JN. 1999. Substrate and enzyme characteristics that limit cellulose hydrolysis. Biotechnology Progress 15:804-816.

Matthews JF, Skopec CE, Mason PE, Zuccato P, Torget RW, Sugiyama J, Himmel ME, Brady JW. 2006. Computer simulation studies of microcrystalline cellulose I beta. Carbohydrate Research 341:138-152.

Mayer F, Coughlan MP, Mori Y, Ljungdahl LG. 1987. Macromolecular Organization of the Cellulolytic Enzyme Complex of *Clostridium-Thermocellum* as Revealed by Electron-Microscopy. Applied and Environmental Microbiology 53:2785-2792.

Mcginnis K, Wilson DB. 1993. Disulfide Arrangement and Chemical Modification of Beta-1,4-Endoglucanase-E2 from *Thermomonospora-Fusca*. Biochemistry (N Y) 32:8151-8156.

Medve J, Karlsson J, Lee D, Tjerneld F. 1998. Hydrolysis of Microcrystalline Cellulose by Cellobiohydrolase I and Endoglucanase II from *Trichoderma reesei*: Adsorption, Sugar Production Pattern, and Synergism of the Enzymes. Biotechnol Bioeng 59:621-634.

Medve J, Stahlberg J, Tjerneld F. 1997. Isotherms for Adsorption of Cellobiohydrolase I and II from *Trichoderma reesei* on Microcrystalline Cellulose. Applied Biochemistry and Biotechnology 66:39-56.

Moran-Mirabal JN, Santhanam N, Corgie SC, Craighead HG, Walker LP. 2008. Immobilization of Cellulose Fibrils on Solid Substrates for Cellulase-Binding Studies Through Quantitative Fluorescence Microscopy. Biotechnol Bioeng 101:1129-1141.

Neuman RP, Walker LP. 1992. Solute Exclusion from Cellulose in Packed-Columns - Experimental Investigation and Pore Volume Measurements. Biotechnol Bioeng 40:218-225.

Nidetzky B, Claessens M. 1994. Specific Quantification of *Trichoderma reesei* Cellulases in Reconstituted Mixtures and its Application to Cellulase-Cellulose Binding Studies. Biotechnol Bioeng 44:961-966.

Nidetzky B, Steiner W. 1993. A New Approach for Modeling Cellulase Cellulose Adsorption and the Kinetics of the Enzymatic-Hydrolysis of Microcrystalline Cellulose. Biotechnol Bioeng 42:469-479.

Nidetzky B, Steiner W, Hayn M, Claeyssens M. 1994. Cellulose Hydrolysis by the Cellulases from *Trichderma reesei:* a New Model for Synergistic Interaction. Biochemical Journal 298:705-710.

Nishiyama Y, Langan P, Chanzy H. 2002. Crystal structure and hydrogen-bonding system in cellulose 1 beta from synchrotron X-ray and neutron fiber diffraction. Journal of the American Chemical Society 124:9074-9082.

Nutt A, Sild V, Pettersson G, Johansson G. 1998. Progress curves. A mean for functional classification of cellulases. European Journal of Biochemistry 258:200-206.

Ohmine K, Ooshima H, Harano Y. 1983. Kinetic-Study on Enzymatic-Hydrolysis of Cellulose by Cellulase from *Trichoderma-Viride*. Biotechnol Bioeng 25:2041-2053.

Okazaki M, Mooyoung M. 1978. Kinetics of Enzymatic-Hydrolysis of Cellulose - Analytical Description of a Mechanistic Model. Biotechnol Bioeng 20:637-663.

O'Neill MA, York WS. 2003. The composition and structures of primary cell walls. In: Rose JKC, editor. The Plant Cell Wall. Boca Raton, FL:CRC Press. p 1-54.

Palonen H, Tenkanen M, Linder M. 1999. Dynamic interaction of *Trichoderma reesei* cellobiohydrolases Ce16A and Ce17A and cellulose at equilibrium and during hydrolysis. Applied and Environmental Microbiology 65:5229-5233.

Pauly M, Keegstra K. 2008. Cell-wall carbohydrates and their modification as a resource for biofuels. Plant J 54:559-568.

Pinto R, Amaral AL, Carvalho J, Ferreira EC, Mota M, Gama M. 2007. Development of a method using image analysis for the measurement of cellulose-binding domains adsorbed onto cellulose fibers. Biotechnol Prog 23:1492-1497.

Pinto R, Amaral AL, Ferreira EC, Mota M, Vilanova M, Ruel K, Gama M. 2008. Quantification of the CBD-FITC conjugates surface coating on cellulose fibres. BMC Biotechnol 8:1.

Rabinovich ML. 2006. Ethanol production from materials containing cellulose: The potential of Russian research and development. Appl Biochem Microbiol 42:1-26.

Reese ET, Siu RGH, Levinson HS. 1950. The Biological Degradation of Soluble Cellulose Derivatives and its Relationship to the Mechanism of Cellulose Hydrolysis. Journal of Bacteriology 59:485-496.

Rouvinen J, Bergfors T, Teeri T, Knowles JKC, Jones TA. 1990. 3-Dimensional Structure of Cellobiohydrolase II from *Trichoderma-Reesei*. Science 249:380-386.

Ryu DDY, Kim C, Mandels M. 1984. Competitive Adsorption of Cellulase Components and its Significance in Synergistic Mechansim. Biotechnol Bioeng 26:488-496.

Ryu DDY, Lee SB. 1986. Enzymatic-Hydrolysis of Cellulose - Determination of Kinetic-Parameters. Chem Eng Commun 45:119-134.

Ryu DDY, Lee SB, Tassinari T, Macy C. 1982. Effect of Compression Milling on Cellulose Structure and on Enzymatic-Hydrolysis Kinetics. Biotechnol Bioeng 24:1047-1067.

Sakon J, Irwin D, Wilson DB, Karplus PA. 1997. Structure and mechanism of endo/exocellulase E4 from *Thermomonospora fusca*. Nat Struct Mol Biol 4:810-818.

Scalettar BA, Abney JR, Owicki JC. 1988. Theoretical Comparison of the Self-Diffusion and Mutual Diffusion of Interacting Membrane-Proteins. Proc Natl Acad Sci U S A 85:6726-6730.

Schatten G, Pawley JB. 1988. Advances in Optical, Confocal, and Electron-Microscopic Imaging for Biomedical Researchers. Science 239:G164-&.

Schubert C. 2006. Can biofuels finally take center stage? Nat Biotechnol 24:777-784.

Schwarz WH. 2001. The cellulosome and cellulose degradation by anaerobic bacteria. Applied Microbiology and Biotechnology 56:634-649.

Scott S, Dagher M, Miles E, Tilman A. 2002. Identifying energy needs and biomass resources within the state of Mississippi. 2009:6.

Shen H, Meinke A, Tomme P, Damude HG, Kwan E, Kilburn DG, Miller RC, Warren RAJ, Gilkes NR. 1995. *Cellulomonas fimi* cellobiohydrolases. Enzymatic Degradation of Insoluble Carbohydrates. p 174-196.

Shoemaker S, Watt K, Tsitovsky G, Cox R. 1983. Characterization and Properties of Cellulases Purified from *Trichoderma-Reesei* Strain-L27. Bio-Technology 1:687-690.

Shoham Y, Lamed R, Bayer EA. 1999. The cellulosome concept as an efficient microbial strategy for the degradation of insoluble polysaccharides. Trends in Microbiology 7:275-281.

Spezio M, Wilson D, Karplus PA. 1993. Crystal structure of the catalytic domain of a thermophilic endocellulase. Biochemistry 32:9906-9916.

Spiridonov NA, Wilson DB. 2001. Cloning and biochemical characterization of BglC, a beta-glucosidase from the cellulolytic actinomycete *Thermobifida fusca*. Current Microbiology 42:295-301.

Spiridonov NA, Wilson DB. 1998. Regulation of Biosynthesis of Individual Cellulases in *Thermomonospora fusca*. Journal of Bacteriology 180:3529-3532.

Stahlberg J, Johansson G, Petterson G. 1991. A New Model for Enzymatic Hydrolysis of Cellulose Based on the Two-Domain Structure of Cellobiohydrolase I. Bio/Technology 9:286-290.

Stephanopoulos G. 2007. Challenges in Engineering Microbes for Biofuels Production. Science; Science 315:801-804.

Stone JE, Scallan AM, Donefer E, Ahlgren E. 1969. Digestibility as a simple finction of a molecule of a similar size to a cellulase enzyme. Adv. Chem. Ser. 95:219-241.

Teeri TT. 1997. Crystalline cellulose degradation: New insight into the function of cellobiohydrolases. Trends in Biotechnology 15:160-167.

Teleman A, Koivula A, Reinikainen T, Valkeajarvi A, Teeri TT, Drakenberg T, Teleman O. 1995. Progress-Curve Analysis shows that Glucose Inhibits the Cellotriose Hydrolysis Catalyzed by Cellobiohydrolase II from *Trichoderma-Reesei*. Eur J Biochem 231:250-258.

Tomme P, Warren RAJ, Gilkes NR. 1995a. Cellulose hydrolysis by bacteria and fungi. London:Academic Press. p 2-81.

Tomme P, Warren RAJ, Miller RC, Kilburn DG, Gilkes NR. 1995b. Cellulose-binding domains: Classification and properties. Enzymatic Degradation of Insoluble Carbohydrates. p 142-163.

Tormo J, Lamed R, Chirino AJ, Morag E, Bayer EA, Shoham Y, Steitz TA. 1996. Crystal structure of a bacterial family-III cellulose-binding domain: A general mechanism for attachment to cellulose. Embo Journal 15:5739-5751.

Valjamae P, Sild V, Nutt A, Pettersson G, Johansson G. 1999. Acid hydrolosis of bacterial cellulose reveals different modes of synergistic action between cellobiohydrolase I and endoglucanase I. European Journal of Biochemistry 266:327-334.

Valjamae P, V S, Pettersson G, Johansson G. 1998. The Initial Kinetics of Hydrolysis by Cellobiohydrolases I and II is Consistent with a Cellulose Surface - Erosion Model. European Journal of Biochemistry 253:469-475.

Varrot A, Schulein M, Davies GJ. 1999. Structural changes of the active site tunnel of *Humicola insolens* cellobiohydrolase, Cel6A, upon oligosaccharide binding. Biochemistry 38:8884-8891.

Viëtor RJ, Mazeau K, Lakin M, Pérez S. 2000. A priori crystal structure prediction of native celluloses. Biopolymers 54:342-354.

Vinzant TB, Adney WS, Decker SR, Baker JO, Kinter MT, Sherman NE, Fox JW, Himmel ME. 2001. Fingerprinting *Trichoderma reesei* hydrolases in a commerical cellulase preparation. Applied Biochemistry and Biotechnology 91-3:99-107.

Walker, L. P., Wilson, D. B. & Irwin,D.C. 1990. Measuring fragmentation of cellulose by *Thermomonospora fusca* cellulase. Enzyme Microb. Technol. 12:378-386.

Walker LP, Belair CD, Wilson DB, Irwin DC. 1993. Engineering Cellulase Mixtures by Varying the Mole Fraction of *Thermomonospora fusca* E5 and E3, *Trichoderma reesei* CBH I, and *Caldocellum saccharolyticum* B-Glucosidase. Biotechnol Bioeng 42:1019-1028.

Walker LP, Wilson DB. 1991. Enzymatic Hydrolysis of Cellulose: An Overview. Bioresource Technology 36:3-14.

Watson DL, Wilson DB, Walker LPW. 2002. Synergism in Binary Mixtures of *Thermobifida fusca* Cellulases Cel6B, Cel9A and Cel5A on BMCC and Avicel. Applied Biochemistry and Biotechnology 101:97-111.

Wilson DB. 2004. Studies of T*hermobifida fusca* plant cell wall degrading enzymes. The Chemical Record 4:72-82.

Wilson DB. 1988. Cellulases of *Thermomonospora fusca*. Methods in Enzymology 160:314-323.

Wilson DB, Irwin DC. 1999. Genetics and Properties of Cellulases. Advances in Biochemical Engineering Biotechnology: Recent Progress in Bioconversion 65:1-21S.

Wood TM. 1988. Preparation of Crystalline, Amorphous, and Dyed Cellulase Substrates. Methods in Enzymology 160:19-25.

Wood TM. 1975. Properties and Mode of Action of Cellulases. Biotechnol Bioeng Symposium 5:111-137.

Wood TM. 1968. Cellulolytic Enzyme System of *Trichoderma Koningii* - Separation of Components Attacking Native Cotton. Biochem J 109:217-&.

Wood TM, Bhat KM. 1988. Methods for Measuring Cellulase Activities. Methods in Enzymology 160:87-112.

Wood TM, McCrae SI. 1979. Synergism Between Enzymes Involved in the Solubilization of Native Cellulose. In: Brown RD,Jr and Jurasek L, editors. Hydrolysis of Cellulose: Mechanisms of Enzymatic and Acid Catalysis. Washington, D. C.:American Chemical Society. p 181-209.

Wood TM, Mccrae SI. 1978. Cellulase of *Trichoderma-Koningii* - Purification and Properties of some Endoglucanase Components with Special Reference to their Action on Cellulose when Acting Alone and in Synergism with Cellobiohydrolase. Biochem J 171:61-72.

Wood TM, Mccrae SI, Bhat KM. 1989. The Mechanism of Fungal Cellulase Action - Synergism between Enzyme Components of *Penicillium-Pinophilum* Cellulase in Solubilizing Hydrogen Bond-Ordered Cellulose. Biochem J 260:37-43.

Woodward J. 1991. Synergism in Cellulase Systems. Bioresourse Technology 36:67-75.

Woodward J, Lima M, Lee NE. 1988a. The Role of Cellulase Concentration in Determining the Degree of Synergism in the Hydrolysis of Microcrystalline Cellulose. Biochemical Journal 255:895-899.

Woodward J, Hayes MK, Lee NE. 1988b. Hydrolysis of Cellulose by Saturating and Non-Saturating Concentrations of Cellulase: Implications for Synergism. Bio/Technology 6:301-304.

Wyman CE, Dale BE, Elander RT, Holtzapple M, Ladisch MR, Lee YY. 2005. Comparative sugar recovery data from laboratory scale application of leading pretreatment technologies to corn stover. Bioresource Technology 96:2026-2032.

Zhang S, Barr BK, Wilson DB. 2000. Effects of noncatalytic residue mutations on substrate specificity and ligand binding of *Thermobifida fusca* endocellulase Cel6A. European Journal of Biochemistry 267:244-252.

Zhang S, Lao G, Wilson DB. 1995. Characterization of a *Thermomonospora fusca* Exocellulase. Biochemistry 34:3386-3395.

Zhang S, Wolfgang DE, Wilson DB. 1999. Substrate heterogeneity causes the nonlinear kinetics of insoluble cellulose hydrolysis. Biotechnol Bioeng 66:35-41.

Zhou W, Irwin DC, Escovar-Kousen J, Wilson DB. 2004. Kinetic Studies of *Thermobifida fusca* Cel9A Active Site Mutant Enzymes. Biochemistry 43:9655-9663.

Zhu L, O'Dwyer JP, Chang VS, Granda CB, Holtzapple MT. 2008. Structural features affecting biomass enzymatic digestibility. Bioresour Technol 99:3817-3828.

CHAPTER 3

A HIGH-THROUGHPUT ASSAY TO MEASURE CELLULASE BINDING AND SYNERGISM IN TERNARY MIXTURES[1]

Abstract

A rapid high-throughput cellulase binding assay using microwell plates was developed to quantify cellulose-bound fractions of fluorescently labeled *Thermobifida fusca* cellulases Cel5A, Cel6B and Cel9A alone or in ternary mixtures. These cellulases were labeled with Alexa Fluor® 594, Alexa Fluor® 350 and Alexa Fluor® 488, respectively, without losses in activity on bacterial micro-crystalline cellulose (BMCC). Controlled experiments were conducted (1) to ascertain whether individual labeled cellulase species could be accurately quantified using[1] 96-well micro plates; (2) to investigate whether the fluorescence emission of one labeled cellulase species could be reliably distinguished from the fluorescence emissions of other labeled cellulases in ternary mixtures to accurately quantify individual cellulases; (3) to verify the thermostability of the fluorescence of labeled cellulases; and (4) to assess cooperative or competitive cellulase binding in ternary mixtures. Experiments demonstrated that microwell plates yielded accurate measurements of cellulase concentrations in single cellulase reactions as well as in multi-cellulase mixtures. In addition, fluorescence remained stable at 50°C over the entire 4h time course of the experiments. This high-throughput measurement system also revealed 13% greater binding for Cel6B-AF350 and 11% lower binding for Cel9A-AF488 in ternary mixtures than was observed when these cellulases individually reacted with cellulose.

---

[1]This work has been published as Santhanam N, Walker LP. 2008. A high-throughput assay to measure cellulase binding and synergism in ternary mixtures. Biol Eng 1:1–19

Overall, the cellulases did not exhibit any cooperative or competitive binding in ternary synergistic mixtures.

3.1 Introduction

A "cellulase cocktail," a reconstituted mixture of cellulases that exploits the concerted action of the various catalytic modes of cellulases (exocellulases, endocellulases and processive endocellulases) is necessary for efficient hydrolysis of crystalline cellulose to fermentable sugars (Irwin et al. 1993; Walker et al. 1993). Individual cellulases exhibit very low specific activities on microcrystalline cellulose. However, the ratio of cellulases in crude mixtures secreted by micro-organisms is such that the activity of the crude mixture is much higher than one would predict from summing the activities of the individual cellulases. The enhanced activity displayed by a mixture of cellulases is termed synergism. A measure of synergism, the Degree of Synergistic Effect (DSE) is defined as the ratio of the activity of a cellulase mixture to the sum of activities of individual cellulases.

Several factors can influence the synergism observed in cellulase mixtures including: (1) the ratio of individual cellulases and the total molar cellulase loading (Henrissat et al. 1985; Woodward et al. 1988b; Woodward et al. 1988a; Walker et al. 1993; Nidetzky and Claessens 1994; Baker et al. 1998; Watson et al. 2002; Jeoh et al. 2002) (2) the accessibility of the substrate (Lee et al. 1982; Ryu et al. 1984; Kyriacou, A., et al. 1989; Medve et al. 1994) and (3) the physico-chemical properties of the substrate (Fan et al. 1980; Henrissat et al. 1985). It has been argued that due to their different binding affinities and modes of attack, the bound cellulase fractions can be very different from the cellulase fractions of the loaded cocktail (Beldman et al. 1987; Bothwell et al. 1993; Medve et al. 1994; Kim et al. 1995). Thus, assessing the bound

cellulase fractions is essential to understanding synergistic interactions (Sharrock 1988; Ooshima et al.1991; Jeoh et al. 2002).

Studies on the effect of enzymatic pretreatment of the substrate led Nidetzky et al. (1993) to conclude that a sequential attack was as effective in hydrolyzing the substrate as a simultaneous attack by two enzymes. They also observed that the adsorption of individual cellulase components onto enzymatically pretreated substrate remained unchanged compared to that on untreated substrate. A similar study (Jeoh et al. 2006) on the effect of binary mixtures of *Thermobifida fusca* cellulases Cel5A,Cel6B and Cel9A on enzymatically pre-hydrolyzed BMCC revealed, however, that the DSE values for all the mixtures were lower on pre-hydrolyzed BMCC than on untreated BMCC. This could imply that a simultaneous concerted action, in the presence of the endocellulase, is required for continuous synergistic hydrolysis. An important question yet unanswered is how the DSE correlates with the bound fractions of the components of a ternary mixture.

Both indirect and direct methods have been used to measure the concentration of multiple cellulases in the supernatant to determine the bound fractions of cellulases in mixtures. Indirect methods employing cellulase activity measurements on substrates such as carboxymethylcellulose (CMC) and filter paper (FP) have been used to distinguish endocellulases from exocellulases (Walker et al. 1993; Ooshima et al. 1991; Ryu et al. 1984, Bothwell et al. 1993). These assays are not very specific as exoglucanases also release reducing sugars from CMC to some extent (Wood 1975). Chromophoric substrates such as 2'-chloro, 4'-nitrophenyl β-D-glycosides of lactose, cellobiose and cellotriose have been used in activity studies to specifically differentiate the cellulases of *Trichoderma reesei* (Van Tilbeurgh and Claeyssens 1985; Van Tilbeurgh et al. 1988; Nidetzky and Claessens 1994). However, the kinetic

constants of each individual cellulase on these substrates need to be determined with the appropriate use of inhibitors in order to apply this technique.

Direct methods of measuring cellulase activity include enzyme linked immunosorbent assays (ELISA) (Kolbe and Kubicek 1990; Nieves et al. 1995; Spiridonov and Wilson 1998; Buhler 1991), radiolabeling (Kyriacou et al. 1989, Bothwell et al. 1993), fast protein liquid chromatography (FPLC) (Medve et al. 1998) and capillary electrophoresis (Jorgensen et al. 2003). While immunoassays are extremely specific, they require the production of antibodies exclusive to the enzymes being studied by a laborious process. Radiolabeling techniques are very sensitive, but their use in mixtures is limited to the number of different radio isotopes available for labeling proteins. Capillary electrophoresis suffers from the disadvantage of protein interaction with the capillary surface at low pH (Jorgensen et al. 2003). More recently, fluorescently labeled cellulases have been employed to study cellulase binding and synergism in binary mixtures (Jeoh et al. 2002). A key feature of this method is that the concentration of bound cellulase is measured directly from the fluorescence of cellulases bound to substrate. Fluorescence labeling has the advantage of high sensitivity, a greater range of linearity and the potential for conducting simultaneous measurements of multiple species by using different colored fluorescent probes.

Jeoh et al. (2002) conducted their binding reactions individually in spin-filter tubes and samples needed to be transferred one-by-one to 96-well plates for subsequent fluorescence measurements. This task is labor intensive requiring several days of experimentation and is not conducive to rapid assay of multiple cellulases. Also, their study was limited to binary mixtures. Our research group has been particularly interested in having an assay platform that would allow the simultaneous evaluation of ternary mixtures composed of “classical” endo- and exo-cellulases, and a

processive endocellulase. Thus, the major objective of this study was to develop a high-throughput cellulase binding assay using 96 well plates that reduced the logistics of conducting hydrolysis, binding and synergism studies down to one experimental platform. In moving to the 96-well platform, there was a need to verify that temperature had no effect on sample fluorescence. In addition, there was a need to quantify the effect of the substrate autofluorescence on cellulase concentration measurements, and to test for overlaps in the excitation and emission wavelengths of the three fluorophores used to label the cellulases. A final objective was to verify that this high-throughput method yielded hydrolysis, binding and synergism results consistent with results obtained by Jeoh et al. (2002) using spin-filters, and to assess cellulase bound fraction on BMCC and the DSE of ternary cellulase mixtures.

3.2 Materials and Methods

3.2.1 Preparation of Bacterial Microcrystalline Cellulose (BMCC)

BMCC (Cellulon, Microfibrous Cellulose, Industrial Grade – Prilled, Lot # 61025P, 18.1% solids) was obtained as a gift from CP Kelco (Atlanta, GA). Twenty-five grams were resuspended in 500 ml distilled water and stirred overnight at 4°C. Sodium azide (0.02%) was added to prevent microbial growth. The suspension was rinsed five times with 0.5 L of distilled water on a scintered glass filter with frequent stirring. BMCC was then resuspended in 350-ml distilled water and the concentration was determined by measuring the dry weight of triplicate aliquots.

3.2.2 Fluorescent labeling of Thermobifida fusca cellulases:

The *T. fusca* cellulases Cel5A (an endocellulase), Cel6B (an exocellulase) and Cel9A (a processive endocellulase) used in this study were prepared as described by Jeoh et al. (2002). Cel5A, Cel6B and Cel9A were labeled using the Alexa Fluor® 594

(AF594), Alexa Fluor® 350 (AF350) and Alexa Fluor® 488 (AF488) Protein Labeling kits respectively (Invitrogen Corporation, Carlsbad, CA). Characteristics of the fluorophores have been summarized in Table 3.1. These three fluorophores were selected to minimize overlap of their respective emission spectra so they could be distinguished from each other by the use of appropriate optical filters. Stock enzyme solutions were diluted to 2mg/ml in 0.1 M Sodium Bicarbonate, pH 8.3, and 300 µl were added to one dye vial provided with the Alexa Fluor® Protein Labeling kit containing the desired dye. One tenth of the reaction volume (30 µl) of 1M Sodium Bicarbonate, pH 8.3, was added to the same vial to further raise the pH of the reaction mixture, since the ester moieties in the dye react efficiently with primary amines on the protein only at an alkaline pH. The reaction mixture was stirred for 1 h at room temperature.

3.2.3 Purification of labeled proteins:

Separation of unconjugated dye from labeled protein was performed using 0.5ml Zeba Desalt Spin Columns (Pierce Biotechnology, Inc., Rockford, IL). The spin columns were first centrifuged to remove the resin storage buffer (PBS, pH 7.2). In order to store the labeled cellulases in 50mM sodium acetate (pH 5.5), buffer exchange was performed on the columns by four washes with sodium acetate buffer. The columns were placed in new collection tubes and 60-75 µl of the labeling reaction mixture were carefully applied to the top of the resin and centrifuged to separate labeled cellulases from unconjugated dye. In order to determine the capacity of the spin columns to retain unconjugated dye, a control mixture of cellulase and dye was prepared at the same concentration as used for the labeling reaction but using a buffer

Table 3.1 Physical and optical properties of fluorophores and cellulases

Species	Extinction Coefficient ε (M-1)	Correction Factor (C.F.)	Molecular Weight (Daltons)	Excitation Wavelength (nm)	Emission Wavelenth (nm)
AF 594	73000	0.56	820	590	617
AF 350	19000	0.19	410	346	442
AF 488	73000	0.11	643	494	519
Cel5A	97100	-	46300		-
Cel6B	115150	-	59600		-
Cel9A	210670	-	90400		-

at pH < 8.3. The reactive groups on the dye are pH sensitive, so the buffer pH ensured that the control mixture was not conducive for dye–protein conjugation. An aliquot of this control mixture was saved, the rest was applied to a spin column and the flow through was collected. The absorbance spectrum of the saved aliquot was compared with that of the flow through.

3.2.4 Determination of cellulase concentrations and degree of labeling of cellulase

The concentration of labeled cellulase (*P*) was calculated as follows:

$$P = \frac{\left\lfloor A_{280} - A_{dye} \times CF \right\rfloor \times DF}{\varepsilon_{protein}} \qquad (3.1)$$

where:

P = Labeled cellulase concentration, M

$C.F.$ = Correction factor for absorbance of the dye at 280 nm

$D.F.$ = Dilution factor

A_{280} = Absorbance of the conjugate at 280 nm

A_{dye} = Absorbance of the conjugate at the excitation maximum of the dye

$\varepsilon_{protein}$ = Extinction coefficient of the protein (M^{-1}).

The degree of labeling (moles dye per mole of protein) of each conjugated cellulase was determined as below:

$$DoL = \frac{A_{dye} \times DF}{\varepsilon_{dye} \times P} \qquad (3.2)$$

where

$D.o.L$ = degree of labeling (dimensionless)

ε_{dye} = Extinction coefficient of the dye (M^{-1})

All constants used in equations 3.1 and 3.2 are listed in Table 3.1.

3.2.5 Activity of labeled cellulases

To verify that there was no loss of activity due to labeling, the activities of labeled and unlabeled cellulases on 1mg/ml BMCC in 50mM sodium acetate buffer (pH 5.5) over 18hr at 50°C were measured. Reactions were stopped by centrifugation and the reducing sugars produced were measured using the PAHBAH method as described by Lever (1972). Briefly, 5% parahydroxybenzoic acid hydrazide in 0.5M HCl was mixed with 0.5M NaOH in a ratio of 1:4 by volume, immediately before the assay. A 1.5 ml aliquot of this mixture was added to 50 µl of reaction supernatant and samples were boiled for 6 minutes followed by absorbance measurement at 410 nm. A standard curve in the range of 0.4-2.4 mM glucose was prepared using 1 mg/ml glucose standard solution.

3.2.6 Quantification of fluorescently labeled cellulases

A Synergy HT Multi-Detection Microplate Reader (BioTek Instruments, Inc., Winooski, VT) was used for all fluorescence and absorbance measurements. Automatic sensitivity adjustment available in the KC4 software was used for all measurements. A brief description of the fluorescence data acquisition by the Synergy HT is as follows. The emitted photons from the fluorophores are collected by optical fibers. The excitation beam reflected by the wells was blocked by an emission filter but allowed the emission beam alone to pass through the well. The emission beam is collected and amplified by a Photo Multiplier Tube (PMT) that generates an electrical signal .The degree of amplification is related to the "sensitivity parameter" set in the software.

The following relationship (Biotek , Winooski, VT) is applied for sensitivity adjustment of fluorescence measurements :

$$M = \left(\frac{S}{S_0} \right)^{7.8} \qquad (3.3)$$

where,

S = Measured sensitivity (dimensionless)

S0 = Default sensitivity (dimensionless)

M = Multiplication factor for sensitivity adjustment (dimensionless)

Fluorescence values where calculated using the following equation:

$$F = M \times F_0 \tag{3.4}$$

where,

F = Fluorescence value (Relative Fluorescence Units, RFU)

F0 = Default fluorescence value (RFU)

The fluorescence read obtained as raw data is the average number obtained thus, the scale (0 to 50,000 RFU) being proportional to the charge of the integrating circuit. Automatic sensitivity adjustment was enabled for all measurements.

3.2.7 Precision of fluorescence quantification

The precision of fluorescence quantification was determined by comparing the concentration obtained from the standard curves with the known concentration from absorbance measurements of the stock labeled cellulases.

3.2.8 Crosstalk between fluorophores

In order to examine the overlap of the excitation and emission wavelengths of the three fluorophores, mixture standard curves were prepared by serial dilutions of equimolar ternary mixtures of the labeled cellulases and compared with individual standard curves at same enzyme concentrations.

3.2.9 Background fluorescence

To determine the significance of background signal due to BMCC, fluorescence of control samples containing only BMCC, was measured at all three wavelengths and subtracted from the corresponding total fluorescence.

3.2.10 Thermostability of labeled cellulases:

The effect of temperature on the enzyme mixture fluorescence was observed for the following temperatures: 22, 30, 40 and 50°C. Standard curves of measured fluorescence were obtained for labeled cellulases incubated at these temperatures and times of 0.5, 1, 2, 3, 4 and 5 h.

3.2.11 Binding assays

All binding assays were conducted in black AcroPrep™ (Pall Life Sciences, Ann Arbor, MI) 96 wells filter plates with 0.45 μm membranes made of hydrophilic polypropylene as shown in Figure 3.1. To examine the extent of any post-filtration non-specific binding of cellulases to these membranes, the fluorescence of samples was measured before and after filtration and compared to a control well whose contents were not filtered through.

For all binding reactions 200-μl of individual cellulases or cellulase mixture were added to the wells to achieve a total cellulase loading of 0.5 μM. For cellulase mixtures, the proportion of Cel5A-AF594 was fixed at 10% of the total enzyme loading while the input ratio of the other two cellulases was varied between 0-90%. The Cel5A-AF594 proportion was fixed because previous studies have shown that only 10% of Cel5A-AF594 is required to obtain maximum synergistic effects on BMCC (Watson et al. 2002; Jeoh et al. 2006).

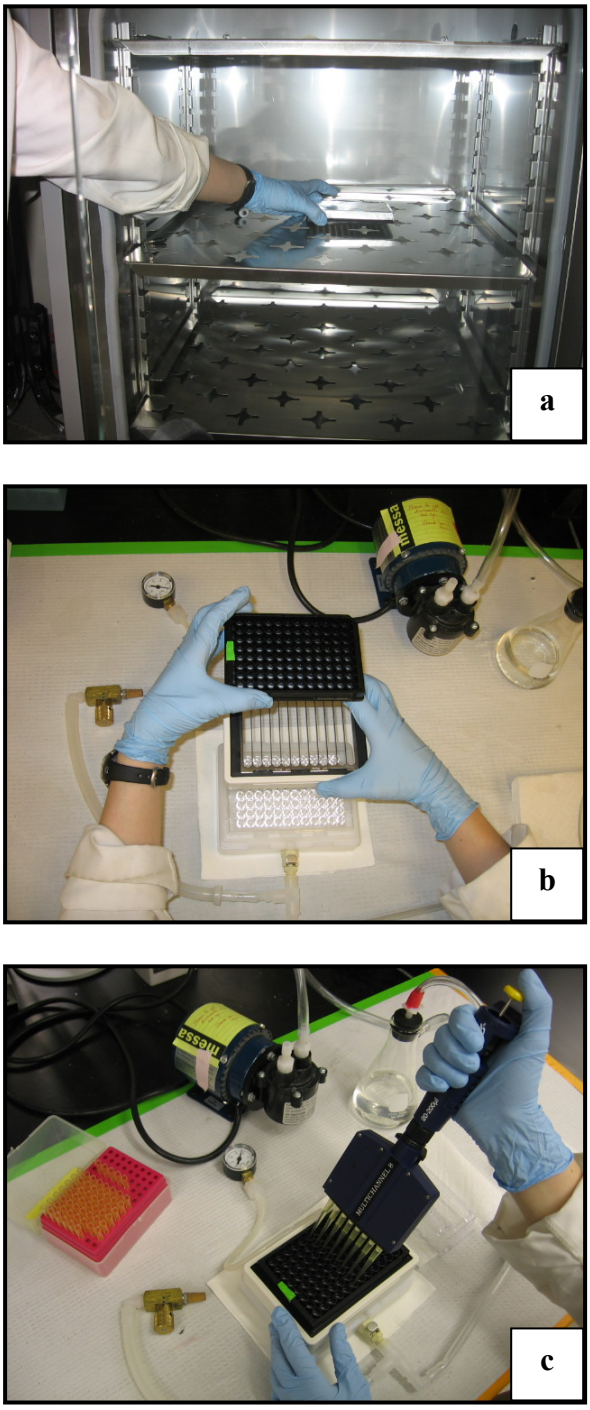

Figure 3.1 Plate binding assay (a) all binding reactions were conducted at 50°C; (b) the reactions were stopped by filtration using a Millipore MultiScreen Filtration System Manifold; and (c) retentates were resuspended in 250 µl buffer.

All ternary mixture studies were conducted at non-saturating total enzyme loadings in order for them to lie in the range necessary for observing synergism (Jeoh et al 2002). The plates were pre-incubated with BMCC at 50°C for 30 min. The reactions were started by adding 50 µl of 5mg/ml BMCC to all wells for a substrate concentration of 1 mg/ml. Reactions were carried out for 1, 2, 3 and 4 h. Before termination of reactions, the total fluorescence of all wells at each emission wavelength was measured to determine the initial total cellulase loadings, thus eliminating the need for enzyme blanks for measuring initial cellulase concentrations. The reactions were stopped by filtration with a Millipore MultiScreen Filtration System Manifold (Millipore, Billerica, MA) at a vacuum manifold pressure of 15" Hg. The filtrates were collected in clear 96 well plates and frozen for reducing sugar measurements. The retentates were re-suspended in 250-µl of 50mM sodium acetate buffer and transferred to a clean black 96-well plate for bound cellulase fluorescence measurements. The total bound cellulase concentration for mixtures was obtained by summing the measured bound cellulase concentration of each cellulase in the mixture. Standard curves for the labeled cellulases were prepared with every plate to account for variability between plates. All measurements were made in triplicate.

3.3 Results and Discussion

3.3.1 Activities of labeled and unlabeled cellulases

Listed in Table 3.2 are the specific activities of labeled and unlabeled cellulases. From these results it can be concluded that fluorescence labeling of the cellulases did not inhibit cellulose hydrolysis.

Table 3.2 Comparison of specific activities of unlabeled and fluorescence-labeled cellulases

Cellulase Species	Specific BMCC Activity on 1mg/ml (μmoles cellobiose/min/μmol cellulase)	
	Unlabeled	Fluorescence-labeled
Cel5A	0.61 ± 0.025	0.55 ± 0.038
Cel6B	0.15 ± 0.015	0.16 ± 0.036
Cel9A	1.59 ± 0.123	1.66 ± 0.054

3.3.2 Purification efficiency

Comparison of the absorbance spectra of the buffer alone, control mixture of free dye and unlabeled Cel9A, and the flow through from the spin column are shown in Figure 3.2. The difference in the peaks at 488 nm (the absorption maximum for the dye used in the control) shows that 93.88% of the total dye in the mixture is retained by the column. The use of spin columns ensured minimal retention of free dye in the labeled cellulase sample in an easy and efficient way and offered an improvement over the elution columns used in earlier studies (Jeoh et al. 2002) which required pooling of fractions based on naked-eye detection of two separate bands on the elution columns, of free dye and labeled protein.

3.3.3 Correlation of fluorescence with cellulase concentration

Figure 3.3 is a plot of measured cellulase concentration versus known cellulase concentration for Cel5A-AF594 alone and in a ternary mixture. Similar results were obtained for Cel6B-AF350 and Cel9A-AF488 (data not shown). The equation $y = ax$ was fitted to the data yielding slopes of approximately 1.0 for Cel5a-AF594 measured alone and in a ternary mixture, as shown. The R^2 values obtained for the curve fits were 0.996 and 0.998 for Cel5A-AF594 alone and in ternary mixture, respectively. This indicates that cellulase concentrations measured using fluorescence standard curves are in close agreement with the original loaded cellulase concentrations for individual as well as mixtures of cellulases.

The need for a particular cellulase to be detected in a ternary mixture with the same sensitivity as when detected in the absence of other cellulases is important for accurate quantification of cellulases in mixtures. Figures 3.4 shows the Relative Fluorescence Units (RFU) versus moles of cellulase for the three cellulases

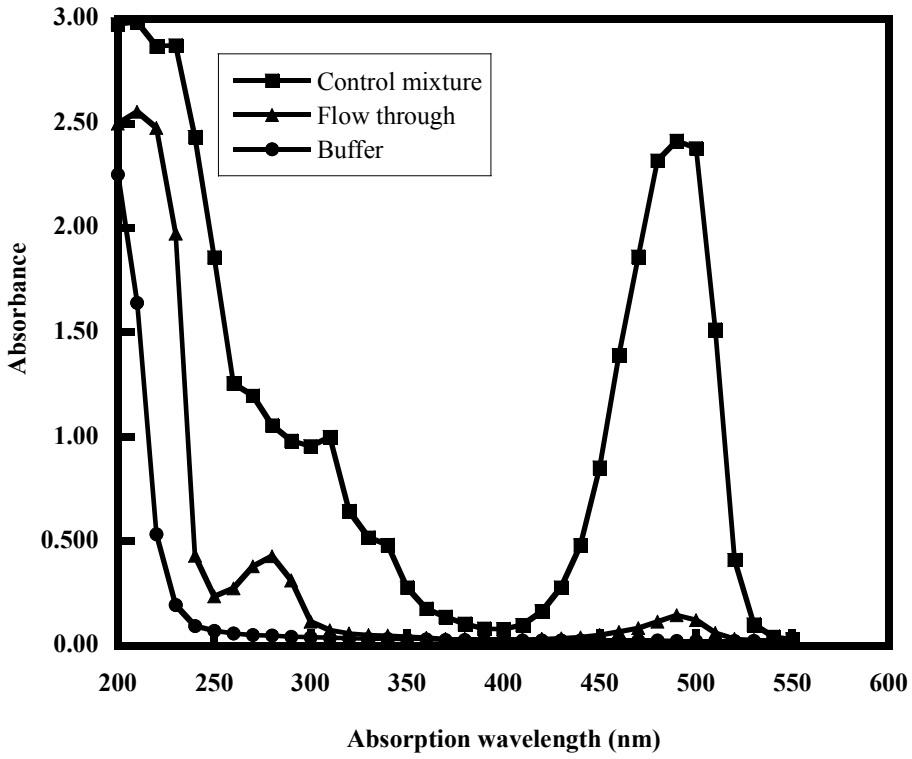

Figure 3.2 Dye retention capacity of Zeba Desalt spin columns showing absorbances of the buffer, of the control mixture (unreactive Alexa Fluor 488 dye and Cel9A), and of the flow through from the Zeba Desalt Spin Column.

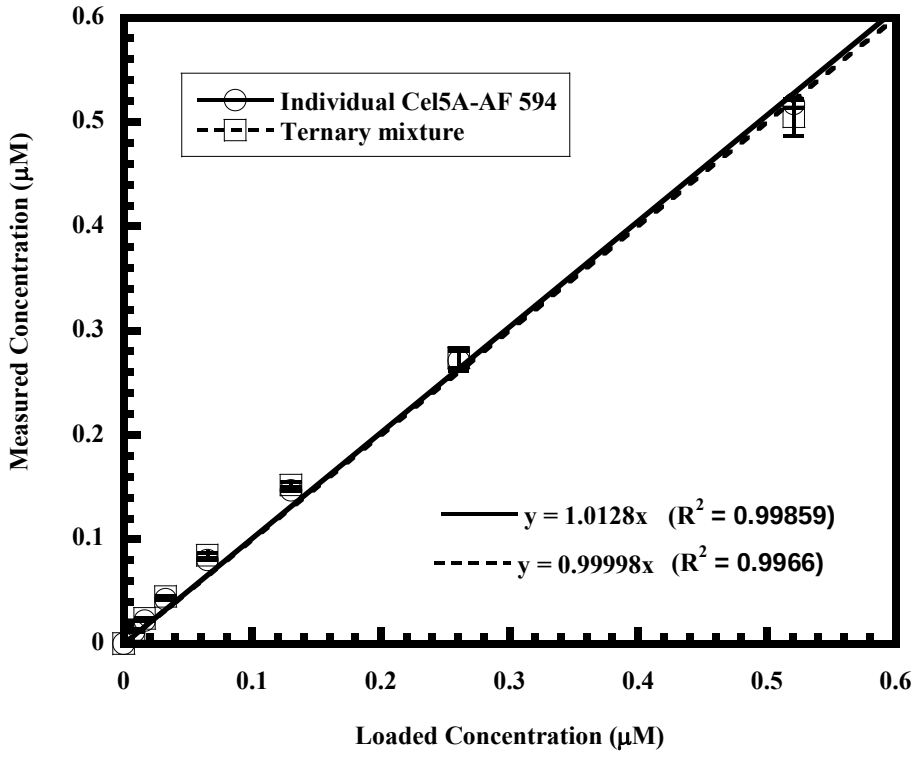

Figure 3.3 Comparison of total concentrations obtained from fluorescence quantification, with the loaded total concentration: Cel5A-AF594 individual (○), Cel5A-AF594 in a ternary mixture (□). Error bars indicate standard error.

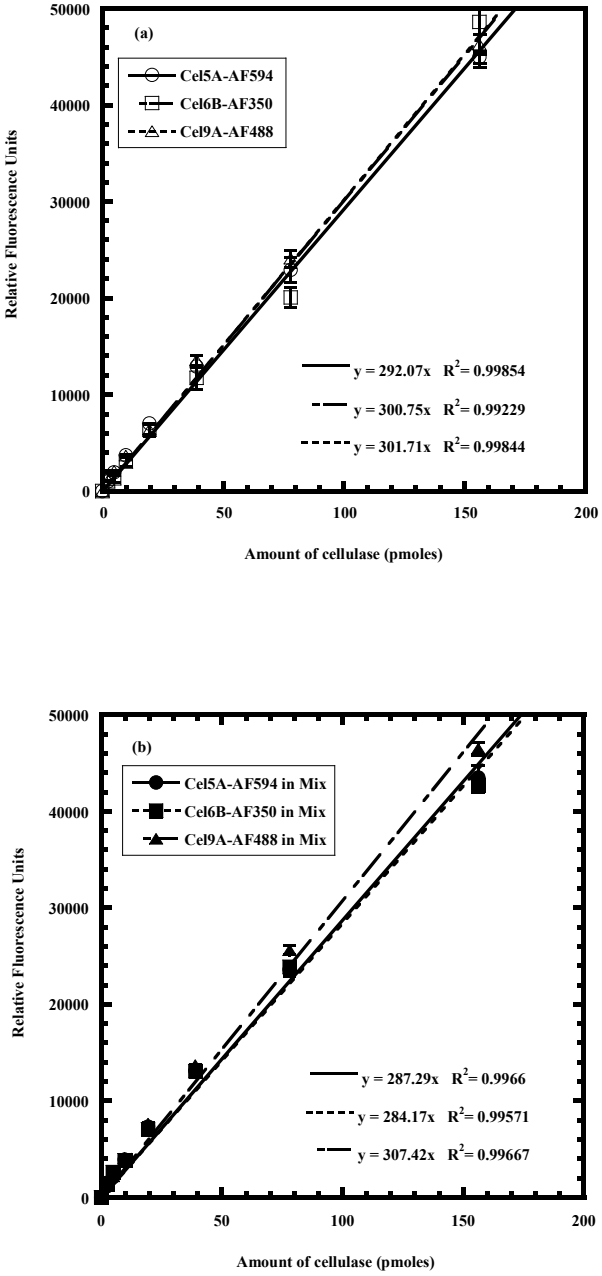

Figure 3.4 Comparison of fluorescence standard curves: (a) individual cellulases (b) equimolar ternary mixtures of the three cellulases. Error bars indicate standard error.

alone (Figure 3.4a) and for the three cellulases in the presence of equimolar concentration of the other two cellulases (Figure 3.4b). A linear correlation between relative fluorescence and cellulase concentration was observed in the range of concentrations studied. The slopes of the standard curves obtained for each enzyme alone (Figure 3.4a) and in a mixture (3.4b) were comparable, with a relative difference between their slopes being 0.8 – 2.8 %. This implies that the maximum error associated with measurement of concentration of each enzyme in mixtures is 3% relative to concentration measurements for individual cellulases.

3.3.4 Thermostability of labeled cellulases

The results of fitting a linear relationship between fluorescence and known cellulase concentration for each cellulase in ternary mixtures at different temperatures and incubation times are listed in Table 3.3. Since all binding assays were conducted at 50°C the fluorescence of samples was tested over 0-5 h at this temperature and observed to have a coefficient of variance (CoV) of less than 3%. Between 22 and 50°C, temperature was found not to appreciably affect the total well fluorescence.

3.3.5 Non-specific binding of cellulases to filters

Hydrophobic binding sites on filter membranes are usually blocked by incubation with a suitable blocking solution containing a protein, such as Bovine Serum Albumin (BSA), that does not interfere with the reaction system under investigation. This step is particularly important when the filtrate is used for measurements and requires several buffer washes to ensure complete removal of unbound blocking solution. Since the filtrate was not used for any cellulase concentration measurements in the present study, the membrane blocking step was

Table 3.3 Effect of temperature on the slope of the linear standard curves for Cel5A-AF594, Cel6B-AF350, Cel9A-AF488 in equimolar ternary mixtures. Slope expressed in units of RFU/pmole (RFU = Relative Fluorescence Units)

Temperature Time (h)	Cel5A-AF594 Slope	R^2	Cel6B-AF350 Slope	R^2	Cel9A-AF488 slope	R^2
22ºC						
0.5	392.84	0.978	303.05	0.971	397.27	0.983
1	394.00	0.980	306.83	0.971	401.40	0.984
30ºC						
0.5	402.90	0.998	303.51	0.994	393.78	0.999
1	410.68	0.998	289.06	0.994	365.44	0.999
40ºC						
0.5	407.94	0.996	320.51	0.986	373.24	0.998
1	408.73	0.995	301.52	0.984	381.82	0.998
50 ºC						
0.5	395.88	0.996	285.56	0.996	388.82	0.998
1	395.50	0.996	292.49	0.997	396.31	0.999
2	383.84	0.996	292.55	0.988	393.74	0.999
3	376.76	0.996	290.77	0.995	390.62	0.998
4	371.10	0.996	285.14	0.991	387.49	0.998
5	370.87	0.996	293.32	0.987	389.40	0.998
Mean at 50ºC	382.32		289.96		391.06	
C.o.V. at 50ºC	0.029		0.012		0.007	

deemed dispensable. However, it was necessary to ascertain whether the fluorescence of the membrane-bound cellulases produced any significant background signal that could affect fluorescence measurements of cellulose-bound cellulases. Residual fluorescence was observed in wells after the filtration of labeled cellulase samples. A linear fit was applied to fluorescence in wells after filtration vs fluorescence in wells before filtration and the slopes and correlation coefficients were obtained (Table 3.4). The fluorescence of the wells after filtration was between 10-13% of the fluorescence before filtration. The observed extent of non-specific binding was significant enough to require a transfer of the resuspended cellulase-bound BMCC from the filter plate to a clean blank 96-well plate before measuring bound enzyme.

3.3.6 Hydrolysis by individual cellulases

The percentage of substrate hydrolyzed by *T. fusca* Cel5A-AF594, Cel6B-AF350 and Cel9a-AF488 individually, at 50°C over 1, 2, 3 and 4 h was observed to increase over time for all three cellulases. Cel9A-AF488 showed the highest extent of hydrolysis while Cel5A-AF594 and Cel6B-AF350 had comparable hydrolytic capabilities within the range of concentrations used (data not shown).

3.3.7 Binding isotherms for individual cellulases

The individual binding of *T. fusca* cellulases Cel5A-AF594, Cel6B-AF350 and Cel9A-AF488 at 50°C at 4 h are shown in Figure 3.5. At low cellulase concentrations the classical Langmuir model predicts a linear relationship between bound cellulase concentration and free cellulase concentration. Cellulase binding data have error

Table 3.4 Non-specific binding of cellulases to filter plate bottom

Labeled Cellulase	% of Well fluorescence after filtration vs before filtration	R^2
Cel5A-AF594	13.2	0.981
Cel6B-AF350	10.5	0.984
Cel9A-AF488	10.9	0.985

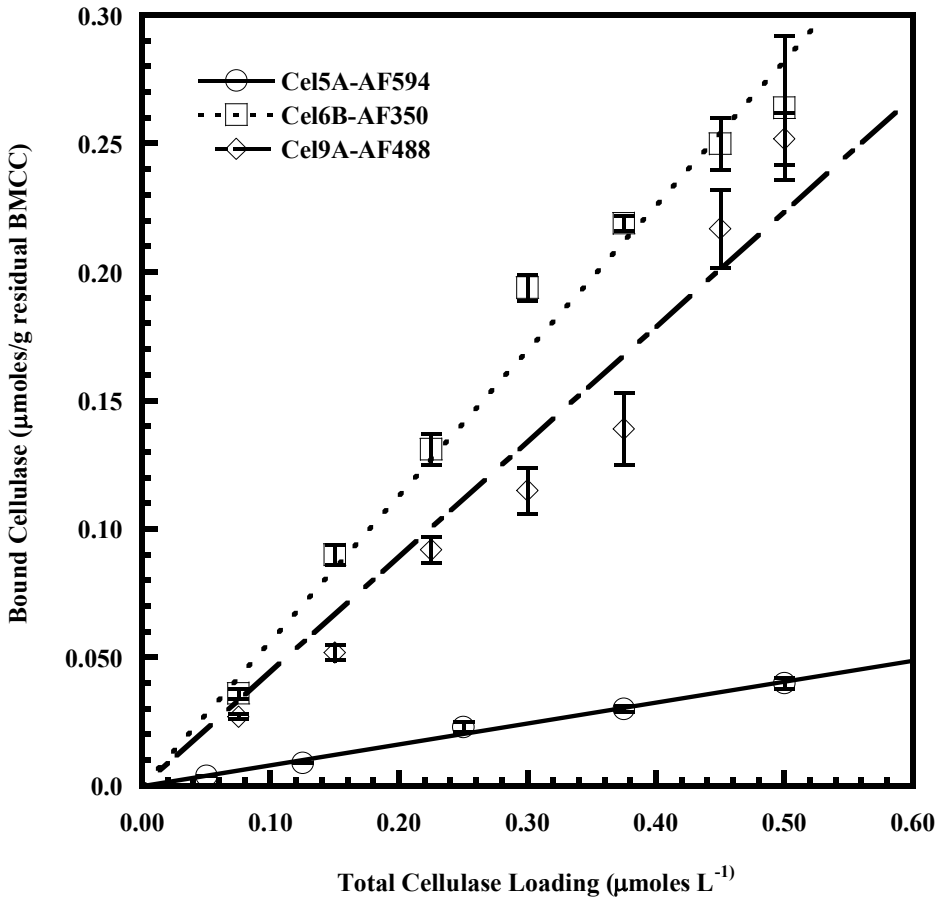

Figure 3.5 Individual cellulase binding isotherms for *T. fusca* Cel5A, Cel6B and Cel9A on BMCC at 50°C after 4 h. Error bars indicate standard error.

associated with the independent variable and the dependent variable (Bothwell and Walker 1995); bound cellulase concentration was measured experimentally and free cellulase concentration was determined by subtracting the bound concentration from total cellulase concentration. Since total cellulase loading is the only controlled input variable, the approximation for low concentration was applied to the Langmuir binding model equation relating bound cellulase concentration to total cellulase concentration (Bothwell and Walker 1995) and the following relationship was obtained:

$$E_b = \beta \times E_t \tag{3.4}$$

where

E_b = Bound cellulase concentration (μmole/g residual BMCC)

E_t = Total cellulase concentration (μmole/L)

β = Linear coefficient (L/g)

The β values obtained were

Cel5A-AF594 : β = 0.081 L/g (R^2 = 0.989),

Cel6B-AF350 : β = 0.565 L/g (R^2 = 0.977) and

Cel9A-AF488 : β = 0.447 L/g (R^2 = 0.957)

Cel6B-AF350 is observed to have the highest binding affinity, followed by Cel9A-AF488 while Cel5A-AF594 is seen to have the lowest binding affinity. Cel9A-AF488, being a processive endocellulase, can be expected to have a binding affinity that lies between the binding affinities of an exocellulase and a classical endocellulase. The R^2 values for Cel5A-AF594 and Cel6B-AF350 were higher in comparison to that of Cel9A-AF488. The bound enzyme concentration is dependent on the amount of residual BMCC in a reaction, which is determined by the extent of hydrolysis. The greater extent of hydrolysis by Cel9A-AF488 than Cel5A-AF594 or Cel6B-AF350 leads to a much more rapidly changing substrate concentration which

could be the cause for greater variability in bound Cel9A-AF488 measurements. These results are in agreement with previous predictions for individual cellulase binding isotherms for Cel6B-AF350 and Cel9A-AF488, which are the two principal cellulases whose synergistic binding behavior is being investigated in the current study. Cel5A-AF594 shows lower binding affinity than previously predicted (Jeoh et al. 2002, Bothwell et al. 1996). However, its activity on BMCC was uninhibited and SDS PAGE analysis demonstrated that the cellulase had not undergone any proteolysis (data not shown). Inefficient separation of unconjugated dye from labeled cellulases in the earlier work may have led to higher predictions for bound Cel5A concentrations. Such a possibility has been addressed in the present investigation by the use of the Zeba Desalt spin columns (Figure 3.2).

3.3.8 Binding behavior of cellulases in mixtures

The bound cellulase concentration of Cel6B-AF350 and Cel9A-AF488 in mixtures varied linearly with increasing cellulase loading. A linear curve fit of the following form was applied to describe the mixture binding phenomenon.

$$E_{b,i} = \beta_{mix} \times E_{t,i} \tag{3.5}$$

where :

$E_{b,i}$ = Bound concentration of cellulase i in ternary mixture (μmol/g residual BMCC)

$E_{t,i}$ = Total concentration of cellulase i in ternary mixture (μM)

β_{mix} = Linear coefficient (L/g)

Figure 3.6 shows the binding of Cel6B-AF350 and Cel9A-AF488, alone and in ternary mixtures, after a 4 hr reaction at 50°C. β values for cellulases acting alone and in mixtures are listed in Table 3.5. The β values for individual reactions differed from those estimated for the mixture reactions. The β_{mix} of Cel6B in the ternary mixtures

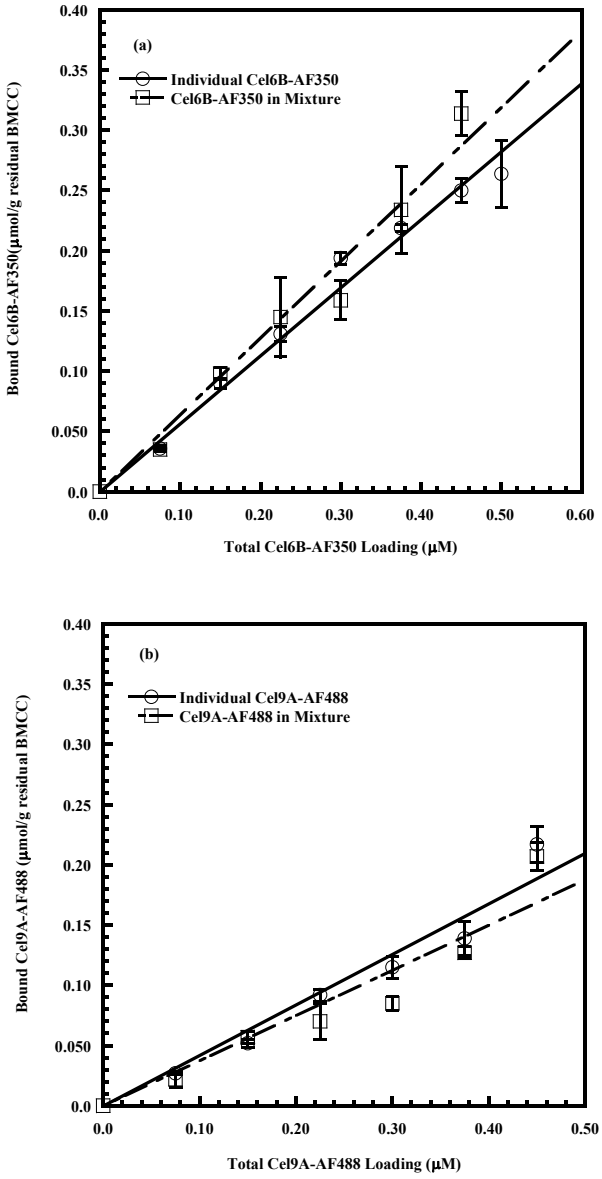

Figure 3.6 Binding isotherms for cellulases in mixtures a) Cel6B-AF350 alone and in ternary mixture b) Cel9A-AF488 alone and in ternary mixture. Error bars indicate standard error.

Table 3.5 Linear coefficients for individual binding and binding in mixtures

Species	Individual Binding		Binding in Mixture	
	β	R^2	β_{mix}	R^2
Cel6B-AF350	0.565	0.977	0.638	0.975
Cel9A-AF488	0.420	0.952	0.376	0.917

was observed to be greater than the β for individual binding reactions by 13% while the β_{mix} of Cel9A was observed to be 10.5% lower in ternary mixtures than the β value measured when alone. For both Cel6B and Cel9A, the highest cellulase loading yielded binding levels higher than this linear model. This observation along with the linear binding behavior of the cellulases when reacting alone (see Figure 3.5) suggests an enhancement of binding at higher cellulase concentrations.

3.3.9 Hydrolysis by cellulase mixtures and Degree of Synergistic Effect

Percent of hydrolysis and DSE at 4h are presented in Figure 3.7a and 3.7b, respectively. The degree of synergistic effect for all ternary mixtures was calculated as follows (Walker et al. 1993a):

$$DSE_{\chi} = \frac{\chi_{mix}}{\sum_{i=1}^{3} \chi_i} \qquad (3.6)$$

where:

DSE_{χ} = degree of synergistic effect for the extent of hydrolysis (dimensionless)

χ_{mix} = extent of hydrolysis of 1mg/ml BMCC achieved by a ternary mixture

χ_i = extent of hydrolysis of 1mg/ml BMCC achieved by the *i*th component of the mixture when acting alone but at the same concentration as in the mixture.

Figure 3.7a shows the extent of hydrolysis of BMCC achieved by summing the extent of the Cel5A, Cel6B and Cel9A alone and measured extent of hydrolysis for the ternary mixtures of these cellulases. The extent of hydrolysis for mixtures of the cellulase increased approximately linearly with increasing Cel6B mole ratio, decreasing Cel9A mole ratio, up to the point where Cel6B represented 75% of the total cellulase loaded. Thus, the highest extent of hydrolysis observed occurred at loaded mole ratios of 0.75, 0.15, and 0.10 for Cel6B, Cel9A, and Cel5A, respectively. This is

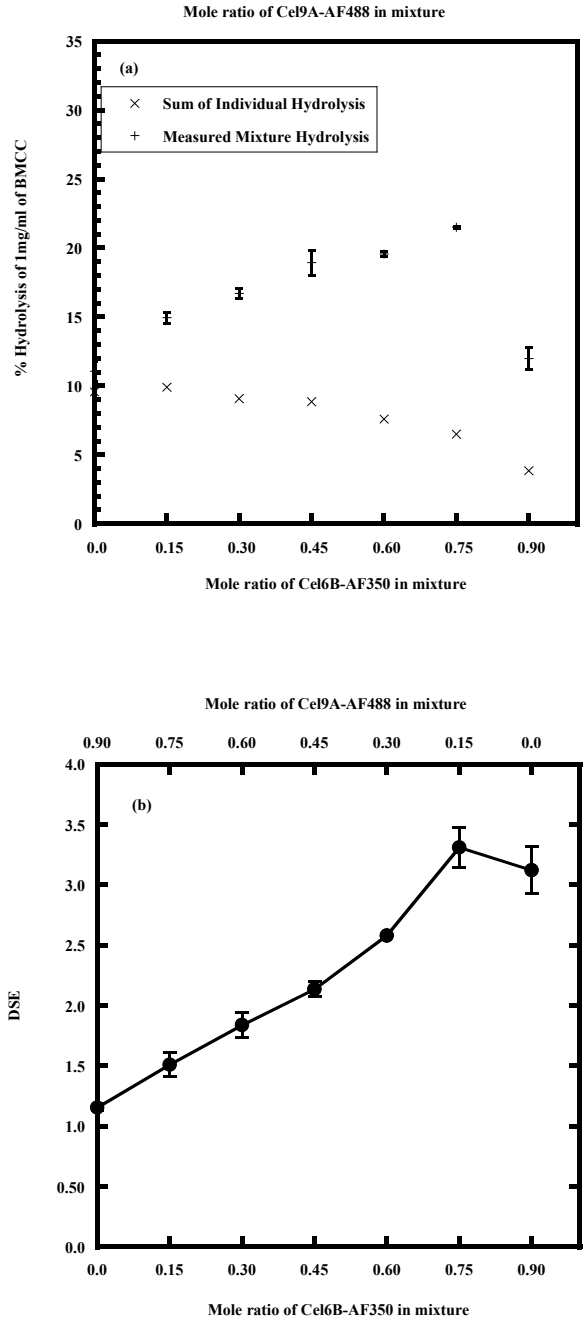

Figure 3.7 Effect of varying molar ratios of Cel6B and Cel9A at fixed total loading on (a) the extents of hydrolysis on BMCC and (b) the degree of synergistic sffect at 4 h. Error bars indicate standard error. Total protein concentration was 0.5μM. BMCC concentration was 1 mg/ml.

consistent with other studies which have suggested that maximum synergy is observed when an exo-cellulase represents 70 to 80% of the mixture (Walker et. al. 1993; Watson et. al. 2002). What was not apparent in the earlier studies was the extent to which the exo-cellulase dominated the total bound cellulase. For the highest extent of hydrolysis, Cel6B represented 90% of the bound cellulases as opposed to 75% of the total cellulase loading, with Cel9A and Cel5A representing 8 and 2% of the total bound cellulases, respectively (data not shown). When Cel9A was eliminated from the mixture the extent of hydrolysis dropped from 22% to 12%. This indicated that the presence of Cel5A and Cel9A, albeit at low concentrations, was essential for increasing the extent of hydrolysis by a mixture.

A similar trend of increasing DSE with increasing Cel6B mole ratio was observed (see Figure 3.7b). However the drop in the DSE when Cel9A was eliminated from the mixture was not as significant, from a value of 3.3 to 3.1. While looking at DSE data it is important to keep in mind that the DSE is sensitive to changes in the value of the sum of extents of hydrolysis. Hence, in the final analysis, much more insight is gained by looking at the extent of hydrolysis rather than the degree of synergistic effect alone.

3.3.10 Extent of binding and Degree of Synergistic Binding

Extent of binding and degree of synergistic binding (DSB) at 4h are presented in Figure 3.8a and 3.8b, respectively. DSB values were calculated as follows (Jeoh et al. 2002):

$$DSB = \frac{\dfrac{E_{b,mix}}{S_{res,mix}}}{\displaystyle\sum_{i=1}^{3}\left[\frac{E_{b,individual}}{S_{res,individual}}\right]} \qquad (3.7)$$

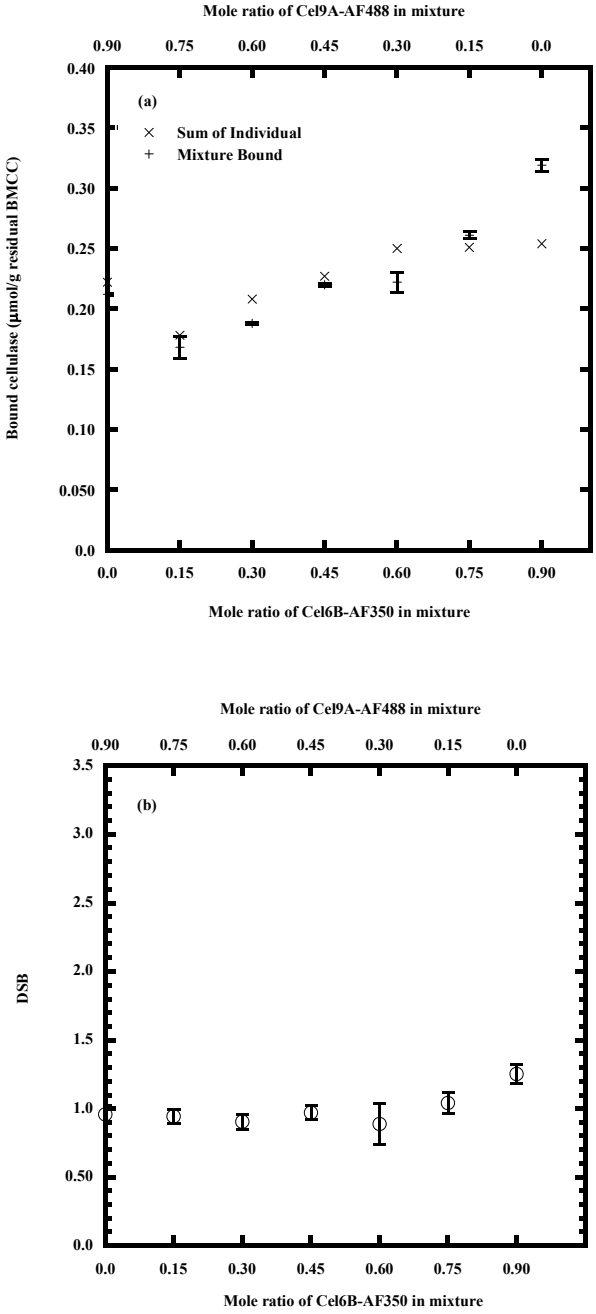

Figure 3.8 Effect of varying molar ratios of Cel6B and Cel9A at fixed total loading on (a) the extents of hydrolysis on BMCC and (b) the degree of synergistic sffect at 4 h. Error bars indicate standard error. Total protein concentration was 0.5µM. BMCC concentration was 1 mg/ml

where:

DSB = degree of synergistic binding (dimensionless)

$E_{b,mix}$ = bound concentration of enzyme in the mixture (μM)

$S_{res,mix}$ = concentration of residual BMCC in the mixture (g/L)

$[E_{b,individual}]_i$ = bound concentration of enzyme *i* when acting individually (μM)

$[S_{res,individual}]_i$ = concentration of residual BMCC in the individual component reaction (g/L)

The sum of individual cellulases bound alone and the total bound cellulase of mixtures are presented in Figure 3.8a. Both variables initially increased approximately linearly with increasing Cel6B mole ratio for Cel6B mole fraction of 0.0 to 0.6. However, at a Cel6B mole ratio of 0.6 the sum of the individual cellulases bound alone bEG Ins to level off, but the measured total bound cellulase of the mixture continues to increase. At a Cel6B mole fraction of 0.90 there is a 22% difference between binding level predicted by summing the binding of the cellulases alone versus the actual measured total bound cellulase of the mixture. Measurement of the Cel6B bound fraction for this maximum bound cellulase concentration revealed that Cel6B represented 98% of the bound cellulase with Cel5A representing only 2% of the total.

Figure 3.8b shows the DSB values at varying molar ratios of Cel6B-AF350 in ternary mixtures at 4 h. All DSB values were observed to range between 4 -11 % of unity except the binary mixture of Cel5A-AF594:Cel6B-AF350 in the ratio 0.1:0.9 which has a DSB value 25% greater than unity indicating that there was a significant increase in the bound cellulase concentration of this binary mixture. As noted earlier, this synergism in binding was due to an increase in bound Cel6B at the expense of Cel5A and Cel9A. In addition, this increase in bound Cel6B did not result in an increase in

the extent of hydrolysis or DSE. Instead, this increase in bound Cel6B resulted in a 22% drop in extent of hydrolysis (Figure 3.7a). These results indicated that the presence of Cel5A and Cel9A, albeit at low concentrations, is essential for optimal cellulose hydrolysis. Higher resolution of cellulase binding measurements around Cel6B mole ratio of 0.6 to 0.9 would allow for a more precise determination of the mole fraction needed to obtain maximum extent of hydrolysis and DSE.

3.4 Conclusion

A high-throughput fluorescence method for studying synergistic interactions between a "classical" endocellulase, an exocellulase, and a processive endocellulase has been developed and optimized. This method has been shown to yield reliable, reproducible, and accurate results at elevated temperature that are consistent with other methods using spin-tubes. Maximum error observed in measuring bound cellulase concentration was less than 3% across a number of cellulase mixtures and filter-bottom microwell plates. Much of this measurement error was controlled by selection of fluorophores which minimized crosstalk. Crosstalk can occur in fluorescence measurements when the excitation and/or emission spectra of two or more fluorophores in a sample overlap, making it difficult to isolate the fluorescence of one flurophore alone. This aspect will become even more important as we seek to expand the number of cellulases studied in synergistic mixtures. Also, the use of fluorescence to assay bound fractions is not limited by the substrate-specific activity of cellulases and hence can be applied to study binding trends of cellulases in the presence of other species having similar hydrolytic properties or in mixture studies involving inactive mutants.

The use of filtration plates allowed swift separation of insoluble BMCC from unbound cellulases, and direct measurement of fluorescence of bound cellulases

eliminated the errors associated with non-specific binding to filtration membranes. This additional step was necessary to negate the effect of the non-specific binding of cellulases on the micro-plate filters that represented 10-13% of the fluorescence signal. However, plate readers equipped with robotics would allow efficient management of this step.

The results of this study clearly demonstrate that all three cellulases were needed to maximize the extent of hydrolysis, and they confirm that an exocellulase mole fraction of 0.75 is needed for optimal hydrolysis. However, the more telling story is that the maximum extent of hydrolysis occurs when exocellulases represent upwards of 90% of the total bound cellulase. Exceeding this level of bound exocellulase results in a drop-off in the extent of hydrolysis despite additional binding of Cel6B. The lack of overlap between maximum DSE and maximum DSB suggests that more bound cellulase does not necessary imply higher extent of hydrolysis. In addition, the bound mole fractions for maximum extent of hydrolysis data also underscore the small the amounts of Cel5A and Cel9A that are needed to dramatically change the extent of hydrolysis bringing to light the nonlinearity of the synergism phenomena around optimal molar ratio. Finer experimental resolution of extent of hydrolysis values between Cel6B molar ratio of 0. 6 to 0.9 is likely to yield a more complete picture of this nonlinearity, and this plays to the strength of this high-throughput analysis system. We believe that exploring the limits of the use of fluorescently labeled cellulases in micro-plate reactors will provide a useful tool for accelerated combinatorial mixture binding studies by allowing simultaneous analysis of multiple enzymes.

REFERENCES

Baker, J. O., C. I. Ehrman, W. S. Adney, S. R. Thomas and M. E. Himmel. 1998. Hydrolysis of Cellulose Using Ternary Mixtures of Purified Cellulases. Applied Biochem. Biotechnol. 70-72:395-403.

Beldman, G., A. G. J. Voragen, F. M. Rombouts, M. F. Searle-van Leeuwen and W. Pilnik. 1987. Adsorption and Kinetic Behavior of Purified Endoglucanases and Exoglucanases from *Trichoderma viride*. Biotechnol Bioeng. 30:251-257.

Bothwell, M. K., L. P. Walker, D. B. Wilson, D. C. Irwin and M. Price. 1993. Synergism Between Pure *Thermomonospora fusca* and *Trichoderma reesei* Cellulases. Biomass Bioenergy 4(4): 293-299.

Bothwell, M. K. and L. P. Walker. 1995. Evaluation of Parameter Estimation Methods for Estimating Cellulase Binding Constants. Bioresource Technol. 53:21-29.

Bothwell, M.K., Daughetee, S.D., Chau, G.Y.,Wilson, D.B. and Walker,L.P. 1996. Binding capacities of *Thermomonospora fusca* E3, E4 $_a$nd E5, the E3 $_b$inding domain, and T*richoderma reesei* CBH I on Avicel and bacterial microcrystalline cellulose. Bioresource Technol. 60:169-178.

Buhler, R. 1991. Double-Antibody Sandwich Enzyme-Linked Immunosorbent Assay for Quantitation of Endoglucanase I of *Trichoderma reesei*. Applied Environ. Microbiol. 57(11): 3317-3321.

Fan, L. T., Y. -. Lee and D. R. Beardmore. 1980. Mechanism of the Enzymatic Hydrolysis of Cellulose: Effects of Major Structural Features of Cellulose on Enzymatic Hydrolysis. Biotech.Bioeng. 22:177-199.

Henrissat, B., H. Driguez, C. Viet and M. Schulein. 1985. Synergism of Cellulases from *Trichoderma reesei* in the Degradation of Cellulose. Bio/Technol. 3(8): 722-726.

Irwin, L. Walker, M. Spezio,D.Wilson. 1993. Activity studies of eight purified cellulases: specificity, synergism, and binding domain effects. Biotechnol.Bioeng. 42:1002-1013.

Jeoh, T., D. B. Wilson and L. P. Walker. 2002. Cooperative and Competitive Binding in Synergistic Mixtures of *Thermobifida fusca* Cel5A, Cel6B and Cel9A. Biotechnol. Progress 18(4): 760-769.

Jeoh, T., D. B. Wilson and L. P. Walker. 2006. Effect of Cellulase Mole Fraction and Cellulose Recalcitrance on Synergism in Cellulose Hydrolysis and Binding. Biotechnol. Progress 22(1): 270-277.

Jervis, E.J, C. A. Haynes and D. G. Kilburn, 1997. Surface Diffusion of Cellulases and Their Isolated Binding Domains on Cellulose. J. Biochem. 272(38): 24016-24023.

Jorgensen, H., J. P. Kutter and L. Olsson. 2003. Separation and quantification of cellulases and hemicellulases by capillary electrophoresis. Analytical Biochem. 317(1): 85-93.

Kim, D. W., Y. K. Jeong, Y. H. Jang and J. K. Lee. 1995. Adsorption Characteristics of Endo II and Exo II Purified from *Trichoderma viride* on Microcrystalline Celluloses with Different Surface Area. Bulletin Korean Chem. Soc. 16(6): 498-503.

Kolbe, J. and C. P. Kubicek. 1990. Quantification and Identification of the Main Components of the *Trichoderma* cellulase comples with Monoclonal Antibodies using an Enzyme-Linked Immunosorbent Assay (ELISA). Applied Microbiol. Biotechnol. 34:26-30.

Kyriacou, A., Neufeld, R.J., & Mackenzie,C.R. 1989. Reversibility and Competition in the adsorption of *Trichoderma reesei* cellulase components. Biotechnol. Bioeng. 33:631-637.

Lee, S. B., H. S. Shin and D. D. Y. Ryu. 1982. Adsorption of Cellulase on Cellulose: Effect of Physicochemical Properties of Cellulose on Adsoprtion and Rate of Hydrolysis. Biotechnol. Bioeng. 24:2137-2153.

Lever, M. 1972. A New Reaction for Calorimetric Determination of Carbohydrates. Analytical Biochem. 47:273-279.

Li, Y., D.C. Irwin and D. B. Wilson. 2007. Processivity, Substrate Binding and Mechanism of Cellulose Hydrolysis by Thermobifida fusca Cel9A. Appl. Environ. Microbiol. AEM Accepts, published online ahead of print on 16 March 2007

Medve, J., J. Stahlberg and F. Tjerneld. 1994. Adsorption and Synergism of Cellobiohydrolase I and II of *Trichoderma reesei* During Hydrolysis of Microcrystalline Cellulose. Biotechnol. Bioeng. 44:1064-1073.

Medve, J., J. Karlsson, D. Lee and F. Tjerneld. 1998. Hydrolysis of Microcrystalline Cellulose by Cellobiohydrolase I and Endoglucanase II from *Trichoderma reesei*: Adsorption, Sugar Production Pattern, and Synergism of the Enzymes. Biotechnol. Bioeng. 59(5): 621-634.

Nidetzky, B. and M. Claessens. 1994. Specific Quantification of *Trichoderma reesei* Cellulases in Reconstituted Mixtures and its Application to Cellulase-Cellulose Binding Studies. Biotechnol.Bioeng. 44:961-966.

Nidetzky ,B. and W. Steiner. 1993. A New Approach for Modelling Cellulase-Cellulose Adsorption and the Kinetics of the Enzymatic Hydrolysis of Microcrystalline Cellulose. Biotechnol. Bioeng. 42(4): 469-479

Ooshima, H., Kurakake, M., Kato, J. and Harano,Y. 1991. Enzymatic activity of cellulase adsorbed on cellulose and its change during hydrolysis. Applied Biochem. Biotechnol. 31:253-266.

Ryu, D. D. Y., C. Kim and M. Mandels. 1984. Competitive Adsorption of Cellulase Components and its Significance in Synergistic Mechanism. Biotechnol. Bioeng. 26:488-496.

Sharrock, K. R. 1988. Cellulase Assay Methods: A Review. J. Biochem. Biophys. Methods 17:81-106.

Spiridonov, N. A. and D. B. Wilson. 1998. Regulation of Biosynthesis of Individual Cellulases in *Thermomonospora fusca*. J. Bacteriol. 180(14): 3529-3532.

Van Tilbeurgh, H. and M. Claeyssens. 1985. Detection and Differentiation of Cellulase Components Using Low Molecular Mass Fluorogenic Substrates. FEBS Letters 187(2): 283-288.

Van Tilbeurgh, H., F. G. Loontiens, C. K. deBruyne and M. Claeyssens. 1988. Fluorogenic and Chromogenic Glycosides as Substrates and Ligands of Carbohydrates. Methods Enzymol. 160:45-59.

Walker, L. P., C. D. Belair, D. B. Wilson and D. C. Irwin. 1993. Engineering Cellulase Mixtures by Varying the Mole Fraction of *Thermomonospora fusca* E5 and E3, *Trichoderma reesei* CBH I, and *Caldocellum saccharolyticum* B-Glucosidase. Biotechnol. Bioeng. 42:1019-1028.

Watson, D. L., D. B. Wilson and L. P. W. Walker. 2002. Synergism in Binary Mixtures of *Thermobifida fusca* Cellulases Cel6B, Cel9A and Cel5A on BMCC and Avicel. Applied Biochem. Biotechnol. 101:97-111.

Wood, T. M. 1975. Properties and Mode of Action of Cellulases. Biotechnol. Bioeng Symp. 5:111-137.

Woodward, J., M. Lima and N. E. Lee. 1988a. The Role of Cellulase Concentration in Determining the Degree of Synergism in the Hydrolysis of Microcrystalline Cellulose. Biochem. J. 255:895-899.

Woodward, J., M. K. Hayes and N. E. Lee. 1988b. Hydrolysis of Cellulose by Saturating and Non-Saturating Concentrations of Cellulase: Implications for Synergism. Bio/Technol. 6(3): 301-304.

CHAPTER 4

AN EXPERIMENTAL SYSTEM FOR MONITORING CELLULASE-CELLULOSE INTERACTIONS USING FLUORESCENCE MICROSCOPY[2]

Abstract

There is still much uncertainty about how cellulases, enzymes that depolymerize cellulose, interact with cellulose on its surface and within its complex porous structure. The mechanism of action of cellulases on crystalline cellulose is a key issue that needs to be resolved before the cellulase-cellulose reaction can be completely understood. This work is focused on using a high resolution fluorescence microscopy technique to study the binding of cellulases on immobilized cellulose with different morphological structures. First, it is demonstrated that both crystalline cellulose and *Thermobifida fusca* cellulases Cel5A, Cel6B and Cel9A can be fluorescently labeled and that labeling does not inhibit the hydrolytic property of these cellulases. Second, the labeled cellulose is spatially confined and immobilized on micro-patterned glass surfaces using a polymer lift-off method. The combination of the fluorescence labeling and the immobilization method yields a system that can be used to investigate cellulase-cellulose interactions using high resolution fluorescence imaging techniques.

4.1 Introduction

Cellulases are industrially significant enzymes capable of degrading cellulose and hence form a key component in the production of bioethanol from lignocellulosic biomass. At the most fundamental level, cellulases must bind to and react on the

---

[2] This work has been published as Moran-Mirabal JM, Santhanam N, Corgie SC, Craighead HG, Walker LP. 2008. Immobilization of Cellulose Fibrils on Solid Substrates for Cellulase-Binding Studies Through Quantitative Fluorescence Microscopy. Biotechnol Bioeng 101:1129-1141.

exposed surface of cellulose fibrils (Chanzy, et al. 1984; Chanzy and Henrissat 1985), bundles of cellulose chains with a width of 5-10 nm and length of the order of hundreds of nanometers (Brown 2004). Current understanding of the mechanism of cellulase action on cellulose has been gained from protein engineering and X-ray crystallography studies. These studies have resolved structural features of cellulases such as catalytic clefts and tunnels, identified essential amino acids in the catalytic core of cellulases and explored the fundamentals of cellulose chain alignment in the active site (Henrissat, et al. 1998; Tomme, et al. 1995; Wilson and Irwin 1999). These experiments used soluble cellooligosaccharides as substrates in order to explain the action of cellulases on insoluble, crystalline cellulose. Hence they have not been able to resolve the on-off rate or the processive behavior of cellulases on the surface of cellulose. They have also not differentiated between cellulase interactions with cellulose fibrils and those with cellulose in more complex morphologies that have an intrinsic pore structure.

In order to completely understand the mechanism of the enzymatic hydrolysis of crystalline cellulose it is essential to develop techniques which will allow the study of interactions of cellulases with cellulose, across a range of dimensions, from the nanoscale of cellulose fibrils, to the microscale aggregates of interwoven fibril bundles, to the sub-millimeter scale of cellulose particles where pore size distribution may play a major role in determining the accessibility of cellulases to reactive surfaces. It has been shown that the irreversibly bound cellulases of *Cellulomonas fimi* move two-dimensionally on the surface of cellulose films in order to seek β-1,4-glucopyranoside linkages (Jervis, et al. 1997). These studies have determined the surface diffusion rates of *C. fimi* cellulases and their CBDs on *Valonia ventricosa* microcrystalline cellulose using the Fluorescence recovery after photobleaching technique. While this work was the first of its kind to establish the surface mobility of

cellulose-bound cellulases, there have been only limited applications of high-resolution optical techniques in the study of cellulases. Recently, Pinto et al. (2007) have developed a method based on image analysis of widefield fluorescence intensity measurements to quantify the surface concentrations of CBD-FITC conjugates bound to cellulose films. These studies indicate the growing potential of the use of optical microscopy to elucidate the fundamental mechanism of cellulase action on cellulose.

Microscopy techniques, such as epifluorescence microscopy and fluorescence correlation spectroscopy, can be used to visualize and quantify the binding diffusion of cellulases on cellulose. The first step towards application of these techniques is the development of an experimental system which allows efficient miniaturization of the cellulase-cellulose reaction while exhibiting fluorescent properties not inherent to cellulases or cellulose. Key features of an optimal system would include: i) fluorescently labeled active cellulases free from unconjugated fluorophore, ii) a uniformly fluorescent, immobilized cellulosic substrate that can be reliably distinguished from, and visualized in the presence of fluorescently labeled cellulases, iii) a buffer with additives that maximize the signal to noise ratio of all fluorophores without interfering with cellulase activity. The objective of this work is to develop and establish such a system that is optimized to facilitate the application of fluorescence microscopy techniques to the study of cellulase-cellulose interactions. The fluorescently labeled cellulose is confined to specific rEG Ions on a glass slide by the use of a polymer lift-off technique, a method that has been successfully applied in the past for the immobilization of biomolecules (Craighead, et al. 2001; Ilic and Craighead 2000; Moran-Mirabal, et al. 2007). Fluorescently labeled cellulases are purified using native polyacrylamide gel electrophoresis so as to eliminate any uncojugated fluorophore that could lead to stray fluorescence in the reaction system.

4.2 Materials and Methods

4.2.1 Fluorescent labeling of BMCC

A stock suspension of Bacterial Microcrystalline Cellulose (BMCC) was made by reconstituting moist BMCC (Monsanto Cellulon, Monsanto Company, San Diego, CA) to a final concentration of 8.42 mg/ml. Fluorescent labeling of cellulose with 5-(4,6-dicholorotriazinyl)-aminofluorescein (DTAF) was carried out according to a previously reported protocol (Helbert, et al. 2003). Briefly, the BMCC was swollen in a 75:25 mixture of Ethylene Diamine (EDA) to water at room temperature overnight. The sample was then centrifuged and resuspended in a large volume of methanol and allowed to stand for a few hours. Six alternating methanol washes and EDA swellings were done for complete conversion, followed by extensive washing with de-ionized water to remove any traces of EDA that may be present in the BMCC. DTAF labeling of treated cellulose was carried out by dissolving 6 mg of DTAF in 10ml of 0.2 N NaOH containing a 100 mg suspension of the treated cellulose and stirring the mixture at room temperature for 24 h. The cellulose was then extensively washed with water to remove excess DTAF and then washed with and resuspended in 50 mM Sodium acetate buffer pH 5.5. The final concentration of treated and labeled BMCC was determined by measuring the oven-dried weight of triplicate 5ml samples. Scanning Electron Microscopy (SEM) images of treated and untreated BMCC were taken to observe the changes in morphology brought about by the treatment.

4.2.2 Fluorescent labeling of cellulases

T. fusca Cel5A, Cel6B, and Cel9A cellulases were labeled with amine-reactive Alexa Fluor 647 (AF647) succinimidyl ester following the protocol provided by the manufacturer (Invitrogen Corporation, Carlsbad, CA). The enzymes were diluted to a concentration of 1 mg/mL in sodium acetate buffer. Then, 500 μL of the enzyme

solution were added to a vial containing the reactive dye, mixed thoroughly, and 50 μL of 1M sodium bicarbonate were added to raise the pH of the solution to 9. The labeling reaction was carried out shielding the mixture from light for 1 hr under continuous stirring at room temperature, after which the cellulase-fluorophore mixture was stored at 4 °C.

4.2.3 Purification of labeled cellulases

Labeled cellulases were separated from free unreacted dye by native polyacrylamide gel electrophoresis (n-PAGE). The gels for cellulase purification were made with 4% acrylamide stacking gel in Tris 0.6M pH 6.8, and 15% acrylamide resolving gel, 15% w/v glucose, in Tris 1.5M pH 8.3. The gel lanes were loaded with 16 μL labeled protein sample and 4 μL of a 1:50 dilution of a loading buffer containing 50/50 Tris 0.6M pH6.8/glycerine and 1mg/mL of bromophenol blue. The low concentration of the bromophenol blue was chosen such that background fluorescence form the marker would not interfere with the quantification of unreacted dye. The gels were run in Tris-glycine buffer pH 8.3 at 100V for 45 min and 160 V for 75 min. After the electrophoresis step was complete, the bands containing the labeled enzymes were excised and stored in Tris-glycine buffer at 4°C.

The fluorescently labeled enzymes were eluted from the gel slabs using a BioRad 422 Electroeluter (Bio-Rad Laboratories, Hercules, CA) following the manufacturer recommended protocol. The electroelution was run using Tris-glycine buffer pH 8.3, shielding the mixture from light, and at 4°C. Each enzyme preparation was eluted in a separate run to avoid cross contamination. The AF647 labeled enzymes were collected using 3000 Da MWCO membrane caps. The recovered volume from the electroelution was 400-800 μL. Millipore desalt columns (Biomax-5,

Millipore, Bedford, MA) were used to replace the Tris-glycine buffer in which the labeled enzymes were suspended by sodium acetate buffer.

4.2.4 Determination of cellulase concentrations and degree of labeling of cellulase

The concentration of labeled cellulase (P) was calculated as follows:

$$P = \frac{\left[A_{280} - A_{dye} \times 0.03 \right] \times DF}{\varepsilon_{protein}} \tag{4.1}$$

where:

P = Labeled cellulase concentration, M

$D.F.$ = Dilution factor

A_{280} = Absorbance of the conjugate at 280 nm

A_{dye} = Absorbance of the conjugate at the excitation maximum of the dye

$\varepsilon_{protein}$ = Extinction coefficient of the protein (M^{-1}).

The degree of labeling (moles dye per mole of protein) of each conjugated cellulase was determined as below:

$$DoL = \frac{A_{dye} \times DF}{\varepsilon_{dye} \times P} \tag{4.2}$$

where

DoL = degree of labeling (dimensionless)

ε_{dye} = Extinction coefficient of the dye (M^{-1})

All constants used in equations 4.1 and 4.2 are listed in Table 4.1.

4.2.5 Activity of labeled cellulases

To verify that there was no loss of activity due to labeling, the activities of labeled and unlabeled cellulases on 1mg/ml BMCC in 50mM sodium acetate buffer (pH 5.5) over 18hr at 50°C were measured. Reactions were stopped by centrifugation and the

Table 4.1 Molecular weight and extinction coefficients for Alexa Fluor 647 fluorophore and cellulases.

Molecule	AF647	Cel5A	Cel6B	Cel9A
MW (Da)	1250	46,300	59,600	90,400
ε (M^{-1})	239,000	97,100	115,150	210,670

reducing sugars produced were measured using the PAHBAH method (Lever 1972). Briefly, 5% parahydroxybenzoic acid hydrazide in 0.5M HCl was mixed with 0.5M NaOH in a ratio of 1:4 by volume, immediately before the assay. A 1.5 ml aliquot of this mixture was added to 50 µl of reaction supernatant and samples were boiled for 6 minutes followed by absorbance measurement at 410 nm. A standard curve in the range of 0.4-2.4 mM glucose was prepared using 1 mg/ml glucose standard solution.

4.2.6 Test of activity in the presence of additives

Two additives were tested: bovine serum albumin (BSA, (Invitrogen, Ultrapure molecular biology grade) and L-ascorbic acid (AA, Sigma-Ultra AA). BSA was tested as a blocker of non-specific binding with the aim to minimize cellulase adsorption to the glass substrate. AA was used as an oxidation inhibitor to protect the fluorophores attached to the enzymes and prevent photobleaching. The effect of the addition of these additives on the activity of the cellulases was tested using the PAHBAH assay as described above.

4.2.7 Cellulose immobilization

Micropatterned polymer lift-off surfaces were fabricated on 170 µm thick fused silica coverslips (ESCO Products) were prepared by Dr. Jose Moran-Mirabal as previously reported (Moran-Mirabal, et al. 2007). Glass coverslips with the patterned polymer coating were mounted onto plasma-cleaned poly-carbonate Petri dishes containing a cut-out section at the bottom (P35-10-C, MatTek, Ashland, MA). The coverslips were attached to the Petri dish using medical grade, solvent-free, UV-curable adhesive (1161M, Dymax, Torrington, CT). Curing was done by 30 min exposure to UV light in a trans-illuminator, after which the coverslip was permanently

bonded to the dish. This allowed the incubation of patterned cellulose material with up to 5 mL volume of solution containing the cellulases.

Cellulose immobilization onto the patterned surfaces was achieved by directly applying 10 μL of a 1 mg/mL solution of cellulose suspended in water to each patterned motif and allowing the solution to evaporate on a hotplate set at 70°C. After 1 hr drying, the sample was rehydrated in deionized water and the polymer was lifted-off, removing the excess cellulose and yielding a thin layer of immobilized fibrils. The sample was then rinsed 3 times with deionized water to remove any remaining cellulose in solution and stored overnight at 4°C to achieve complete cellulose rehydration. To block non-specific adhesion of cellulases onto the Petri dish surface and the unpatterned sections of the coverslip, the sample was incubated for one hour with 3 mL of 5 mg/mL bovine serum albumin (Invitrogen, Ultrapure molecular biology grade) in 50 mM sodium acetate buffer (pH 5.5). Then, the sample was washed three times with 50 mM sodium acetate buffer containing ascorbic acid. Cellulase solutions at the desired enzyme concentrations were prepared separately in sodium acetate buffer supplemented with ascorbic acid, and allowed to mix for one hour before addition to the patterned cellulose. This was done to avoid concentration gradients that could skew the cellulase binding onto the cellulose fibrils.

4.2.8 Optical set-up for imaging

Imaging of the patterned cellulose fibrils and the binding of labeled cellulases was done using an Olympus IX-71 inverted microscope and a 60x/1.2NA UPLAPO Olympus water immersion objective. DTAF-labeled cellulose was imaged using a 475AF40 excitation filter, a 505DRLP dichroic mirror, and a 525AF45 emission filter (Chroma Technology Corp., Rockingham, VT). Imaging of the Alexa 647 labeled cellulases was done using a 630AF50 excitation filter, a 650DRLP dichroic mirror,

and a 680AF40 emission filter (Chroma Technology Corp., Rockingham, VT). Images were recorded through a highly sensitive CascadeII EMCCD camera with exposures varying between 100 and 2000ms. All images were recorded through IPLab software (Scanalytics, BD Biosciences, Bioimaging, Rockville, MD).

4.3 Results and Discussion

4.3.1 Efficiency of removal of unconjugated dye

Cellulases labeled with amine reactive AF647 succinimidyl ester probes were found to contain free dye after sample purification through two successive size-exclusion spin columns (3000 Da MWCO). Native gel purification allowed the separation of bands of AF647 labeled Cel5A, Cel6B and Cel9A from unconjugated flourophore. Band intensity measurements were used to calculate the free dye fluorescence as a percentage of total sample fluorescence. The average values of free dye fluorescence were found to be 78 ± 3% for Cel5A, 46 ± 6 % for Cel6B and 66 ± 2% for Cel9A. Thus the n-PAGE purification step indicated that the free dye contributed to as much as 80% of total sample fluorescence after the use of two successive size exclusion spin columns. The presence of unconjugated fluorophore in the labeled cellulase sample is undesirable as it would lead to overprediction of the amount of cellulase present in a reaction system. It would introduce background fluorescence that can interfere with accurate quantification of cellulase binding via fluorescence spectroscopy. The high purity of labeled enzymes achieved with the n-PAGE protocol, allows the use of these cellulases in experiments where enzyme concentration is quantified via fluorometric measurements. It also qualifies these labeled cellulases for use in high resolution optical microscopy studies which require samples with virtually no unconjugated dye.

The degree of labeling of Cel5A, Cel6B and Cel9A were found to be 0.3, 0.5 and 0.5 as calculated from absorbance measurements at 280 and 650 nm, and equations 4.1 - 4.2. This meant that only a fraction of the total enzyme content is labeled with one fluorophore while the rest is unlabeled. This degree of labeling was found to have sufficient signal intensity for wide-field and epifluorescence imaging. Furthermore, the percentage of total protein recovered after labeling and n-PAGE purification ranged between 40- 70%, suggesting that the labeling protocol is well suited for the recovery of small amounts of high-purity labeled enzymes.

4.3.2 Activity of labeled cellulase on labeled BMCC

Comparison of the enzymatic activity of labeled and unlabeled cellulases on untreated, EDA treated, and labeled cellulose revealed slight changes of activity after enzyme labeling with AF647. Upon labeling Cel5A and Cel6B cellulases showed a small decrease in their hydrolytic capacity on all three types of substrate, as shown in Table 4.2. However, this decrease was not directly proportional to the amount of labeled cellulase, which allowed us to conclude that the cellulase activity is not inhibited by labeling. On the other hand, upon labeling, Cel9A shows an increase in activity on treated substrates. Increase in Cel9A activity after labeling has been noted in previous work from our group for enzymes labeled with Alexa488 (Jeoh, et al. 2002). Some of the observed changes in activity could be due to either the number of negative charges present both on the enzymes and the AF647 dye, or the relative hydrophobicity of the dye when compared to the binding face on the CBM of the cellulases. Additionally, the position of the labeled lysine can have a strong impact on the activity of the enzyme, especially if the labeled lysine is located near the CBM or the CD. In order to elucidate the specific effects of labeling on the different lysines, a more detailed study is required.

Table 4.2 Activity measurements (nmol cellobiose/min/nmol enzyme) with standard deviations for unlabeled and AF647 labeled *T.fusca* Cel5A, Cel6B and Cel9A on untreated BMCC (U-BMCC), EDA treated BMCC (T-BMCC) and labeled BMCC (L-BMCC)

	Enzyme (pmoles)	U-BMCC	T-BMCC	L-BMCC
U-Cel5A	45	0.121 ± 0.005	0.180 ± 0.007	0.319 ± 0.046
L-Cel5A		0.093 ± 0.004	0.153 ± 0.011	0.232 ± 0.020
U-Cel6B	100	0.195 ± 0.016	0.149 ± 0.010	0.171 ± 0.011
L-Cel6B		0.145 ± 0.006	0.150 ± 0.012	0.174 ± 0.018
U-Cel9A	50	0.596 ± 0.065	0.527 ± 0.018	0.499 ± 0.028
L-Cel9A		0.581 ± 0.009	0.635 ± 0.043	0.604 ± 0.032

4.3.3 Effect of EDA treatment on BMCC morphology and cellulase activity

The use of EDA treatment swells cellulose as it disrupts the tight metastable crystalline packing of cellulose sheets found in nature and introduces sheet to sheet hydrogen bonds that decrease the crystallinity of cellulose transforming it from cellulose I to cellulose III_I (Frey et al. 2006; Helbert et al. 2003). Cellulose treatment with EDA and treatment followed by labeling with DTAF in most cases led to an increased ability of the cellulases to hydrolyze the cellulose polymers and produce fermentable sugars (Table 4.2). The increase in activity after treatment can be explained in terms of greater substrate accessibility. Furthermore, labeling of the cellulose with DTAF increased the ability of the cellulases to hydrolyze the cellulose fibrils. Previous reports have indicated that the labeling of cellulose with DTAF might hinder processive exo- or endo-glucanases, but that it should have little or no effect on classical endoglucanases (Helbert, et al. 2003). Our results show that activity is significantly hindered only for the unlabeled processive endo-glucanase enzyme Cel9A. Furthermore, the activity of the classical endo-cellulase Cel5A is greatly enhanced. The observed increase in activity could be due to local changes in cellulose sheet arrangements as large dye molecules are incorporated onto hydroxyl moieties, or due to the interaction between the hydrophobic DTAF moiety and the CBM.

4.3.4 Patterning of fluorescent cellulose

When suspended cellulose was dried on a polymer surface and the polymer was subsequently lifted-off, a number of cellulose morphologies were observed as shown in Figure 4.1. On the most fundamental scale were cellulose fibrils, tightly packed arrays of cellulose polymers with typical fiber widths of 5-10 nanometers and length of hundreds of nanometers (Figure 4.1d). A second morphology was composed of interwoven cellulose fibrils, in the form of cellulose fibril bundles (Figure 4.1c) or

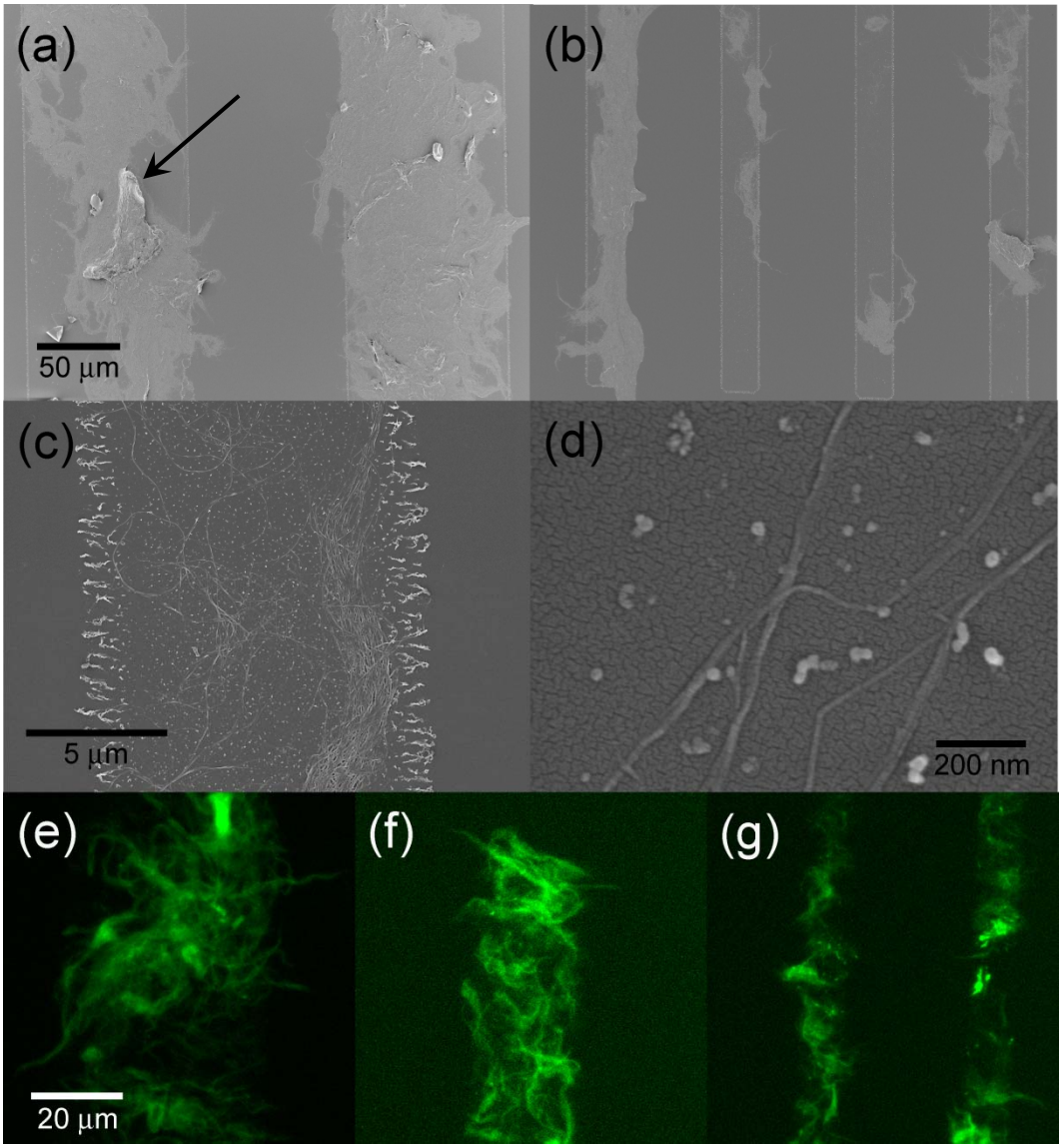

Figure 4.1. Micro-patterned immobilized cellulose imaged by scanning electron microscopy (a-d) and wide field fluorescence (e-f): (a) cellulose deposited through 100 µm patterns shows cellulose particle (arrow) and cellulose mat morphologies; (b) cellulose deposited through 20 µm patterns shows cellulose mat morphology; (c) cellulose deposited through 10 µm patterns shows individual cellulose fibril and fibril bundle morphologies; (d) single cellulose fibril morphology as deposited through 10 µm patterns; (e-g) fluorescence images of cellulose deposited through 50, 20, and 10 µm patterns.

mats (Figure 4.1a-b), with dimensions in the solid surface plane on the micrometer scale, but with axial dimensions below one micron. Finally, there were cellulose particles, conformed by tightly packed cellulose fibrils with dimensions exceeding a few microns in all dimensions (arrow in Figure 4.1a). We These different morphologies are pointed out to underscore the advantages of cellulose fibril immobilization through the polymer lift-off technique. When cellulose was dried from aqueous solutions, mostly cellulose fibril mats and cellulose particles were observed on the polymer/glass surface, similar to those observed when the samples were dried on unpatterned surfaces. However, after the polymer was lifted-off the cellulose left behind in the patterned areas appeared as thin fibril mats (Figure 4.1b), fibril bundles (Figure 4.1c) and even individual cellulose fibrils with 5-10 nm diameter (Figure 4.1d). The cellulosic material left behind after polymer lift-off was well adhered to the substrate and did not dislodge or shift position even after repeated vigorous washing. The polymer lift-off technique also allowed the confinement of immobilized cellulose to predefined areas, a feature that enables repeated localization of structural features in multiple readings over a time-lapsed experiment. The immobilized, fluorescently labeled cellulose could then be imaged through fluorescence microscopy (Figure 4.1e-g) or via scanning electron microscopy.

4.3.5 Photo-bleaching reduction through addition of ascorbic acid

Constant illumination of cellulases labeled with AF647 and bound to immobilized cellulose fibrils resulted in significant photo-bleaching. Illumination of samples with either 100 or 25% total arc lamp power (17 ± 1 and 4.3 ± 0.2 W/cm2 respectively measured at the focal plane) in 50mM sodium acetate buffer pH 5.5 resulted in a $1/e$ decay of fluorescence due to photobleaching in 32 and 86 s respectively, which is similar to decay times reported for cellulases labeled with FITC

(Pinto, et al. 2007). Photo-bleaching of fluorescent samples is a common obstacle in experiments where time-lapsed or dynamic information is desired. Several studies have focused on techniques to minimize this problem through the addition of oxygen scavengers (Dittrich and Schwille 2001; Longin et al. 1993; Rasnik et al. 2006; van den Berg et al. 2001). Depending on the temporal resolution required, oxygen scavengers can interfere with the fluorescence intensity measurements (Rasnik et al. 2006). The goal was to optimize this system to obtain information of cellulase binding to cellulose in the minute to hour range, with exposures well above the millisecond range. Thus, addition of ascorbic acid as an oxygen scavenger to reduce photo oxidation and the resulting photo-bleaching did not interfere significantly with intensity measurements.

4.3.6 Effect of additives on activity of cellulases

The effect of addition of AA and BSA on the activity of Cel6B was tested and the results obtained are shown in Figures 4.2 (a) and 4.3 (a), respectively. The effect of the presence of the additives on the assay used to measure activity, in this case the PAHBAH assay, was also investigated and the results are shown in Figures 4.2 (b) and 4.3 (b). This control experiment was performed in order to ensure that any effect observed was due to the additive and not to due to the method used to measure reducing sugar production. At 5mM the ascorbic acid appears to have significant reaction with the PAHBAH reagent indicating the presence of 36% greater reducing sugars than the actual glucose reducing ends present in the reaction. At lower concentrations ascorbic acid does not appear to have any significant effect on the cellulase activity as measured using the PAHBAH assay. In the presence of 5 mg/ml BSA, there appears to be 10% increase in cellulase activity. However, at 5mg/ml the presence of BSA affects the PAHBAH assay which indicates 10% more reducing ends

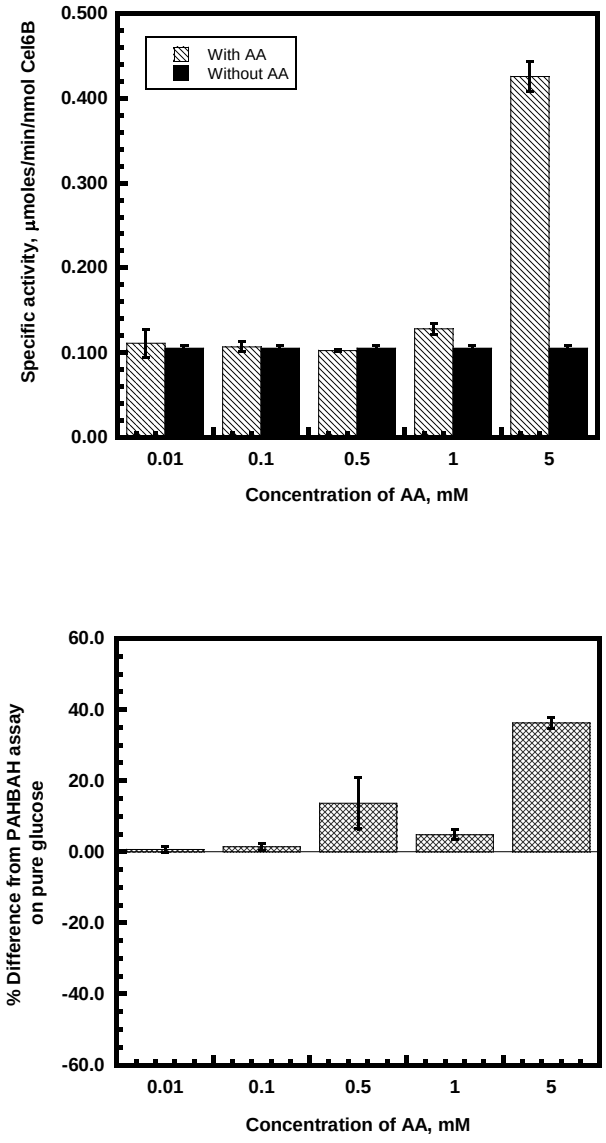

Figure 4.2 Effect of the presence of ascorbic acid (a) on the activity of Cel6B and (b) on the PAHBAH assay.

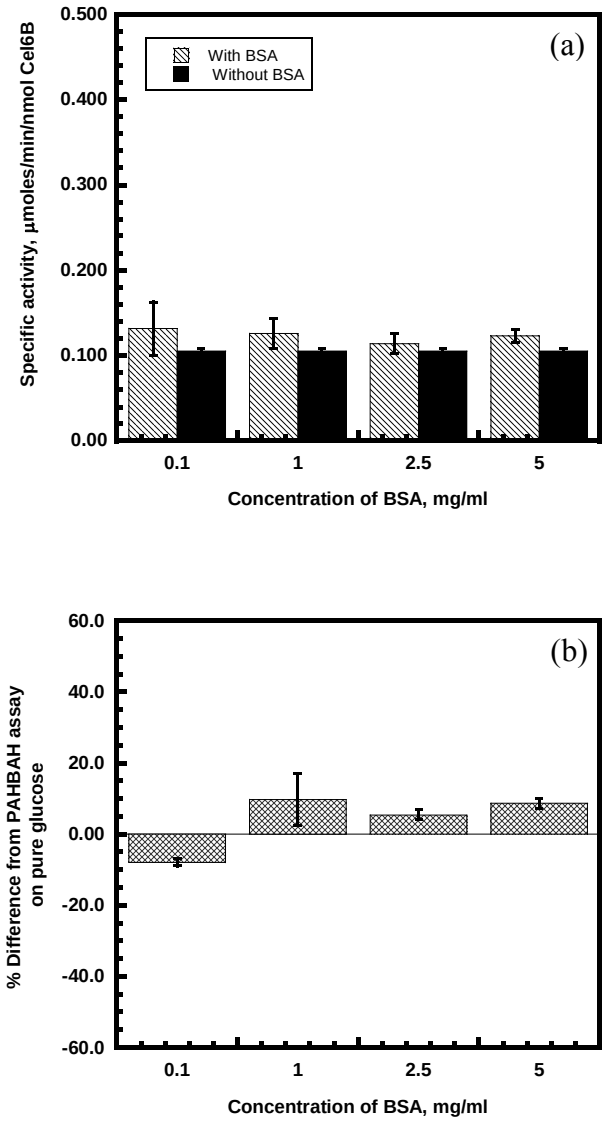

Figure 4.3 Effect of the presence of BSA (a) on the activity of Cel6B and (b) on the PAHBAH assay.

than present in glucose in the solution. This effect on PAHBAH appears to be reflected in the apparent increased activity of all three cellulases indicating that BSA does not cause any enhancement or inhibition of cellulase activity on BMCC. Thus it was ascertained that reagents used for oxygen
scavenging and blocking of non-specific binding sites, did not affect the hydrolytic activity of cellulases.

4.3.7 Imaging of cellulases bound to immobilized cellulose

Cellulase binding by incubation of all three *T. fusca* cellulases with the patterned cellulose was imaged in epifluorescence mode. The binding of fluorescently labeled Cel6B, Cel5A and Cel9A, incubated at 2 nM total enzyme concentration for 90 min is shown in Figure 4.4. Previous studies conducted by our group have shown that Cel5A, Cel6B, and Cel9A bind irreversibly to BMCC at temperatures below 40°C (Jung and Walker 2003). Thus little enzyme desorption was expected from the cellulose substrates after initial incubation and washing. In all panels the green channel represents the DTAF labeled cellulose and the red channel the bound AF647 labeled cellulases. Figure 4.4 clearly shows the contrast between samples where the surface was not blocked against non-specific adsorption (Figure 4.4a, Cel6B) and those where the surface was blocked with BSA treatment (Figures 4.4b-d, Cel6B, Cel5A, and Cel9A respectively). It is evident that if no blocking treatment was used, significant background fluorescence was observed from non-specifically adsorbed cellulases onto the glass surface. The surface treatment with BSA not only significantly reduced the amount of non-specifically bounded cellulases and thus the background fluorescence in the red channel, but also did not introduce any detectable background fluorescence into the red or green channel (Figures 4.4b-d). The blocking treatment was thus an essential part of sample preparation which allowed distinct

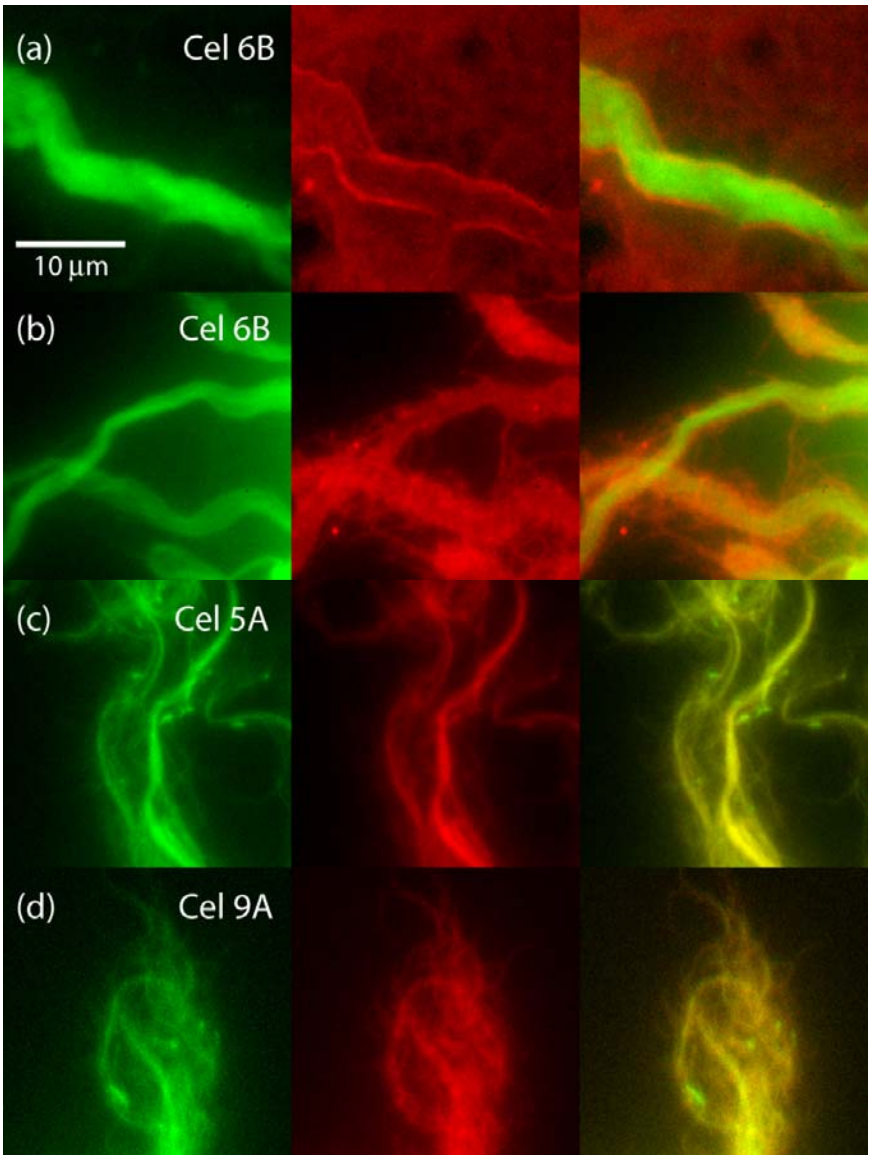

Figure 4.4 Epifluorescence microscopy imaging of 2nM Cel6B, Cel5A and Cel9A bound on immobilized cellulose after 90 min of incubation. Images show the fluorescence acquired from each of the cellulases incubated with immobilized cellulose (a) Cellulose incubated with AF647 labeled Cel6B – sample prepared without surface blocking for nonspecific binding; and (b)-(d) Cellulose incubated with Cel6B, Cel5A, and Cel9A AF647-labeled cellulases after surface was blocked through incubation with 5% BSA. Green channel represents DTAF-labeled cellulose, red channel represents AF647-labeled cellulases bound onto the cellulose, and the last panel shows the overlay of both fluorescent images. All images are at the same magnification.

observation of the binding of cellulases to even the smallest sub-micron sized cellulose fibrils.

Incubation of the immobilized cellulose with cellulases revealed binding to the accessible surfaces of cellulose mats and fibrils. All cellulases studied showed similar binding with no striking differences in cellulase distribution over the cellulose morphologies. It was observed however, that after incubation new features became evident in the red channel corresponding to the labeled cellulases that were not seen in the green fluorescence channel corresponding to labeled cellulose. Cellulose labeling is a random process where the fluorophore is attached stochastically to all accessible sites and where the resulting fluorescence is proportional to the total amount of cellulose in the labeled particles. Thus one would expect to have very little fluorescence present in single cellulose fibrils as compared to that for larger fibril bundles and mats. The green channel fluorescence (DTAF) from individual cellulose fibrils could sometimes be so faint that it was obscured by the scattered light from larger aggregates. However, upon incubation with cellulases, small features such as single fibrils became more evident. This is particularly striking in images such as those presented in Figure 4.4b, where numerous individual fibrils become evident in the red channel (AF647). These features were either absent in the green fluorescence or obscured by scattered and out of focus light from larger neighboring aggregates.

The fact that new features can be observed much more easily through cellulase binding than cellulose labeling arises from the uniform coating of accessible cellulose surfaces by cellulases versus uniform labeling of the whole cellulose volume with DTAF. When cellulose is labeled, the incubation time is large and the fluorophore small enough that full interstice penetration of the DTAF molecules into the cellulose particles is achieved, resulting in uniform labeling throughout the whole volume. On the other hand, short incubations and the larger size of cellulases yield hindered

interstice penetration of the cellulases into the volume of the cellulose fibril aggregates, resulting in cellulase binding only to the most accessible surfaces, reducing the amount of total fluorescence per volume. This effect is more evident in cellulose particles with dimensions beyond a few micrometers, where cellulase binding happens preferentially to the outside surface of the aggregate, and there is hindered diffusion into the core of it. This is well exemplified in the red channel for Figure 4.4a, where the surface of the cellulose particle is significantly brighter than the core.

4.4 Conclusion

A miniaturized cellulase-cellulose reaction system exhibiting fluorescent properties for the study of cellulase binding to cellulose at the nanoscale has been developed for the application of high resolution microscopy techniques. One of the key challenges of labeling of proteins is the efficient removal of unconjugated fluorophore. This issue has been addressed through the use of native PAGE and the removal of free dye, which accounted for up to 70% of the total sample fluorescence, was achieved. The hydrolytic activity of fluorescently labeled cellulases on fluorescently labeled cellulose was tested and labeling was found not to inhibit cellulase activity. The immobilization of labeled cellulose by drying on micro-patterned polymer lift-off surfaces was found to be an efficient method for confining cellulose microfibrils to specific well defined rEG Ions on the glass slide. By controlling cellulose concentration and the width of the patterned features it was possible to exert some control over various morphologies spanning from nanoscale cellulose fibers, to microscale cellulose fibril mats to sub-millimeter scale cellulose particles. Epifluorescence microscopy was used to visualize immobilized cellulose as well as cellulases bound to it. The use of 5% BSA was found to be effective in

blocking non-specific binding of cellulases to the glass surface and the addition of ascorbic acid as an oxygen scavenger was found to have no inhibitory effect on the cellulases.

This study allowed direct visualization of the effect of hindered interstice penetration on the binding of cellulases onto cellulose aggregates in terms of different fluorescence intensities observed for cellulose in the form of isolated fibrils as compared to cellulose aggregates with complex morphologies. Hindered interstice penetration into cellulose particles has been described in terms of its impact in the recalcitrance of cellulose to cellulase degradation, and has been taken into account in models that describe cellulase binding as a function of cellulase concentration (Jung, et al. 2002; Jung and Walker 2003). Thus, a well characterized and optimized system has been developed to lay the foundation for future work involving high resolution fluorescence spectroscopy.

REFERENCES

Brown RM. 2004. Cellulose structure and biosynthesis: What is in store for the 21st century? Journal of Polymer Science Part a-Polymer Chemistry 42:487-495.

Chanzy H, Henrissat B. 1985. Unidirectional Degradation of Valonia Cellulose Microcrystals Subjected to Cellulase Action. FEBS 184:285-288.

Chanzy H, Henrissat B, Vuong R. 1984. Colloidal Gold Labelling of 1,4-Beta-D-Glucan Cellobiohydrolase Adsorbed on Cellulose Substrates. FEBS 172:193-197.

Craighead HG, James CD, Turner AMP. 2001. Chemical and topographical patterning for directed cell attachment. Current Opinion in Solid State and Materials Science 5:177-184.

Helbert W, Chanzy H, Husum TL, Schulein M, Ernst S. 2003. Fluorescent cellulose microfibrils as substrate for the detection of cellulase activity. Biomacromolecules 4:481-487.

Henrissat B, Teeri TT, Warren RAJ. 1998. A scheme for designating enzymes that hydrolyse the polysaccharides in the cell walls of plants. Febs Letters 425:352-354.

Ilic B, Craighead HG. 2000. Topographical Patterning of Chemically Sensitive Biological Materials Using a Polymer-Based Dry Lift Off. Biomed Microdevices 2:317-322.

Jeoh T, Wilson DB, Walker LP. 2002. Cooperative and Competitive Binding in Synergistic Mixtures of *Thermobifida fusca* Cel5A, Cel6B and Cel9A. Biotechnology Progress 18:760-769.

Jervis EJ, Haynes CA, Kilburn DG. 1997. Surface diffusion of cellulases and their isolated binding domains on cellulose. J Biol Chem 272:24016-24023.

Jung H, Walker LP. 2003. Binding and Reversibility of *Thermobifida fusca* Cel5A, Cel6B and Cel48A and Their Respective Catalytic Domains to Bacterial Microcrystalline Cellulose. Biotechnol Bioeng 84:151-159.

Jung H, Wilson DB, Walker LP. 2002. Binding Mechanisms for *Thermobifida fusca* Cel5A, Cel6B and Cel48A Cellulose-Binding Modules on Bacterial Microcrystalline Cellulose. Biotechnol Bioeng 80:380-392.

Lever M. 1972. A New Reaction for Calorimetric Determination of Carbohydrates. Analytical Biochemistry 47:273-279.

Moran-Mirabal JM, Tan CP, Orth RN, Williams EO, Craighead HG, Lin DM. 2007. Controlling Microarray Spot Morphology with Polymer Liftoff Arrays. Anal Chem 79:1109-1114.

Moran-Mirabal JN, Santhanam N, Corgie SC, Craighead HG, Walker LP. 2008. Immobilization of Cellulose Fibrils on Solid Substrates for Cellulase-Binding Studies Through Quantitative Fluorescence Microscopy. Biotechnol Bioeng 101:1129-1141.

Pinto R, Amaral AL, Carvalho J, Ferreira EC, Mota M, Gama M. 2007. Development of a method using image analysis for the measurement of cellulose-binding domains adsorbed onto cellulose fibers. Biotechnol Prog 23:1492-1497.

Tomme P, Warren RAJ, Gilkes NR. 1995. Cellulose hydrolysis by bacteria and fungi. London:Academic Press. p 2-81.

Wilson DB, Irwin DC. 1999. Genetics and Properties of Cellulases. Advances in Biochemical Engineering Biotechnology: Recent Progress in Bioconversion 65:1-21S.

CHAPTER 5

IMPACT OF CELLOBIOSE ON THE BINDING AND ACTIVITY OF THERMOBIFIDA FUSCA CEL9A

Abstract

Enzymatic hydrolysis of cellulose by cellulases is an industrially significant process for the production of biofuels. This process suffers from a characteristic rapid decline in reaction rate after the onset of hydrolysis. This work examines product inhibition of *Thermobifida fusca* Cel9A by cellobiose as a possible cause for the decline in hydrolysis rate. Cel9A is a unique processive endocellulase consiting of a catalytic domain closely linked to a family 3c cellulose binding module followed by a linker domain and a family 2 cellulose binding module. In order to investigate the mechanism of product inhibition, intact *T. fusca* Cel9A (Cel9A-90) and its construct Cel9A-68 which lacks the family 2 cellulose binding module were tested for cellobiose inhibition through measuring release of fluorescence from fluorescently labeled bacterial microcrystalline cellulose. Time courses of activity and binding of Cel9A-90 and Cel9A-68 at varying cellobiose concentrations were conducted using DTAF labeled BMCC (FBMCC). Increasing cellobiose concentrations were observed to decrease the initial reaction rate, with 60 mM cellobiose leading to a 30% decrease in the initial rate. No definitive correlation was observed between binding and cellobiose concentrations for both species indicating that the presence of cellobiose does not lead to significant enhancement or inhibition of binding.

5.1 Introduction

Cellulosic biomass has the potential to serve as a plentiful resource of soluble sugars that can be fermented to produce liquid fuel, reducing green house gas emissions and the dependence on petroleum (Tilman, et al. 2006). The production of cellulosic ethanol is hinged around the enzymatic hydrolysis of cellulose, which is an inherently slow process (Himmel, et al. 2007). The rate of hydrolysis falls rapidly as hydrolysis proceeds leading to low yields, long process times and the need for high enzyme loadings (Merino and Cherry 2007; Stephanopoulos 2007). The observed decrease in the rate of hydrolysis has been studied using mixtures of cellulases (Eriksson, et al. 2002; Holtzapple, et al. 1984) as well as purified cellulases (Valjamae, et al. 1998; Zhang, et al. 1999). Product inhibition by cellobiose (Kruus, et al. 1995; Teleman, et al. 1995), slow inactivation of adsorbed cellulases (Converse, et al. 1988; Eriksson, et al. 2002; Gan, et al. 2003) and the heterogeneity of the substrate (Eriksson, et al. 2002; Valjamae, et al. 1998; Zhang, et al. 1999) have been considered as possible causes for the sharp decline in hydrolysis rate. The addition of β-glucosidase, which could relieve cellobiose inhibition, was found to stimulate the hydrolytic activity of synergistic mixtures of cellulases (Walker, et al. 1993) but not that of purified cellulases (Zhang, et al. 1999). However Zhang et al. (1999) (Zhang, et al. 1999) examined the effect of the presence of β-glucosidase by measuring the extent of hydrolysis after a 20 h incubation period during which time the influence of other factors such as substrate transformation by hydrolysis could have come into play. Investigation of the effect of product inhibition during the initial stages has the advantage that it minimizes the influence of other possible rate retarding factors such as enzyme inactivation and structural transformation of the substrate with the progress of hydrolysis (Gusakov and Sinitsyn 1992).

An important constraint in assessing product inhibition through initial rates is that a significant quantity of product must be added to the system at the start of the reaction to elicit inhibitory effects; thus decreasing the signal to noise ratio. (Gusakov and Sinitsyn 1992). Gruno et al. (2004) used [^{3}H] – reducing end labeled bacterial cellulose to investigate cellobiose inhibition of purified *Trichoderma reesei* cellulases. Their study indicated that the competitive inhibition constants for exoglucanases were hundred fold higher on crystalline cellulose as compared to that on low molecular weight substrates. The effect of cellobiose on endoglucanases was found to be lower than that on exoglucanases. However their experimental system suffered from the instability of radioactive label to alkalification, which was used to terminate reactions. The purpose of this study is to investigate the impact of cellobiose on purified cellulases using a stable fluorescently labeled substrate that can be used as reliable alternate measure of cellulase activity.

The aerobic filamentous soil bacterium *Thermobifida fusca* secretes different kinds of hydrolytic enzymes that can degrade plant cell wall polysaccharides (Wilson 2004). Six *T. fusca* cellulases have been purified and characterized of which three are endocellulases – Cel9B, Cel5A and Cel6A, two are exocellulases – Cel6B and Cel48A and one is a unique, processive endocellulase – Cel9A (Wilson 2004). Our study focuses on Cel9A because it has the highest activity of any individual *T. fusca* cellulase on crystalline cellulose (Irwin, et al. 1993). Cel9A also has relatively high activity on the soluble substrate carboxy methyl cellulose (CMC) which is the property of endocellulases. However it also produces 87% soluble reducing ends from filter paper and only 13% insoluble reducing ends. Classical endocellulases produce 30-40% insoluble reducing ends from filter paper while classical exocellulases produce only 5-8% insoluble reducing ends as a result of their processive action on filter paper (Irwin, et al. 1993). Processivity is the ability of a cellulase molecule to

adsorb to a cellulose chain, perform hydrolytic cleavage, translate along the same chain and continue to cleave bonds without dissociating until an obstruction or the end of the chain is reached (Wilson and Irwin 1999). Cel9A also synergizes with endocellulases as well as with both reducing end and non-reducing end exocellulases while classical endocellulases do not synergize with each other (Irwin, et al. 1993). Furthermore, Cel9A retains greater than 70% of its activity between pH 4.7 and pH 10.1 (Irwin, et al. 1998). Hence this unique, highly active endocellulase exhibiting processivity has the potential to become an industrially relevant enzyme. Structurally, Cel9A is made up of four domains; a 51.4 kDa N terminal family 9 catalytic domain (CD), a family 3c cellulose binding module (CBM), a fibronectin-like Pr/Ser/Thr rich linker and a family 2 cellulose binding module at the C-terminus (Irwin, et al. 1998). Cel9A-68, a construct which has only the CD and the family 3c domain has been extensively characterized by mutation studies (Li, et al. 2007) and its crystal structure has been solved (Sakon, et al. 1997).

The adsorption of cellulases to the insoluble cellulose surface is a prerequisite for any hydrolysis to occur; hence the rate of hydrolysis is essentially expected to be a function of the bound enzyme concentration (Bothwell, et al. 1993; Lee and Fan 1982; Walker and Wilson 1991). The effect of cellobiose on the adsorption of *Trichoderma reesei* Cel7A and its individual domains was investigated by Stahlberg et al. (1991) (Stahlberg, et al. 1991) by adding excess cellobiose in the order of 10-100 mM. The binding of the intact Cel7A and its CBM were found to be unaffected by cellobiose, but the extent of binding of the CD increased over time in the presence of cellobiose. A similar study was conducted by Palonen et al. (1999) (Palonen, et al. 1999) at lower cellobiose concentrations ranging from 0.02 mM to 16 mM. Palonen et al. (1999) (Palonen, et al. 1999) found that binding of the CDs of both *T. reesei* Cel7A and

Cel6A were increased two-fold and five-fold respectively, by cellobiose even at concentrations as low as 1.5 mM.

A key objective in this study was to compare the hydrolytic and binding behavior of the intact Cel9A (Cel9A-90) and Cel9A-68 in the presence of high cellobiose concentrations. In making these comparison I expect to gain some insights into actual molecular mechanism by which Cel9A interacts with the substrate at high product concentrations. The underlying hypothesis for this work is that binding of cellobiose to the active site would prevent binding to the cellulose chains on the insoluble substrate. This would result in a decline in hydrolytic activity. Does the presence of cellobiose lead to enhanced non-productive binding of the Cel9A catalytic domain as suggested by some investigators (Palonen, et al. 1999; Stahlberg, et al. 1991) or does it inhibit the binding of the catalytic domain? This can in effect strengthen or weaken the argument that cellobiose is a competitive inhibitor. How does the measured bound fraction of cellulase correlate with the observed decline in activity? The objective of this work is to address these key questions.

5.2 Materials and Methods

5.2.1 Enzyme production and purification

Cel9A-90-Streptomyces lividans strain S130, was grown overnight at 30°C in 300 mL of Tryptic Soy Broth (TSB) with 10 μg/mL of thiostrepton (tsr) (Irwin, et al. 1998) . This starter culture was used to inoculate a 10 L Microferm MF-114 10-L fermentor (New Brunswick Scientific Co., Inc., New Brunswick, NJ) containing TSB with 5 μg/mL tsr. The fermentor was run for 40 h at 30°C, maintaining pH at 7.2, D.O. at 40%, air flow at 10-12 L/min and agitation at 300 rpm. Cells were harvested by centrifugation at 4000 rpm for 30 minutes. Ammonium sulfate was added to the supernatant to a final concentration of 1M and the solution was centrifuged again at

8000 rpm for 30 min. The supernatant was filtered using a 0.2 micron membrane BetaPure Filter Cartridge (Cuno Incorporated, CT, USA) at pressure less than 2 psi. The supernatant was loaded onto a CL-4B 100 mL phenyl Sepharose column and washed with 200 mL 1M (NH4)2SO4 followed by 300 mL 0.5 M (NH4)2SO4 + 0.01 M NaCl + 5 mM KPi. Cel9A-90 was eluted with 5 mM KPi at pH 6. Fractions containing maximum Cel9A-90 as determined by SDS gel electrophoresis were pooled and applied to a 100 mL Q-Sepharose column as described in previous work (Zhou, et al. 2004). Protein was eluted from the Q-Sepharose column using 5 mM Bis Tris, pH 5.7 + 10 % glycerol buffer containing NaCl gradients (0.1 M to 0.6 M). Purity of pooled fractions was determined using SDS gels. Protein was concentrated using Amicon ultrafiltration and stored in 5 mM sodium acetate buffer, pH 5.5 containing 10% glycerol. Cel9A-68 was produced and purified as in earlier work (Li, et al. 2007).

5.2.2 Substrate preparation

Bacterial microcrystalline cellulose (BMCC) (Cellulon, Microfibrous Cellulose, Industrial Grade – Prilled, Lot # 61025P, 18.1% solids) was prepared as previously described (Santhanam and Walker 2008). Fluorescent labeling of BMCC with DTAF (5-(4,6-dichlorotriazinyl) aminofluorescein) was carried out as detailed by Helbert et al. (Helbert, et al. 2003) with one exception; the treatment with ethylenediamine and successive methanol/ethylenediamine wash steps were omitted to prevent the conversion of BMCC from Cellulose I to Cellulose III_I. Briefly, 80 mg of DTAF were added to 20 ml of 10mg/ml BMCC in 0.2 N NaOH and stirred for 24 h at room temperature. The DTAF labeled BMCC (FBMCC) was separated from unreacted DTAF by repeated washing with distilled water followed by centrifugation. Fluorescence of the filtrate was compared with that of water to ensure complete

removal of unconjugated dye. The FBMCC was finally resuspended in 50 mM sodium acetate pH 5.5. Dry weight measurements were made to determine the concentration of the BMCC and FBMCC suspensions.

5.2.3 Binding assays

All binding assays were conducted in 350 µL wells of black AcroPrep™ (Pall Life Sciences, Ann Arbor, MI) 96 wells filter plates with 0.45 µm membranes made of hydrophilic polypropylene. Filter plates were incubated for 0.5h with 300 µL of 5% bovine serum albumin (BSA) prior to reaction to block non-specific binding sites on the filter. Wells were rinsed repeatedly with 300 µL, 50 mM sodium acetate, pH 5.5 and flow through was tested for absence of residual BSA before reaction set up. Cel9A-90 or Cel9A-68 were added to a final concentration of 1.6 µM in a 300 µL reaction volume containing 4.2 mg/ml of BMCC or FBMCC. Sodium acetate at 50 mM , pH 5.5 with 10% glycerol was used as buffer. Reactions were incubated at 4°C for 1h and terminated through filtration by centrifugation. Unbound enzyme concentrations were determined using extinction coefficients (Irwin, et al. 1998) and absorbance at 280 nm which was measured using the Synergy™ 2 Multi-Mode Microplate Reader (BioTek Instruments, Inc., Winooski, VT). A series of enzyme dilutions were prepared and the absorbance at 280 nm for triplicates, was measured without filtration and after filtration through BSA-pretreated filter plates to check for nonspecific adsorption of enzyme to the filters.

5.2.4 Fluorescence activity assays

Activity assays were set up exactly as the binding assays except for incubation at 50°C. The plates with buffer and enzyme were pre-incubated at 50°C for 30 min. The substrate was pre-incubated separately at the same temperature for the same

amount of time. The reactions were started by adding 210 µl of 6mg/ml BMCC or FBMCC to all wells to obtain a substrate concentration of 4.2 mg/ml. After the desired time, reactions were stopped by centrifugation and the fluorescence of the filtrate was measured with a Synergy™ 2 Multi-Mode Microplate Reader (BioTek Instruments, Inc., Winooski, VT) using a 485/20 bandpass filter. The "automatic sensitivity adjustment" feature was used in order to take advantage of the full dynamic range of the instrument for fluorescence detection. The "scale to high well" option was selected and an unfiltered FBMCC control sample was added to a reference well in the collection plate. The Synergy 2 plate reader allows a maximum detection of 10^6 counts of fluorescence for signal in the reference well. The target for the reference well was set at 10^5 counts in order to make allowance for other wells in case they had more signal than the reference well. The fluorescence of all sample wells was then expressed as a percentage of the fluorescence of the reference well. The filtrates were frozen and used to measure the reducing sugars produced using the PAHBAH method as described by Lever (1972).

5.2.5 Cellobiose inhibition

The effect of cellobiose was studied by adding cellobiose (≥99.0%, HPLC grade,Sigma-Aldrich, St. Louis, MO) to final concentrations of 5mM, 10 mM, 20 mM, 60 mM and 80 mM to the enzyme and pre-incubating at the desired temperature. Binding and activity assays as described above were conducted with FBMCC as substrate. A corresponding reaction with no cellobiose was also set up in the same plate. All reactions were run in triplicate. Blanks with no enzyme were set up to correct for substrate absorbance. Control samples with no substrate were set up to measure total enzyme concentrations for each species at each time point.

5.3 Results and Discussion

5.3.1 Fluorescence release and reducing sugar production

The hydrolysis time courses for BMCC and FBMCC, at 50°C over 12 h, are shown in Figure 5.1 for Cel9A-90 and Cel9A-68, respectively. The extent of conversion of FBMCC by both Cel9A species is found to be in close agreement with the extent of conversion of BMCC, with a maximum difference of 4% at 8h for Cel9A-90. The hydrolytic activities of Cel9A-90 and Cel9A-68 were not affected by the fluorescent labeling of BMCC as shown previously (Helbert, et al. 2003; Moran-Mirabal, et al. 2008). For the purpose of this study, FBMCC was found to closely mimic BMCC at all the time points examined and could thus be used for inhibition experiments.

At labeling conditions similar to those used in this study, the degree of substitution of FBMCC has been documented to be 0.005 (Helbert, et al. 2003) which corresponds to the grafting of 1 DTAF molecule about every 200 glucose units. A fixed blank fluorescence release of 13.73 ± 1.31% was observed on filtration of FBMCC incubated with no enzyme at all time points at both 50°C and 4°C studied. This value was subtracted from all measurements of total fluorescence released in the presence of enzyme to determine the actual percentage of fluorescence released due to enzymatic activity. The constant blank fluorescence released from FBMCC in the control sample incubated without enzyme showed that the fluorescent substrate was stable, with no dissociation of dye over time at the temperatures studied. This ensured that the enzyme alone was responsible for any dye release greater than the blank fluorescence, just as it was responsible for any reducing sugar production.

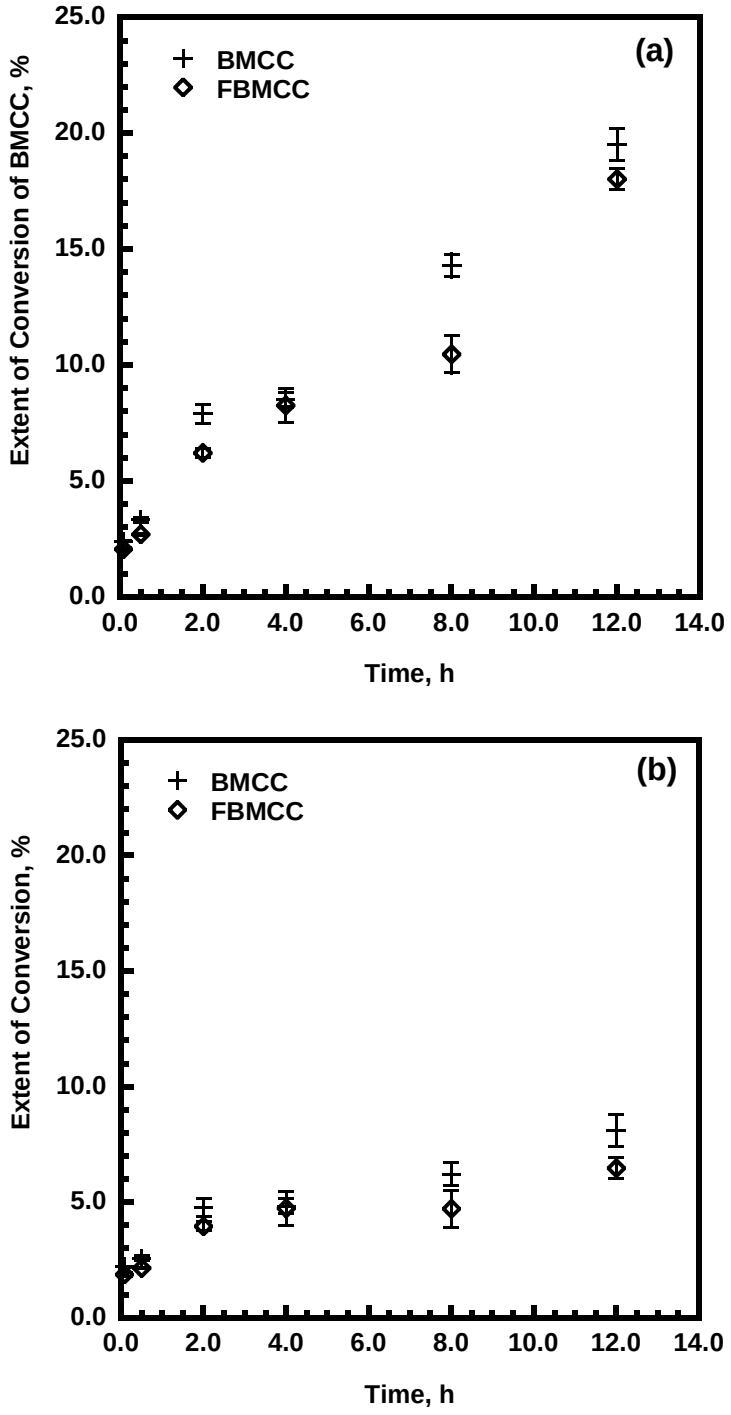

Figure 5.1 Time course of activity of (a) Cel9A-90 and (b) Cel9A-68 on BMCC and F-BMCC at 50°C. Enzyme concentrations used: 1.6 µM. Substrate concentration was fixed at 4.2 mg/ml in a total reaction volume of 300 µL. Error bars indicate standard deviation of triplicate samples.

Figure 5.2 is a plot of fluorescence released as a function of the extent of conversion of FBMCC for Cel9A-90 and Cel9A-68. A strong linear correlation exists between the fluorescence released and the reducing sugars produced over the 12 h period examined. The slopes of the linear plots for Cel9A-90 and Cel9A-68 are found to be in close agreement, being within 1.5 % of each other. This indicates that though the extents of activity are different for the two cellulases, the ratio of fluorescence released to the reducing sugars produced is the same for both. For instance, at 12h, while Cel9A-90 releases 55% fluorescence as a result of 11% conversion of FBMCC while Cel9A-68 releases 35% fluorescence as a result of 7% conversion. Since Cel9A exhibits endocellulolytic activity (Irwin, et al. 1998), the random cleavage of labeled cellulose results in rapid formation of soluble fluorescent oligosaccharides similar to the observations of Helbert et al. (Helbert, et al. 2003) for endocellulase Cel6B of *Humicola insolens*. Figure 5.2 thus indicates that the labeling of cellulose throughout the volume of DTAF is uniform, allowing fluorescence released to be directly and linearly proportional to the reducing ends released by Cel9A-90 and Cel9A-68 up to 12% conversion of BMCC by Cel9A-90 which is achieved after 8 h of reaction. Since 8 h of reaction would involve the diffusion of cellulases into the porous structure of BMCC, this implies that the DTAF not only reacts with hydroxyl groups on the surface of BMCC but also with the hydroxyl groups on cellulose chains in the interior pores of BMCC.

The extent of hydrolysis of FBMCC up to 8 h derived from fluorescence released is shown in Figure 5.3. A comparison of these values with the extent of conversion in Figure 5.1 indicates that the correlation provides an accurate estimate of the percentage of reducing sugars produced. For the time periods and the enzyme

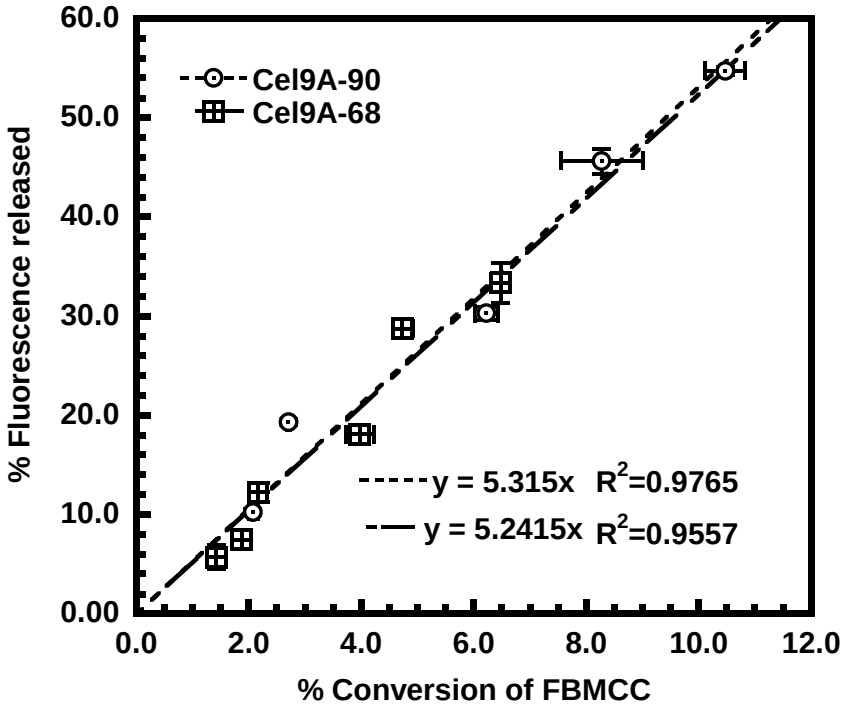

Figure 5.2 Linear correlation between fluorescence released and soluble reducing ends produced by Cel9A-90 and by Cel9A-68 at 50°C. Enzyme concentrations used: 1.6 µM. Substrate concentration was fixed at 4.2 mg/ml in a total reaction volume of 300 µL. Error bars indicate standard deviation of triplicate samples.

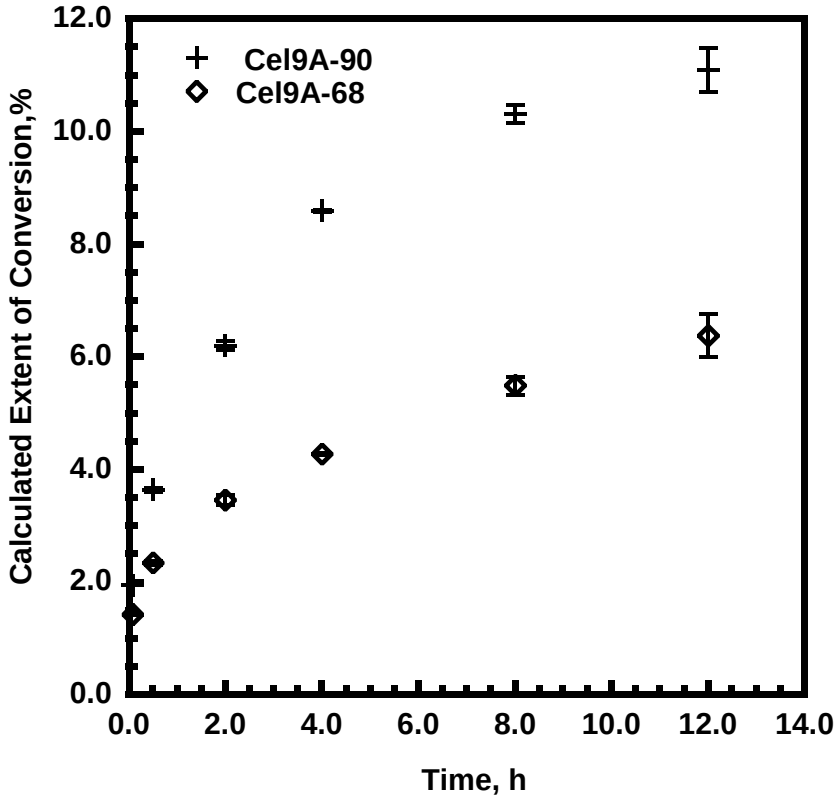

Figure 5.3. Time course of extent of conversion calculated from fluorescence released by Cel9A-90 and Cel9A-68 from F-BMCC at 50°C. Enzyme concentrations used: 1.6 µM. Substrate concentration was fixed at 4.2 mg/ml in a total reaction volume of 300 µL. Error bars indicate standard deviation of triplicate samples.

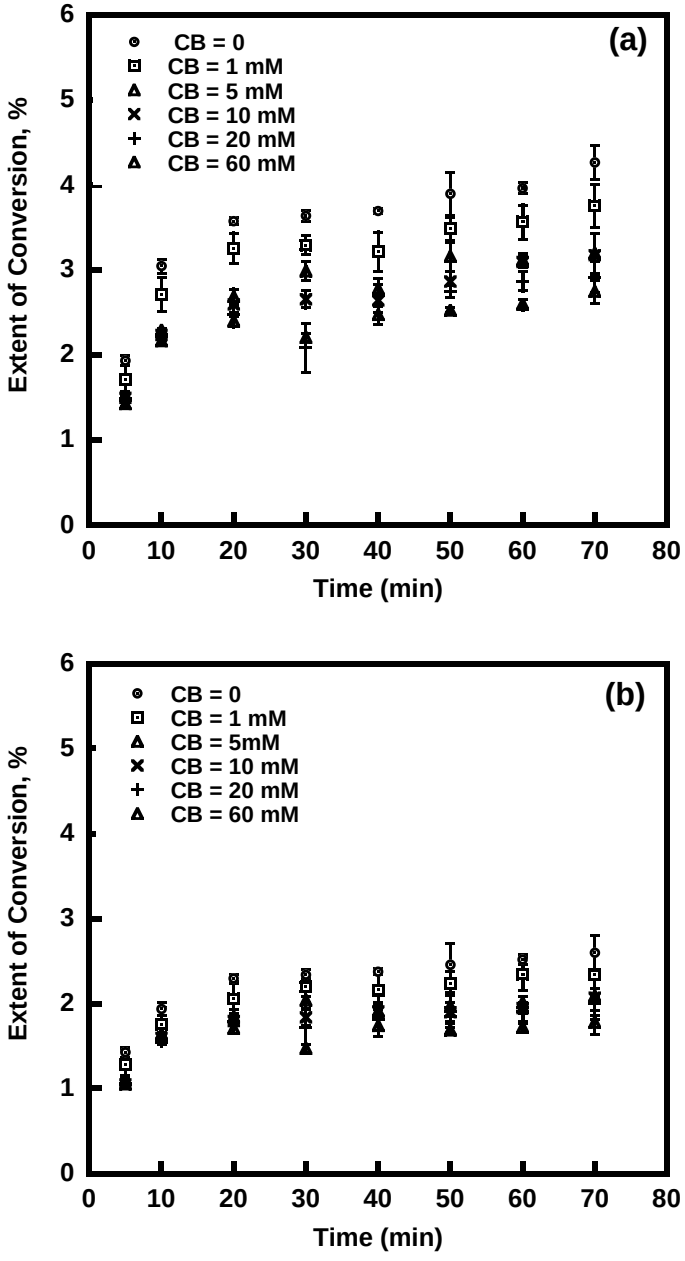

Figure 5.4. Time course of the fluorescence released by (a) Cel9A-90 and (b) Cel9A-68 in the absence and presence of cellobiose at 50°C. Enzyme concentrations used: 1.6 µM. Substrate concentration was fixed at 4.2 mg/ml in a total reaction volume of 300 µL.

loadings used in this study, the linear correlation observed between the extent of conversion and the fluorescence released allows the fluorescence released to be used as a reliable alternative for quantifying cellulase activity with the advantage of higher resolution at short reaction times.

5.3.2 Impact of cellobiose on activity

The time course of fluorescence released by Cel9A-90 and Cel9A-68 at 10 min intervals up to 1.2 h in the absence and presence of excess exogenous cellobiose are shown in Figure 5.4. All reactions at any particular time point were conducted in the same microplate. The released fluorescence increases linearly initially and then bEG Ins to deviate from the linearity. As expected, the rate of fluorescence release was found to decrease continuously over the time period studied. To investigate the effect of cellobiose on the reaction rate, initial rates of fluorescence released at each cellobiose concentration were estimated by applying a linear fit forced through t = 0 to the time course data in Figure 5.4. The initial rate values obtained at varying cellobiose concentrations are listed in Table 5.1. For Cel9A-90, a 10 % decrease in the initial rate is observed in the presence of 1 mM cellobiose. Increasing cellobiose concentrations appear to decrease the initial rate further but the addition of a 60 times higher cellobiose concentration is found to decrease the initial rate only by 30% . For Cel9A-68, 1 mM cellobiose causes the initial rate to drop by 10.5% and increasing cellobiose concentrations appear to cause the initial rate to decline. As for Cel9A-90, a 60 mM cellobiose addition only decreases the initial rate by 24 %. These results indicate that Cel9A is sensitive to cellobiose inhibition up to a concentration of 5mM as the rate of fluorescence released does not decrease continuously with increasing inhibitor concentration between 5mM – 60 mM. For a classical competitive mechanism, at a fixed substrate concentration and a fixed value of substrate

Table 5.1 Initial velocity estimates for FBMCC hydrolysis by Cel9A-90 and Cel9A-68 at varying exogenous cellobiose concentrations.

Cellobiose Concn. (mM)	Initial Velocity Estimate (%Fl/min)			
	Cel9A-90	R^2	Cel9A-68	R^2
0	1.13	0.8929	0.727	0.8713
1	1.02	0.901	0.651	0.8671
5	0.855	0.8851	0.531	0.8491
10	0.828	0.8805	0.572	0.8734
20	0.803	0.8662	0.566	0.8723
60	0.775	0.8646	0.553	0.8521

concentration corresponding to half the limiting rate of fluorescencence released, the initial rate of release of fluorescence would be inversely proportional to the inhibitor concentration. However, the initial rate as shown in Figure 5.5, does not decrease with increasing cellobiose concentrations between 5mM - 60 mM, indicating that the inhibition is not classical competitive inhibition in this range. The fact that the extents of inhibition for both Cel9A-90 and Cel9A-68 were found to be of the same order indicate that while the activity of Cel9A-68 is lower than that of Cel9A-90, the mechanism of inhibition of catalytic activity for both species is similar. It may also be inferred that the presence of the family 2 CBM does not affect the extent of inhibition by cellobiose, which is in agreement with the fact that CBMs of families II have no affinity for small oligosaccharides such as cellobiose (Arai et al. 2003).

The crystal structure of Cel9A-68 determined by X-ray crystallography at 1.9 Å resolution (Sakon et al 1997) shows that the CD is rigidly attached to the family 3c CBM and a shallow cleft runs through the CD and forms the substrate binding site. With the help of enzyme-oligosaccharide complexes the Cel9A active site was identified and the locations of six glycosyl binding sites numbered -4,-3,-2,-1,+1,+2 from the non-reducing end to the reducing end were established (Sakon et al 1997). At high cellobiose concentrations the probability of cellobiose entering the active site would be higher and if our hypothesis that cellobiose blocks the active site leading to a reduced reaction rate were true, a greater decrease in the initial rate would be observed with increasing cellobiose concentrations. However, this is not the case with Cel9A, indicating that cellobiose does not compete with the cellulose chain to gain access to the active site.

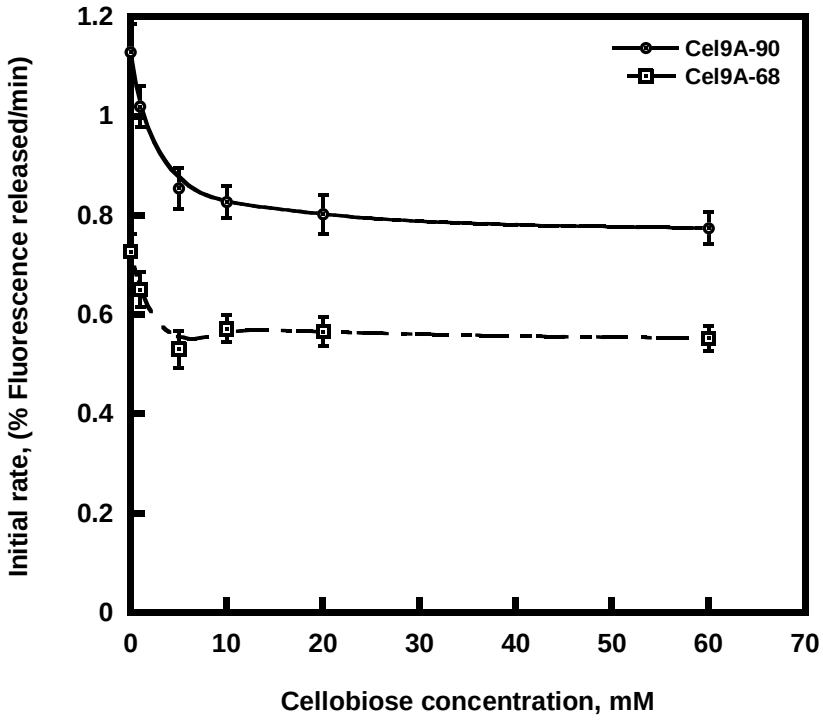

Figure 5.5 Effect of cellobiose on the initial rates for FBMCC hydrolysis by Cel9A-90 and Cel9A-68. Initial rates were estimated by applying linear fits to the fluorescence release data and extrapolating to t = 0.

5.3.3 Binding to fluorescent cellulose

While it has been shown previously that DTAF labeling of BMCC does not inhibit cellulase activity (Helbert, et al. 2003; Moran-Mirabal, et al. 2008), the binding behavior of cellulases to FBMCC has not been directly compared with their binding on BMCC. Figure 5.6 shows the extent of binding of Cel9A-90 and Cel9A-68 on BMCC and FBMCC at 50˚C over 6 h. Bound fractions are expressed as a function of residual BMCC to account for the depletion of substrate as a result of activity over time. Cel9A-90 is found to bind up to an extent of 69 % within 5 minutes to both BMCC and FBMCC. Its binding to FBMCC is found to match its binding to BMCC up to 4 h. After 6 h of reaction, the binding to FBMCC is found to be 16 % lower than that to BMCC indicating that differences in binding extents bEG In over long reaction times. Hence binding time courses in the presence of cellobiose were conducted only up to 1.2 h in order to minimize any influence of FBMCC on the binding behavior. Cel9A-68 is found to bind very weakly to BMCC as well to FBMCC at 50˚C, with an average extent of binding of 2% at the time points studied. It has been shown previously that Cel9A-68 does not bind to BMCC even at room temperature (Irwin, et al. 1998).

5.3.4 Impact of cellobiose on binding

The time courses of binding of Cel9A -90 and Cel9A-68 to FBMCC at 50˚C over 1.2 h, at varying cellobiose concentrations, are shown in Figure 5.7. The bound concentration is expressed as the μmoles of cellulase bound per mass of residual FBMCC. For reactions containing cellobiose, the correlation between the fluorescence activity and percentage conversion was used to determine the residual FBMCC. There is considerable variability in the bound fractions of Cel9A-90

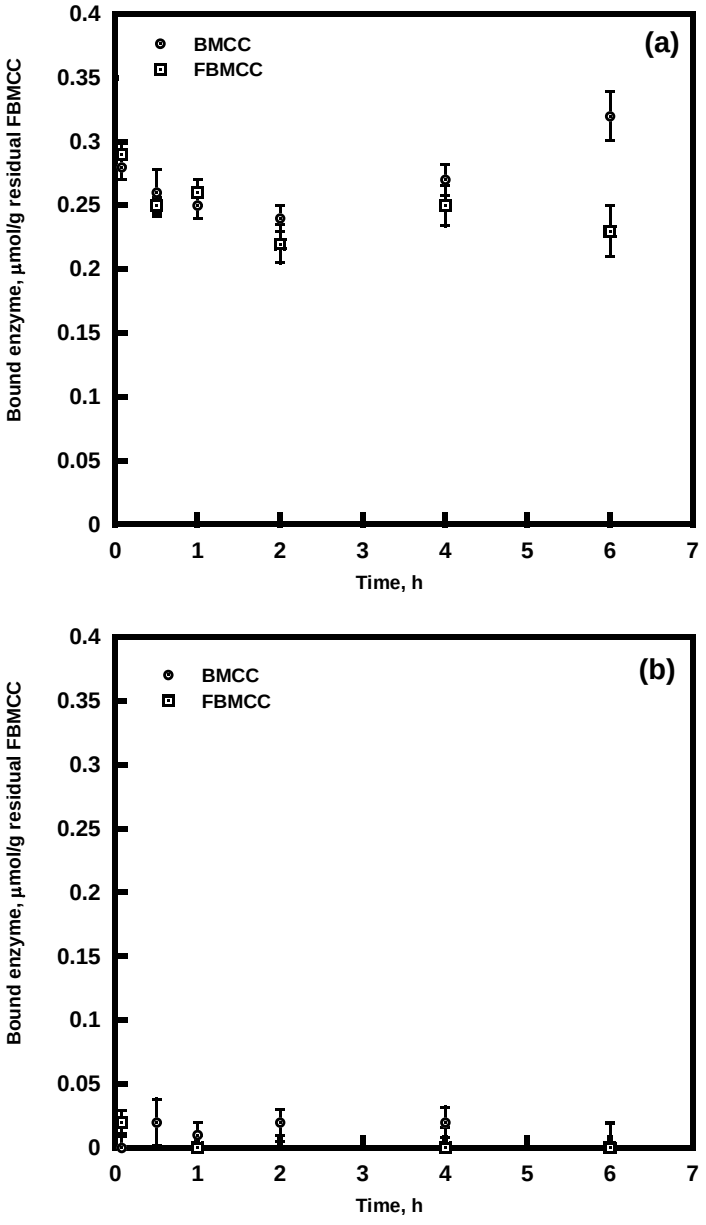

Figure 5.6. Time course of binding of Cel9A-90 and Cel9A-68 at 50°C over 6h. FBMCC concentration was fixed at 4.2 mg/ml in a total reaction volume of 300 µL. Enzyme concentrations used : 1.67 µM Cel9A-90 and 2.17 µM Cel9A-68.

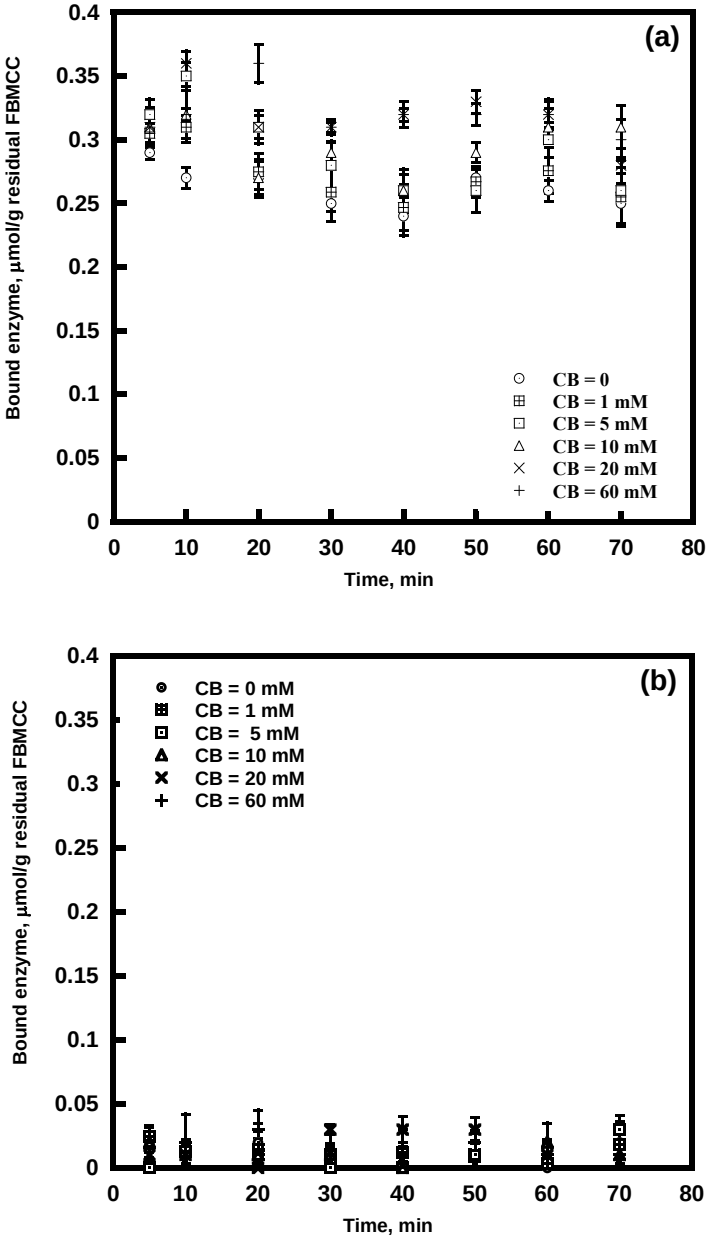

Figure 5.7 Time course of binding of Cel9A-90 and Cel9A-68 to FBMCC in the absence and presence of cellobiose at 50°C. FBMCC concentration was fixed at 4.2 mg/ml in a total reaction volume of 300 µL. Enzyme concentrations used : 1.67 µM Cel9A-90 and 2.17 µM Cel9A-68.

measured in the presence of cellobiose. Two factors may be responsible for the variation in bound fractions observed, namely, the variability in substrate loading between wells and non-specific adsorption to filter plates. Bacterial microcrystalline cellulose, while being a good model substrate in terms of its simple morphology and high crystallinity, is still a non-homogeneous slurry whose density can vary from sample to sample depending on the extent of mixing before a sample is pipetted out. While it is a suitable substrate for cellulose hydrolysis kinetics, its inherent variability and heterogeneous nature contribute significantly to variability in binding measurements especially at low enzyme-substrate ratios. Low enzyme-substrate ratios, however, need to be used in order to observe binding prior to saturation of binding sites in the substrate.

The other factor which may be considered responsible for variability between the time points is the nonspecific adsorption of cellulases to the microplate filter. The effect of nonspecific adsorption to microplate wells becomes more significant at low volumes at low enzyme concentrations. Since the unbound enzyme concentration in the filtrate is the measured variable for this study, the effectiveness of BSA-pretreatment in minimizing nonspecific adsorption was tested. Figure 5.8 shows a comparison of the concentration of Cel9A-68 measured directly without filtration (expected concentration) and after filtration through BSA-pretreated microplates (measured concentration). Linear regression analysis of the two variables resulted in a slope of 1.045 indicating that no change was observed in concentrations on filtration through BSA-pretreated microplates at the reaction volumes used.

An analysis of variance was conducted to determine whether there is any linear correlation between bound fractions of Cel9A-90 and the amount of cellobiose added. The null hypothesis that there is no correlation between bound fractions and cellobiose

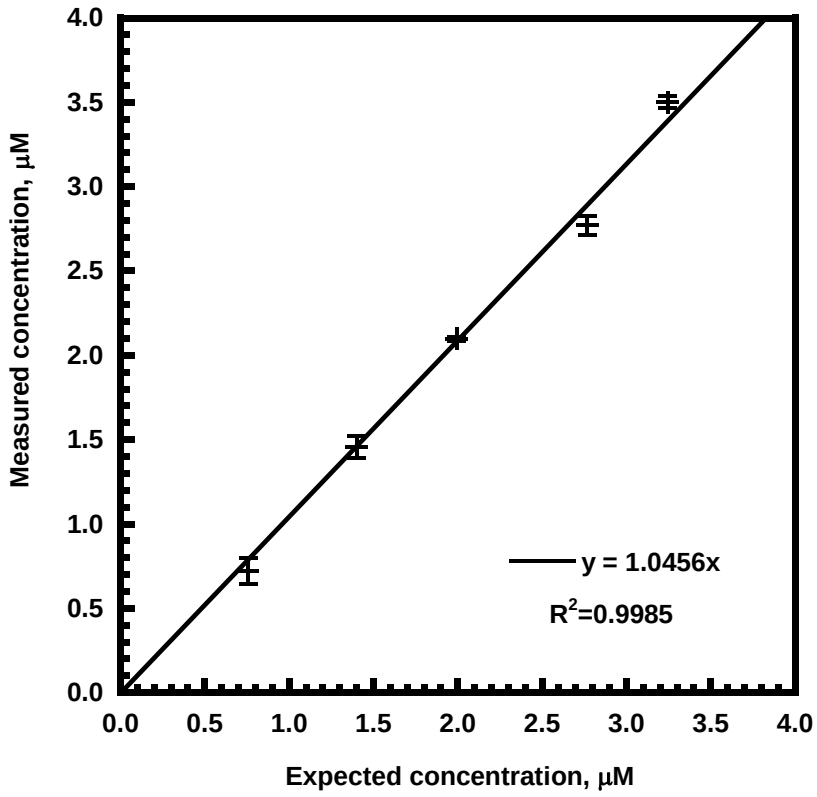

Figure 5.8 Concentration of Cel9A-68 measured using absorbance at 280 nm without filtration (expected concentration) and after filtration through BSA pretreated microplate filter (measured concentration). Error bars indicate standard deviation of the mean for triplicate samples.

concentrations was tested statistically at different time points. The null hypothesis is usually tested by computing an F statistic and its associated probability, *p* value which is also denoted as Prob>F (Lehman et al 2005). The *p* value indicates the probability of obtaining by chance alone an F statistic as large as or larger than the one obtained for a set of data if the null hypothesis were true. Usually when the *p* value is less than 0.05, the null hypothesis can be rejected. For the binding data for Cel9A-90 with respect to cellobiose the Prob > F value was found to be greater than 0.05 for the bound fractions as a function of cellobiose at all the time points studied, indicating that the variation in bound fractions was not directly correlated with the cellobiose concentrations.

5.4 Conclusions

The processive endocellulase *T.fusca* Cel9A exhibits nonlinear kinetics when hydrolyzing BMCC. A fluorescence based assay was successfully used to detect and quantify the extent of hydrolytic activity of intact Cel9A-90 and its construct Cel9A-68 which lacks the family 2 CBM. Fluorescence released was found to have a linear correlation with reducing sugar production. A series of initial rates of hydrolysis were determined for varying cellobiose concentrations at fixed enzyme to substrate ratio. Initial rates for both Cel9A-90 and Cel9A-68 were found to decrease by 30% and 24.5% respectively by the addition of 60 mM cellobiose. The decline in initial rates was not proportionate with the increase in cellobiose concentration indicating that while Cel9A was sensitive to the presence of cellobiose, it did not follow the competitive mechanism of conventional enzyme kinetics over 5 – 60 mM concentration range. The binding of Cel9A-90 and Cel9A-68 to fluorescent BMCC was examined in the presence of cellobiose and no definite enhancement of binding was observed for both species. The variability in bound cellulase concentrations in the

presence of cellobiose could be a result of changes in desorption rates coupled with variability in BMCC concentrations. However, these results indicate that the hydrolyzing activity of Cel9A is not significantly inhibited by high cellobiose concentrations.

Unlike other processive cellulases such as fungal cellobiohydrases which have a tunnel structure that can be blocked by the presence of cellobiose close to the active site (Gruno, et al. 2004), the endocellulase Cel9A has an open structure as described earlier, which would allow cellobiose and other soluble products to freely diffuse away after bond cleavage. It is possible that the variability observed in the bound fractions of Cel9A-90 is due to changes in the desorption rate caused by the cellobiose which would be reflected as changes in bound fractions. However, in this study we did not examine the rate or extent of desorption. Previous work, involving *T. reesei* CBH I and CBH II CDs, has shown that cellobiose leads to increased CD binding (Palonen, et al. 1999; Stahlberg, et al. 1991). However our results indicate that Cel9A-68, which does not bind to crystalline cellulose at 50 º C, remains unaffected by high cellobiose concentrations. The lack of any significant enhancement in binding undermines the hypothesis that the blocking of the active site by cellobiose would lead to increased non-productive binding of *T. fusca* Cel9A.

REFERENCES

Bothwell MK, Walker LP, Wilson DB, Irwin DC, Price M. 1993. Synergism Between Pure *Thermomonospora fusca* and *Trichoderma reesei* Cellulases. Biomass and Bioenergy 4:293-299.

Converse AO, Matsuno R, Tanaka M. 1988. A Model of Enzyme Adsorption and Hydrolysis of Microcrystalline Cellulose with Slow Deactivation of the Adsorbed Enzyme. Biotechnol Bioeng 32:38-45.

Eriksson T, Karlsson J, Tjerneld F. 2002. A model explaining declining rate in hydrolysis of lignocellulose substrates with cellobiohydrolase I (Cel7A) and endoglucanase I (Cel7B) of *Trichoderma reesei*. Appl Biochem Biotechnol 101:41-60.

Gan Q, Allen SJ, Taylor G. 2003. Kinetic dynamics in heterogeneous enzymatic hydrolysis of cellulose: an overview, an experimental study and mathematical modelling. Process Biochemistry 38:1003-1018.

Gruno M, Väljamäe P, Pettersson G, Johansson G. 2004. Inhibition of the *Trichoderma reesei* cellulases by cellobiose is strongly dependent on the nature of the substrate. Biotechnol Bioeng 86:503-511.

Gusakov AV, Sinitsyn AP. 1992. A Theoretical-Analysis of Cellulase Product Inhibition - Effect of Cellulase Binding Constant, Enzyme Substrate Ratio, and Beta-Glucosidase Activity on the Inhibition Pattern. Biotechnol Bioeng 40:663-671.

Helbert W, Chanzy H, Husum TL, Schulein M, Ernst S. 2003. Fluorescent cellulose microfibrils as substrate for the detection of cellulase activity. Biomacromolecules 4:481-487.

Himmel ME, Ding S, Johnson DK, Adney WS, Nimlos MR, Brady JW, Foust TD. 2007. Biomass Recalcitrance: Engineering Plants and Enzymes for Biofuels Production. Science 315:804-807.

Holtzapple MT, Caram HS, Humphrey AE. 1984. The HCH-1 model of enzymatic cellulose hydrolysis. Biotechnol Bioeng 26:775-780.

Irwin D, Shin D-, Zhang S, Barr BK, Sakon J, Karplus PA, Wilson DB. 1998. Roles of the Catalytic Domain and Two Cellulose Binding Domains of *Thermomonospora fusca* E4 in Cellulose Hydrolysis. Journal of Bacteriology 180:1709-1714.

Irwin DC, Spezio M, Walker LP, Wilson DB. 1993. Activity Studies of 8 Purified Cellulases - Specificity, Synergism, and Binding Domain Effects. Biotechnol Bioeng 42:1002-1013.

Kruus K, Andreacchi A, Wang WK, Wu JHD. 1995. Product inhibition of the recombinant CelS, an exoglucanase component of the *Clostridium thermocellum* cellulosome. Appl Microbiol Biotechnol 44:399-404.

Lee YH, Fan LT. 1982. Kinetic-Studies of Enzymatic-Hydrolysis of Insoluble Cellulose - Analysis of the Initial Rates. Biotechnol Bioeng 24:2383-2406.

Li Y, Irwin DC, Wilson DB. 2007. Processivity, Substrate Binding, and Mechanism of Cellulose Hydrolysis by *Thermobifida fusca* Cel9A. Appl. Environ. Microbiol. 73:3165-3172.

Merino ST, Cherry J. 2007. Progress and challenges in enzyme development for Biomass utilization. Biofuels 108:95-120.

Moran-Mirabal JN, Santhanam N, Corgie SC, Craighead HG, Walker LP. 2008. Immobilization of Cellulose Fibrils on Solid Substrates for Cellulase-Binding Studies Through Quantitative Fluorescence Microscopy. Biotechnol Bioeng 101:1129-1141.

Palonen H, Tenkanen M, Linder M. 1999. Dynamic interaction of *Trichoderma reesei* cellobiohydrolases Ce16A and Ce17A and cellulose at equilibrium and during hydrolysis. Applied and Environmental Microbiology 65:5229-5233.

Sakon J, Irwin D, Wilson DB, Karplus PA. 1997. Structure and mechanism of endo/exocellulase E4 from *Thermomonospora fusca*. Nat Struct Mol Biol 4:810-818.

Stahlberg J, Johansson G, Petterson G. 1991. A New Model for Enzymatic Hydrolysis of Cellulose Based on the Two-Domain Structure of Cellobiohydrolase I. Bio/Technology 9:286-290.

Stephanopoulos G. 2007. Challenges in Engineering Microbes for Biofuels Production. Science; Science 315:801-804.

Teleman A, Koivula A, Reinikainen T, Valkeajarvi A, Teeri TT, Drakenberg T, Teleman O. 1995. Progress-Curve Analysis shows that Glucose Inhibits the Cellotriose Hydrolysis Catalyzed by Cellobiohydrolase II from *Trichoderma-Reesei*. Eur J Biochem 231:250-258.

Tilman D, Hill J, Lehman C. 2006. Carbon-Negative Biofuels from Low-Input High-Diversity Grassland Biomass. Science; Science 314:1598-1600.

Valjamae P, V S, Pettersson G, Johansson G. 1998. The Initial Kinetics of Hydrolysis by Cellobiohydrolases I and II is Consistent with a Cellulose Surface - Erosion Model. European Journal of Biochemistry 253:469-475.

Walker LP, Belair CD, Wilson DB, Irwin DC. 1993. Engineering Cellulase Mixtures by Varying the Mole Fraction of *Thermomonospora fusca* E5 and E3, *Trichoderma reesei* CBH I, and *Caldocellum saccharolyticum* B-Glucosidase. Biotechnol Bioeng 42:1019-1028.

Walker LP, Wilson DB. 1991. Enzymatic Hydrolysis of Cellulose: An Overview. Bioresource Technology 36:3-14.

Wilson DB. 2004. Studies of T*hermobifida fusca* plant cell wall degrading enzymes. The Chemical Record 4:72-82.

Wilson DB, Irwin DC. 1999. Genetics and Properties of Cellulases. Advances in Biochemical Engineering Biotechnology: Recent Progress in Bioconversion 65:1-21S.

Zhang S, Wolfgang DE, Wilson DB. 1999. Substrate heterogeneity causes the nonlinear kinetics of insoluble cellulose hydrolysis. Biotechnol Bioeng 66:35-41.

Zhou W, Irwin DC, Escovar-Kousen J, Wilson DB. 2004. Kinetic Studies of *Thermobifida fusca* Cel9A Active Site Mutant Enzymes. Biochemistry 43:9655-9663.

CHAPTER 6

CONCLUSIONS

6.1 Summary of research

There were three major objectives that defined the scope of this dissertation: (1) to assess how bound cellulase fractions in synergistic mixtures correlated with the degree of synergistic effect (DSE), (2) to elucidate the binding mechanism of cellulases to cellulose fibrils using high resolution fluorescence microscopy (3) to investigate whether product inhibition by cellobiose played a major role in the crystalline cellulose hydrolysis kinetics of *T. fusca* Cel9A. These three objectives were met through systematic method development that has been presented in Chapters 3 through 5.

6.1.1 Do cellulases bind cooperatively or competitively in ternary synergistic mixtures?

A comparison of the sum of individual cellulases when bound alone with the total bound cellulases in mixtures showed that they were in close agreement for all cellulase mixtures studied, but one. This indicated that the bound fractions of cellulases were not influenced by the simultaneous binding and hydrolytic activity two other cellulases. Hence the binding in ternary mixtures was found to be additive, unlike the activity in these mixtures, all of which were synergistic. The one exception to this rule was the mixture containing 90% Cel6B, 10% Cel5A and no Cel9A (a binary mixture) where Cel6B represented 98% of the total bound cellulase and Cel5A represented only 2%. Overall, at varying mole ratios of Cel6B and Cel9A, with Cel5A fixed at 10%, binding in ternary mixtures at 50ºC exhibited neither competitive binding nor cooperative binding between the cellulases. Jeoh et al (2002) had

observed enhanced extents of binding at 50ºC for binary mixtures and had concluded that cellulases bind cooperatively due to the increased availability of binding sites created on the substrate by the higher extents of hydrolysis. Of the two binary mixtures studied in the present work, the one containing 90% Cel6B and 10% Cel5A exhibited a 25% enhancement in binding indicating that there was a significant increase in the bound cellulase concentration of this binary mixture. This result seems to be in agreement with the work of Jeoh et al. (2002). It would be expected that in ternary mixtures, the availability of binding sites would increase much more rapidly than in binary mixtures leading to similar enhancement of binding. However, no such enhancement in binding was observed. Hence it is concluded that the binding in ternary mixtures at 50°C is neither competitive nor cooperative.

6.1.2 Binding of cellulases to immobilized cellulose microfibrils

The polymer lift-off technique was found to be successful in controlling the deposition of cellulose morphologies, which spanned from the nanoscale of cellulose fibers to the microscale of cellulose fibril mats to the sub-millimeter scale of cellulose particles. Thus cellulose immobilization was achieved where individual fibrils could be identified. The results of Chapter 4 demonstrated the first successful integration of both cellulase and cellulose labeling into a single experimental system to achieve fluorescence imaging of cellulase-cellulose interactions. Previous studies have focused on the use of either labeled cellulases (Jeoh, et al. 2002; Pinto, et al. 2007), Chapter 3) or labeled cellulose, but have not explored the use of a complete fluorescent assay. This unique system was found to retain the intrinsic activity and binding capabilities of cellulases. Since cellulose hydrolysis occurs at a solid liquid interface, the stagnant boundary layer surrounding the cellulose particles and the changing morphology of the substrate affect the rate at which the cellulases diffuse

onto the surface (Gan, et al. 2003) and into its porous structure. Hence this study successfully developed a system where the effect of complex morphology and internal pore structure can be assessed and compared with the behavior on individual fibrils.

Using this fluorescent cellulose-cellulase system it was shown that the binding behavior of depended strongly on the morphology and complexity of cellulose aggregates, with large aggregates showing effects from hindrance due to penetration into the cellulose pore structure (Moran-Mirabal, et al. 2008). These results support the hypothesis developed by Jung and Walker (2002a, 2002b) the interstice penetration was the cause for the deviation observed in the Langmuir binding isotherms of cellulases, their binding modules and their catalytic domains.

6.1.3 How does cellobiose affect Cel9A binding and activity?

The final objective of this research was to ascertain the influence of high cellobiose concentrations on the behavior of intact Cel9A and its construct lacking the family 2 CBM, Cel9A-68 (Chapter 5). This study used the fluorescence released from the DTAF labeled BMCC to monitor activity at high cellobiose concentrations. The presence of cellobiose at 5 mM led to a 30% decrease in the initial rate of hydrolysis by intact Cel9A. However, increasing the cellobiose concentration further up to 60mM still reduced the initial rate only by 30% indicating that Cel9A activity is sensitive to inhibition by cellobiose only up to 5mM. The active site of Cel9A has been identified and the locations of six glycosyl binding sites numbered -4,-3,-2,-1,+1,+2 from the non-reducing end to the reducing end were established (Sakon, et al. 1997). If the binding of cellobiose to the active site were to saturate the entire enzyme present with inhibitor, the maximum concentration of cellobiose required to do that would be roughly three times the total enzyme concentration, which would be of the order of 5 μM. The exogenous cellobiose concentrations used in this study to elicit

inhibitory effects were several orders of magnitude higher, being in the range of 5-60 mM. It is possible that the system was completely inundated by the cellobiose making it difficult to discern any inhibition. Hence, the mechanism of blocking of active sites by cellobiose could not be used to explain the observed activity trends. Furthermore, the binding of Cel9A in the presence of cellobiose was found to exhibit considerable variability without any significant enhancement or reduction of bound fractions. The observed variability could not be accounted for by any method related factors such as non specific binding to the plate filters.

6.2 Suggestions for future research

The use of microplate readers equipped with a robotic platform will greatly expand the limits of using fluorescence based assays in microplate reactors. They will enable automated combinatorial mixture binding, activity and inhibition studies that can rapidly provide useful information about the different aspects of a complex study. The experimental system developed in Chapter 4 can be used as a foundation for the application of high resolution fluorescence spectroscopy techniques to study cellulase-cellulose interactions at the single molecule level. An analysis of the time course of production of all the soluble cellooligosaccharides released as a result of Cel9A activity could lead to useful clues regarding Cel9A hydrolysis kinetics. Products other than cellobiose that could have possible inhibitory effects should also be integrated into a product inhibition study to allow for a complete mechanistic description of hydrolysis Cel9A.

REFERENCES

Gan Q, Allen SJ, Taylor G. 2003. Kinetic dynamics in heterogeneous enzymatic hydrolysis of cellulose: an overview, an experimental study and mathematical modelling. Process Biochemistry 38:1003-1018.

Jeoh T, Wilson DB, Walker LP. 2002. Cooperative and Competitive Binding in Synergistic Mixtures of *Thermobifida fusca* Cel5A, Cel6B and Cel9A. Biotechnology Progress 18:760-769.

Jung H, Walker LP. 2002. Binding of *Thermobifida fusca* CD_{Cel5A}, CD_{Cel6B} and CD_{Cel48A} to Easily Hydrolyzable and Recalcitrant Cellulose Fractions on BMCC. Enzyme and Microbial Technology 31:941-948.

Jung H, Wilson DB, Walker LP. 2002. Binding Mechanisms for *Thermobifida fusca* Cel5A, Cel6B and Cel48A Cellulose-Binding Modules on Bacterial Microcrystalline Cellulose. Biotechnol Bioeng 80:380-392.

Moran-Mirabal JN, Santhanam N, Corgie SC, Craighead HG, Walker LP. 2008. Immobilization of Cellulose Fibrils on Solid Substrates for Cellulase-Binding Studies Through Quantitative Fluorescence Microscopy. Biotechnol Bioeng 101:1129-1141.

Pinto R, Amaral AL, Carvalho J, Ferreira EC, Mota M, Gama M. 2007. Development of a method using image analysis for the measurement of cellulose-binding domains adsorbed onto cellulose fibers. Biotechnol Prog 23:1492-1497.

Sakon J, Irwin D, Wilson DB, Karplus PA. 1997. Structure and mechanism of endo/exocellulase E4 from *Thermomonospora fusca*. Nat Struct Mol Biol 4:810-818.